University of Alberta

AGONIST EVOKED STATES OF THE $GABA_A$ RECEPTOR

by

Janna Leanne Kozuska

A thesis submitted to the Faculty of Graduate Studies and Research
in partial fulfillment of the requirements for the degree of

Doctor of Philosophy

Department of Pharmacology

Edmonton, Alberta
Spring 2007

Library and Archives Canada

Published Heritage Branch

395 Wellington Street
Ottawa ON K1A 0N4
Canada

Bibliothèque et Archives Canada

Direction du Patrimoine de l'édition

395, rue Wellington
Ottawa ON K1A 0N4
Canada

Your file Votre référence
ISBN: 978-0-494-29702-5
Our file Notre référence
ISBN: 978-0-494-29702-5

NOTICE:
The author has granted a non-exclusive license allowing Library and Archives Canada to reproduce, publish, archive, preserve, conserve, communicate to the public by telecommunication or on the Internet, loan, distribute and sell theses worldwide, for commercial or non-commercial purposes, in microform, paper, electronic and/or any other formats.

The author retains copyright ownership and moral rights in this thesis. Neither the thesis nor substantial extracts from it may be printed or otherwise reproduced without the author's permission.

AVIS:
L'auteur a accordé une licence non exclusive permettant à la Bibliothèque et Archives Canada de reproduire, publier, archiver, sauvegarder, conserver, transmettre au public par télécommunication ou par l'Internet, prêter, distribuer et vendre des thèses partout dans le monde, à des fins commerciales ou autres, sur support microforme, papier, électronique et/ou autres formats.

L'auteur conserve la propriété du droit d'auteur et des droits moraux qui protège cette thèse. Ni la thèse ni des extraits substantiels de celle-ci ne doivent être imprimés ou autrement reproduits sans son autorisation.

In compliance with the Canadian Privacy Act some supporting forms may have been removed from this thesis.

While these forms may be included in the document page count, their removal does not represent any loss of content from the thesis.

Conformément à la loi canadienne sur la protection de la vie privée, quelques formulaires secondaires ont été enlevés de cette thèse.

Bien que ces formulaires aient inclus dans la pagination, il n'y aura aucun contenu manquant.

Canada

To my parents, Michael and Leanne

Abstract

Multiple conductance states and populations of mean single channel current duration have been reported in gamma-aminobutyric acid type A receptors ($GABA_AR$) by numerous investigators. This thesis describes all of the distinguishable conductance states of the $GABA_AR$ and their relationship to agonist concentration in an attempt to define the role(s) these states play in channel activation.

From single channel recordings of $\alpha1\beta2\gamma2L$ $GABA_ARs$, we identified three different conductance amplitudes of 7 pS (mini-conductance), 16 pS (sub-conductance) and 29 pS (full-conductance). Open duration analysis indicated a single population of mini-conductance currents, but two populations each of the sub- and full-conductance currents. In total, five activated states of the $GABA_AR$ were identified.

The frequency of occurrence of the conductance amplitudes was determined from time blocks of 500 ms at various concentrations of the endogenous ligand, γ-aminobutyric acid (GABA), or the partial agonists, 4,5,6,7-tetrahydroisoxazolo-[5,4-c]pyridin-3-ol (THIP) or piperidine-4-sulphonic acid (P4S). The resulting frequency concentration curves for the mini-conductance currents rose sharply to an asymptote at very low agonist concentrations and remained constant thereafter, while both the sub- and full-conductance curves rose in a biphasic manner. The independence of EC_{50} values for each current amplitude is interpreted to indicate separate binding events involving agonist. Comparing the whole cell concentration-effect curves to the frequency-concentration curves of each amplitude state suggests that the majority of current is passed through the full-conductance state at high concentrations of agonist.

A series of novel bisfunctional $GABA_AR$ agonists, the polymethylene digabamides, were also investigated. The whole cell concentration effect curves for these compounds illustrated an increase in intrinsic activity and a decrease in potency with increasing molecular length. All of these compounds are partial agonists in this system. At concentrations of GABA greater than 100 μM, both a fast and slow phase of desensitization was observed. These same components of desensitization were reported with ethylene digabamide and propylene digabamide but the longer compounds only evoked the slow phase of desensitization. These differences in desensitization kinetics are discussed.

Acknowledgements

There are numerous individuals that I would like to thank for their support throughout the course of this program and their contributions to the research described here. I am grateful to my supervisor Dr. William Dryden for giving me the opportunity to work in his laboratory. Throughout the course of my program he never stopped believing in my abilities or the promise of this project and this support was greatly appreciated. I value all of our conversations, both scientific and non-scientific.

I would like to thank the members of my committee, Dr. Susan Dunn and Dr. Glen Baker for their assistance during the course of my degree. I appreciate all the discussions and ideas. I would also like to thank Dr. Ian Martin for his excitement and interest in this work. His encouragement and enthusiasm were always motivating. I also greatly appreciate the critical considerations of Dr. Andy Holt.

I have made a number of friendships with other graduate students over the years that I cherish deeply. These friendships made my time in the department enjoyable and amusing. It has been a pleasure to get to know so many people pursuing interests in science in many different disciplines. I am also thankful to Isabelle Paulsen for her technical assistance and friendship over the years. I loved our long talks and gym dates.

The continued support and encouragement from my parents and friends through all my years of school is greatly appreciated. Thank you for your love and patience throughout the years. To Greg, thank you for your friendship and love.

Table of Contents

Chapter 1 Introduction 1

GABA Overview 2

GABA Receptor Overview 3

The Ligand Gated Ion Channel Superfamily 4

The Acetylcholine Binding Pocket 7

$GABA_AR$ Subunits 13

$GABA_AR$ Assembly and Clustering 15

$GABA_AR$ Binding Sites 17

$GABA_AR$ Agonists 18

The GABA Binding Pocket 18

Channel Opening and Gating 22

Multiple Conductance States 27

Desensitization 34

Expression Systems 38

Aims of the Present Study 39

Bibliography 51

Chapter 2 Methods 67

Cell Culture and Expression of Recombinant Receptors in Culture 68

Patch Clamp Electrophysiology 69

Analysis of Whole-Cell Currents 70

Analysis of Single-Channel Currents 71

Expression in *Xenopus laevis* Oocytes 74

Two-Electrode Voltage Clamp 75

Two-Electrode Voltage Clamp Analysis 76

Drugs Investigated 76

Bibliography 80

Chapter 3 $GABA_AR$ Activation by GABA 81

Introduction 82

Methods 82

Results 83

Activation of $GABA_AR$ by GABA: Whole Cell Currents 83

Single Channel Conductance 83
Frequency of Events 84
Open Channel Duration of $GABA_AR$ 85
Discussion 87
Bibliography 104
Chapter 4 The Single Channel Basis for Partial Agonism at the $\alpha1\beta2\gamma2L$ $GABA_AR$ 107
Introduction 108
Methods 109
Results 110
Concentration-Effect Relationship of THIP and P4S Compared to that of GABA 110
Single Channel Currents 110
Frequency of Channel Openings to the Various Current Amplitudes 111
Open Duration of the Multiple Amplitude Currents 113
Discussion 114
Bibliography 133
Chapter 5 Probing $GABA_AR$ Function With Novel Bisfunctional Ligands: The Polymethlyene Digabamides 134
Introduction 135
Methods 136
Results 136
The Polymethylene Digabamides 136
Whole Cell Currents of $GABA_AR$ Activated by the Polymethlyene Digabamides 136
Desensitization of $GABA_AR$ with Polymethlyene Digabamides 138
Concentration Dependence of $GABA_AR$ Desensitization with GABA or ZAPA 139
Discussion 140
Bibliography 157
Chapter 6 General Discussion 159
General Discussion 160
Bibliography 167

List of Tables

Table 3-1	Open duration analysis summary	102
Table 4-1	Summary of open duration analysis	131
Table 5-1	Maximum distance separating GABA moieties in each of the series of polymethylene digabamides	149
Table 5-2	Potency and intrinsic activity of the series of polymethylene digabamide compounds compared to GABA and ZAPA	152
Table 5-3	Desensitization rates of GABA, ZAPA and the polymethylene digabamides	154

List of Figures

Figure 1-1	The structure of GABA	42
Figure 1-2	Model of a $GABA_AR$ subunit	43
Figure 1-3	Cross section of a nAChR	44
Figure 1-4	View of the cytoplasmic section of a nAChR achieved through cryo-electron microscopy	45
Figure 1-5	Crystal structure of AChBP at 2.7 A	46
Figure 1-6	A model of the five subunits of the most common type of $GABA_AR$	47
Figure 1-7	Model of nAChR gating	48
Figure 1-8	Multiple conductance states of $GABA_AR$	49
Figure 1-9	Models of channel activation and desensitization	50
Figure 2-1	Transfected HEK293 cells	77
Figure 2-2	Examples of channel closures	78
Figure 2-3	*Xenopus* oocyte under two-electrode voltage clamp	79
Figure 3-1	Whole cell $GABA_AR$ currents evoked by GABA	95

Figure 3-2	Amplitude histogram from channel activation with GABA	96
Figure 3-3	Single channel current conductances of $GABA_AR$ activated by GABA	97 & 98
Figure 3-4	Frequency of conductance events at various concentrations of GABA	99
Figure 3-5	Open duration of $GABA_ARs$ activated by GABA: mini-, sub- and full-conductance current durations at 1 μM GABA	100
Figure 3-6	Open duration analysis of $GABA_ARs$ activated by 1 μM GABA	101
Figure 3-7	Proportion of the long and short events with concentration of GABA	103
Figure 4-1	Three $GABA_AR$ agonists	119
Figure 4-2	Whole cell responses to GABA, THIP or P4S	120
Figure 4-3	Sample single channel recordings evoked by THIP	121
Figure 4-4	Sample single channel recordings evoked by P4S	122
Figure 4-5	Amplitude histograms from channel activation with THIP or P4S	123

Figure 4-6	Frequency of conductance events at various concentrations of THIP	124
Figure 4-7	Frequency of conductance events at various concentrations of P4S	125
Figure 4-8	Comparison of the frequency of conductance events at various concentrations of agonists	126
Figure 4-9	Open duration of $GABA_A$Rs activated by THIP: mini-, sub- and full-conductance current durations at 100 μM THIP	127
Figure 4-10	Open duration analysis of $GABA_A$Rs activated by 100 μM THIP	128
Figure 4-11	Open duration of $GABA_A$Rs activated by P4S: mini-, sub- and full-conductance current durations at 10 μM P4S	129
Figure 4-12	Open duration analysis of $GABA_A$Rs activated by 10 μM P4S	130
Figure 4-13	Proportion of long to short sub- or full-conductance openings	132
Figure 5-1	Generic structure of polymethylene digabamides	148
Figure 5-2	Sample whole cell currents elicited by GABA, ZAPA, PCR232, PRC186, PRC233 and PRC187	150

Figure 5-3 Concentration-response curves for polymethylene digabamides compared to GABA and ZAPA 151

Figure 5-4 Two-electrode voltage clamp currents from *Xenopus* oocytes 153

Figure 5-5 Concentration dependence of desensitization 155

Figure 5-6 Proportion of the maximum current entering slow or fast desensitization when exposed to GABA or ZAPA 156

List of Abbreviations

ACh	acetlycholine
AChBP	acetylcholine binding protein
AMPA	α-amino-3-hydroxy-5-methyl-4-isoxazolepropionic acid type glutamate receptors
cDNA	complementary deoxyribonucleic acid
DDF	p-(dimethylamino)-benzenediazonium fluroroborate
EC_{50}	half-maximal concentration for channel activation
E_{max}	maximum response
EGTA	ethylene glycol-bis(β-aminoethylether)-N,N,N',N'-tetra-acetic acid
GABA	γ-aminobutyric acid
GABARAP	γ-aminobutyric acid type A receptor associated protein
$GABA_AR(s)$	γ-aminobutyric acid type A receptor(s)
$GABA_BR(s)$	γ-aminobutyric acid type B receptor(s)
$GABA_CR(s)$	γ-aminobutyric acid type C receptors(s)
GFP	green fluorescence protein
HEK293	human embryonic kidney 293
HEPES	4-(hydroxyethyl)-1-piperazineethanesulfonic acid
$5HT_3R(s)$	5-hydroxytryptamine type 3 receptor(s)
IAA	imidazole-4-acetic acid
IC_{50}	half maximal inhibitory concentration
K_D	equlibrium ligand dissociation constant
LGIC	ligand gated ion channel
MBTA	4-(-N-maleimido)benzyltrimethylammonium
nAChR(s)	nicotinic acetylcholine receptor(s)
NMDA	N-methyl-D aspartate type glutamate receptors
P4S	piperidine-4-sulphonic acid
pKa	-log of acid association constant
4-PIOL	5-(4-piperidyl)-3-isoxazolol

RNA	ribonucleic acid
SCAM	substituted cysteine accessibility method
S.D.	standard deviation
thio-4-PIOL	5-(4-piperidyl)-3-isothiazolol
THIP	4,5,6,7-tetrahydroisoxazolo[5,4-c]pyridin-3-ol
TM	transmembrane
ZAPA	Z-3-[(aminoiminomethyl)thiol]prop-2-enoic acid

CHAPTER 1:

INTRODUCTION

GABA Overview

Gamma-aminobutyric acid (GABA) is an amino acid that serves as a neurotransmitter in the brain. It functions primarily as an inhibitory neurotransmitter in many pathways of the central nervous system, although there are situations during development (Obata *et al.*, 1978; Cherubini *et al.*, 1991; Ben-Ari *et al.*, 1997) and tonic stimulation of adult hippocampal pyramidal neurons (Michelson & Wong, 1991; Staley *et al.*, 1995) when GABA behaves as an excitatory neurotransmitter. Intracellular concentrations of chloride fall progressively with development due to the dominant expression of a chloride transporter, KCC2, which transports chloride out of the cell (for review see Le Van Quyen, 2006). This shifts GABA activity from net excitatory to net inhibitory.

In the late 1950s and early 1960s GABA was initially identified as an inhibitory neurotransmitter at the crustacean inhibitory neuromuscular junction. GABA was shown to increase the conductance of chloride and hyperpolarize the post-synaptic membrane potential (for review see Davidson, 1976). Determining the role of GABA in the mammalian central nervous system proved to be much more difficult due to the complexity of this system and disagreements over the conclusions reached by different groups. By the late 1960s GABA was generally recognized as an inhibitory neurotransmitter in the mammalian central nervous system (Davidson, 1976).

GABA is formed from the principal excitatory neurotransmitter glutamate by glutamic acid decarboxylase using pyridoxal phosphate as a cofactor. After its release into the synaptic cleft, GABA is removed from the synapse by GABA transporters on nerve terminals and glial cells. It is either returned to the nerve terminal where it can be

repackaged and re-released, or it is transported into glial cells where it is metabolized. Glial cells contain GABA transaminase, which converts GABA into succinic semialdehyde. This is converted into either α-hydroxybutyric acid or succinic acid, which can enter the Kreb's cycle. GABA is zwitterionic and, with pKas of 4.23 and 10.43, it is electroneutral at physiological pH (see Figure 1-1). Unlike the primary amino acids, the amino and carboxyl groups of GABA are not attached to the α-carbon but rather are attached to different carbon atoms in the molecule.

GABA Receptor Overview

GABA receptors fall into two major categories, ligand gated ion channels and G-protein coupled receptors. GABA type A receptors ($GABA_ARs$) and GABA type C receptors ($GABA_CRs$) are ligand gated ion channels while GABA type B receptors ($GABA_BRs$) are G-protein coupled receptors. $GABA_A$ and $GABA_C$ receptors have major differences in pharmacology. For instance, $GABA_CRs$ are not sensitive to bicuculline, the classical antagonist at $GABA_ARs$, nor are they sensitive to muscimol, the classical agonist at $GABA_ARs$.. These differences in pharmacology led to the distinction of two classes of ion channel GABA receptors. However, due to the structural homology between $GABA_ARs$ and $GABA_CRs$, $GABA_CRs$ are often referred to as a subtype of $GABA_ARs$. Baclofen is an agonist at $GABA_BRs$, and these receptors are also insensitive to bicuculline, a $GABA_AR$ antagonist.

Activation of GABA receptors usually leads to hyperpolarization of the neuron, thereby effectively lowering the membrane potential. This reduces the probability that an action potential will be generated by the depolarizing action of an excitatory

neurotransmitter. $GABA_A$ and $GABA_C$ receptors achieve this by passing chloride through their integral ion channel into the cell when the receptor is activated. This moves the membrane potential towards the equilibrium potential for chloride, thereby reducing the probability that an action potential will be generated by the depolarizing action of an excitatory neurotransmitter. Unlike the ligand gated ion channel GABA receptors, the $GABA_BR$ is not linked to a chloride channel. Through the inhibition of adenylate cyclase, $GABA_BRs$ can inhibit voltage-gated calcium channels, thereby reducing transmitter release, or through a direct action of the G-proteins, open potassium channels to which they are coupled, leading to a reduction in postsynaptic excitability (see Bowery, 1993 for review). The rest of the work reviewed here will focus on the $GABA_ARs$ and other members of the cysteine-cysteine loop (cys-loop) ligand gated ion channel superfamily.

The Ligand Gated Ion Channel Superfamily

The cys-loop ligand gated ion channel superfamily (LGIC) includes the $GABA_ARs$, the nicotinic acetylcholine receptors (nAChRs), the glycine receptors, and serotonin type 3 receptors ($5HT_3$ Rs) (Schofield *et al.*, 1987; Sieghart, 1988). These receptors all share a common structure as well as high sequence homology among their subunits. Most importantly, there are regions of homology that are conserved in all members of this superfamily. In this class, five subunits arrange in a rosette conformation around a central ion pore (Unwin, 1989; Nayeem *et al.*, 1994). The ion pore in the $GABA_AR$ is chloride selective. Each subunit consists of a large extracellular amino-terminal domain (N-terminal domain) and short extracellular carboxy terminal

domain (C-terminal domain) (Schofield *et al.*, 1987). Closer to the carboxy terminal domain there are four hydrophobic domains (Schofield *et al.*, 1987), each of which is referred to as a transmembrane (TM) domain (see Figure 1-2).

The N-terminal domain of adjacent subunits interacts with ligands, which will be discussed in more detail later. Within this N-terminal domain is a conserved pair of cysteine residues at position 139 and 153 ($GABA_AR$ bovine α1 subunit numbering) (Schofield *et al.*, 1987) that differentiate the cys-loop LGIC superfamily members from other LGICs. Of the four TM domains, the second TM domain, TM2, lines the ion channel pore (Seeburg *et al.*, 1990). Small loops connect TM1 to TM2 and TM2 to TM3 and a large intracellular loop connects TM3 to TM4. This region between TM3 and TM4 shares the least homology between the different subunits (Sieghart & Sperk, 2002), and the significance of this region will be addressed later.

The nAChR is the best characterized member of the cys-loop LGICs and information on its molecular structure has been advanced by cryo-electron crystallography work on nAChRs from the *Torpedo* electric organ performed by Nigel Unwin's group. Initial results confirmed the five subunit arrangement around a central pore which spans the membrane of the cell (Toyoshima & Unwin, 1988). The outer vestibule is approximately 20 Å wide. The extracellular domain is around 65 Å long while the intracellular domain is much shorter (see Figure 1-3). This was later confirmed at 4.6 Å resolution of the receptor by the same group (Miyazawa *et al.*, 1999). The acetylcholine (ACh) binding pockets were identified in the extracellular domain, around 30 Å from the membrane, as cavities in the α subunits (Unwin, 1993). When ACh was bound to the receptor, conformational changes in the receptor and the α subunits were

induced (Unwin, 1995). The 4.6 Å resolution of the receptor illustrated the intracellular end of the receptor, which is composed of projections from the subunits which are approximately 30 Å long and form an inverted cone beneath the membrane spanning domain (Miyazawa *et al.*, 1999). Therefore, ions cannot flow in a linear path through the receptor, but rather divert laterally through narrow openings (portals) between the subunit loops forming this inverted cone shaped structure. Two major openings were identified opposite to the two α subunits which are approximately 8 Å wide and 15 Å long (Miyazawa *et al.*, 1999) (see Figure 1-4). This cytoplasmic domain is formed by the large intracellular M3-M4 loop. For the nAChR, which is a cation-conducting receptor, the net charge of this region is negative, while for anion-conducting receptors such as the glycine receptor and $GABA_AR$, this region is net positive (Unwin, 1989).

Much of the structural information provided by cryo-electron crystallography was supported by the x-ray crystallography studies possible after the crystallization of the acetylcholine binding protein (AChBP) and solving the structure at 2.7 Å resolution (Brejc *et al.*, 2001). This protein was identified in the snail *Lymnaea stagnalis* (Smit *et al.*, 2001) as a protein made and stored in glial cells with the function of binding acetylcholine as a means of inactivating the transmitter. Crystallization of this protein was possible due to its solubility as it lacks the membrane-spanning domains characteristic of the cys-loop LGICs. Numerous conserved residues of the N-terminal domain of the nAChR and of other members of the cys-loop LGIC superfamily are present in the AChBP, and as such this protein has been used as an example of the ligand binding domains of the cys-loop LGICs. The crystal structure of the AChBP was in good agreement with the size of the extracellular domain estimated from cryo-electron

crystallography showing this region as 62 Å high and 80 Å wide with an approximately 18 Å wide central cavitiy (Brejc *et al.*, 2001). The predicted location the ligand binding sites was also very close to that seen in electron microscopy (see Figure 1-5), in the AChBP being 30 Å from the C-termini (Brejc *et al.*, 2001), which, in a cys-loop LGIC, corresponds to the start of the first TM domain. Before, ligand was thought to access the binding pocket from inside the vestibule, as was suggested by the electron microscopy studies (Miyazawa *et al.*, 1999). Recent evidence suggests though that ligand accesses the binding domain from the outside perimeter of the external domain, as suggested from the AChBP (Brejc *et al.*, 2001). In agreement with the earlier electron density map (Miyazawa *et al.*, 1999), the details of the tertiary structure include an N-terminal α-helix followed by ten β-strands arranged in a β-sandwich (Brejc *et al.*, 2001). The authors suggested that the binding site for ligand is formed from loops from one interface and β-strands from the adjacent subunit.

The Acetylcholine Binding Pocket

The nAChR is composed of four different proteins in the stoichiometry of 2α: 1β: 1γ: 1δ (Raftery *et al.*, 1980). The subunits are likely arranged α-γ-α-δ-β counterclockwise around the central ion channel (Pedersen & Cohen, 1990; Czajkowski *et al.*, 1993). The binding site of the nAChR have been characterized through mutagenesis and photoaffinity labeling and further supported by the crystallization of the AChBP.

Using purified *Torpedo* nAChRs, Weill *et al.* (1974) separated the subunits with dodecyl sulfate-acrylamide gel electrophoresis and showed through affinity-alkylation

that the predominant subunit (the α subunit) was covalently labeled with 4-(N-maleimido)benzyl trimethylammonium (MBTA). This led them to suggest that ACh binding occurs exclusively at this subunit. Kao *et al.* (1984) purified nAChRs from *Torpedo* electric tissue and labeled the protein with [^{3}H]-MBTA. Following the reduction of the disulfide bond within the ACh binding site, the α subunit was predominantly labeled with [^{3}H]-MBTA. The α-subunit was isolated and cleaved with cyanogen bromide. High-performance liquid chromatography was used to separate the fragments, and the sequence of the labeled fragment was elucidated using Edman degradation. The [^{3}H]-MBTA labeled fragment contained residues between 179 to 207 and specifically Cys 192 and Cys 193 were the residues labeled. This suggested that these two cysteine residues are close to the ACh binding site. Dennis *et al.* (1988) labeled nAChRs from *Torpedo* with the competitive antagonist [^{3}H]-p-(dimethylamino)-benzenediazonium fluroroborate ([^{3}H]-DDF). Again the α subunits were isolated, cleaved using cyanogen bromide and purified using high-performance liquid chromatography. Trp 149, Tyr 190, Cys 192 and 193 were labeled with [^{3}H]-DDF. They noted that these amino acids lie within hydrophilic domains of the α subunit and may play a role in agonist binding. Abramson *et al.* (1988) used lophotoxin and lophotoxin analog-1, a coral toxin that inhibits the AChR, to further probe the binding site. These compounds covalently react with the α subunit of the nAChR. Using [^{3}H]-lophotoxin analog-1, α subunits were again isolated and digested and the labeled fragment was isolated using sodium dodecyl sulfate-polyacrylamide gel electrophoresis. Once the labeled fragment was sequenced, Trp 190 was identified in the binding of lophotoxin. Using [^{3}H]-DDF labeling, Galzi *et al.* (1990) further identified Tyr 93 (and possibly Trp

86). Binding of [^{3}H]-DDF was inhibited by the agonist carbamoylcholine and the antagonist α-bungarotoxin. Together with the photolabeling experiments done by Dennis *et al.* (1988), Galzi *et al.* (1990) described a three 'loop' model of ACh binding to nAChRs from fish electric organ. These three loops correspond to Tyr 93 (loop A), Trp 149 (loop B) and Trp 190/Cys 192/Tyr 197 (loop C) of the α subunit. Using the agonist [^{3}H]-nicotine, Middleton & Cohen (1991) demonstrated that Tyr 198, Cys 192 and Tyr 190 were labeled with nicotine, indicating that the same regions of the polypeptide chain are involved in agonist and antagonist binding, with the major difference being the degree of labeling of each residue. Using [^{3}H]-acetylcholine mustard (Cohen *et al.*, 1991), alkylation of the receptor occurred at Tyr 93, which further supported its involvement in agonist binding. A number of point mutation studies have been performed to investigate the functional significance of the above amino acid residues. For a review of some of these studies, see Arias (1997). These often resulted in changes in agonist/competitive antagonist binding or channel activation and often resulted in a decrease in agonist affinity compared to wild type receptors. This supports the hypothesis that these residues play a role in agonist binding and/or gating of the receptor complex.

Photoaffinity labeling of the nAChR with [^{3}H]-tubocurarine indicated that the α, γ and δ subunits each covalently interacted with the label (Pedersen & Cohen, 1990). This could be inhibited by either α-bungarotoxin or carbamoylcholine. These results pointed to both the γ subunit and the δ subunit contributing to the binding pocket along with the highly characterized α subunit (Pedersen & Cohen, 1990). This follows from binding studies performed with [^{3}H]-d-tubocurarine that reported biphasic binding of this compound to AChR-rich membranes from *Torpedo* electric organ (Neubig & Cohen,

1979). This work had hinted at the possibility of two separate binding sites for [^{3}H]-d-tubocurarine due to the two affinities reported, which was later deciphered by Blount & Merlie (1989) using subunit expression in fibroblasts as the α-γ subunit interface conferring high affinity and the α-δ subunit interface conferring low affinity for this compound.

With more investigation of the binding pocket, the three loop model of ligand binding has been extended to a six loop model which describes the contribution of individual amino acids from separate regions of the two subunits forming the ligand binding pocket, the α-γ(ε)/δ interface. The major contributions to ACh binding involve loops A, B and C from the α subunit, while loops D, E and F from the γ/δ subunit are described as secondary contributors.

Torpedo nAChRs were equilibrated with [^{3}H]-d-tubocurarine and irradiated with ultraviolet light to identify specific residues that photoincorporated the tritiated antagonist (Chiara & Cohen, 1997). Trp 55 (loop D) of the γ subunit and the corresponding residue in the δ subunit, Trp 57 were identified as residues incorporating the photolabel, as well as residues on the α subunit that had previously been identified, such as Tyr 190, Cys 192 and Tyr 198. Trp 55 of the γ subunit was also identified in agonist binding by labeling with [^{3}H]-nicotine (Chiara *et al.*, 1998). Using [^{3}H]-d-tubocurarine, γ Tyr 111 and Tyr 117 were also labeled (Loop E) (Chiara *et al.*, 1999). The γ subunit amino acid residue Tyr 111 corresponds to δ Arg 113, and point mutations of these two residues led to changes in the binding of α-conotoxin. Czajkowski *et al.* (1993) identified two residues on the δ subunit, Asp 180 and Glu 189 (loop F), that they believed contributed to the ACh binding pocket due to the increase in EC_{50} for ACh and increase in the inhibition of

α-bungarotoxin binding by ACh when these two residues were mutated. Employing chimeras of the γ-δ subunit, point mutations within the δ and γ subunits were introduced and conotoxin M1 binding was investigated (Sine *et al.*, 1995). The amino acid residues γ Lys 34/ δ Ser 36 (loop D), γ Ser 111/ δ Tyr 113 (loop E) and γ Phe 172/ δ Ile 178 (loop F) were identified as contributing to conotoxin M1 selectivity (Sine *et al.*, 1995). Carbamylcholine binding further identified γ Lys 34/ δ Ser 36, γ Phe 172/ δ Ile 178, γ Glu 57/ δ Asp 59 and γ Cys 115/ δ Tyr 117 as residues involved in agonist binding or close to the ACh binding site since introducing point mutations at these locations changed the binding of carbamylcholine (Prince & Sine, 1996). The antagonist, dimethyl d-tubocurarine, identified γ Ile 116/ δ Val 118, γ Tyr 117/ δ Thr 119 and γ Ser 161/ δ Lys 163 as regions involved in antagonist binding (Bren & Sine, 1997).

The two site model of ACh binding to nAChRs has been questioned in the light of evidence that there may be subsites for binding at the high affinity sites (Dunn & Raftery, 1997a, 1997b). After saturation of the high affinity binding sites with [^{3}H]-ACh the authors found that the rate of dissociation was dramatically increased when micromolar concentrations of unlabelled ACh, carbamylcholine or suberyldicholine were added to the dilution buffer compared to the rate of dissociation with dilution buffer without agonist (Dunn & Raftery, 1997a). It was suggested that each high affinity site might have two subsites. Initially [^{3}H]-ACh would bind to site A. With the addition of micromolar concentrations of unlabeled agonist, binding of the unlabeled ligand would occur at site B which would led to a reduction in the affinity of site A, thereby increasing the rate of dissociation from this site. This model was supported by the dissociation rate of [^{3}H]-suberyldicholine, a bis-functional ligand, where this rate was not largely affected by the

addition of micromolar concentrations of agonist (Dunn & Raftery, 1997a). Furthermore, by studying the agonist-induced changes in fluorescence of covalently attached 5-iodoacetamidosalicylic acid, it appears as though ACh can occupy two sites, while suberyldicholine only occupied one (Dunn & Raftery, 1997b). This work has introduced the possibility of additional subsites for agonist binding within the well characterized binding pocket.

Many of the amino acid residues that have been identified either within the binding pocket or as contributing to the binding pocket are aromatic amino acids. This observation led to the suggestion that cation-π interactions may be involved in acetylcholine interaction with the binding pocket (Dougherty & Stauffer, 1990). This is a noncovalent molecular interaction between an aromatic ring, which provides negative electrostatic potential, and a cation. The amino acids most likely to contribute to these interactions are phenylalanine, tyrosine and tryptophan due to the presence of an aromatic ring with π-electrons on the amino acid structures. Zhong *et al.* (1998) studied this interaction at four different tryptophan residues, replacing these residues in series or in combination with a number of tryptophan derivatives. They determined that one of these amino acids, Trp 149, interacts with the quaternary ammonium group of acetylcholine and is probably the primary site of cation-π interaction of the nAChR. However, unlike ACh, nicotine does not show strong cation-π interactions with Trp 149, nor with another likely residue, the Trp γ55/δ57 (Beene *et al.*, 2002). Therefore, it appears that some agonists will interact with the receptor differently from others.

In contrast to these short range cation-π interactions, longer range charge-charge interactions have been proposed to occur between binding domain amino acids that have

acidic side chains and acetylcholine. The negative charge from the acid side chain would interact with the positively charged quaternary ammonium group of ACh. Stauffer & Karlin (1994) determined the mean effective charge of the binding pocket as -2.6. This corresponds to two to three negative charges within the ACh binding domain. Stauffer & Karlin (1994) speculated that these negative charges might be contributed by Asp 180 and Glu 189 of the δ subunit, residues that were identified in contributing to the ACh binding pocket by Czajkowski *et al.* (1993). However, binding of the agonist to the binding pocket is thought to primarily involve cation-π interactions over charge-charge interactions (Dougherty & Stauffer, 1990).

The residues that have been implicated in binding at the nAChR are conserved in the AChBP (Brejc et *al.*, 2001), supporting the proposition that the AChBP is a good model for the N-terminal domain of the nAChR. Together with mutagenesis and binding studies, the AChBP model has also helped provide the identification of possible residues involved in GABA binding (Cromer *et al.*, 2002), residues that couple GABA binding to channel gating (Boileau *et al.*, 2002b), possible drug binding pockets (Ernst *et al.*, 2005) and support for the arrangement of the subunits in the heteropentamer (Trudell, 2002). This will be considered in more detail later.

$GABA_AR$ Subunits

Five subunits assemble to form a $GABA_AR$. These subunits are evolutionarily related, but are encoded by different genes (Barnard *et al.*, 1998). Subunits show 70% sequence similarity within classes and approximately 30% between classes. Numerous classes of subunits are available to assemble into receptors. To date, the subunits that

have been identified are α1-6, β1-4, γ1-3, δ, θ, π, ε, and ρ1-2 (Simeone *et al.*, 2003). The ρ subunits assemble into the so-called $GABA_C$Rs. Splice variants of some of these subunits also occur (eg. γ2 short and long- Whiting *et al.*, 1990). Theoretically, many possible combinations of $GABA_A$Rs could occur, but the true number of $GABA_A$Rs *in vivo* is likely to be substantially fewer (Seeburg *et al.*, 1990; Wisden & Seeburg, 1992; McKernan & Whiting, 1996). The specific subunits that make up a receptor determine the pharmacology of the receptor, as well as the activation, deactivation and desensitization kinetics and conductance values. For example, receptors composed of α1 and β2 subunits display a significantly lower conductance than receptors composed of α1, β2 and γ2 (Seeburg *et al.*, 1990; Angelotti & Macdonald, 1993).

The expression of the various receptor subtypes varies in different cells and brain regions, suggesting a functional specificity of the different types of $GABA_A$Rs (Simeone *et al.*, 2003). For example, α1 mRNA is expressed ubiquitously throughout the brain, while α6 mRNA is only found in the cerebellar granule cells (Wisden *et al.*, 1992). The π subunit seems to be rare or nonexistent in the brain, but is highly expressed in female reproductive organs (Hedblom & Kirkness, 1997). The significance of receptor distribution and the differences in the behaviour of the different receptors may provide important clues into broader functioning within the brain. This differential expression profile, along with the observation that the pharmacological profile of the various receptor subtypes is also often different may provide the opportunity to create novel drugs that can target specific functions through the receptor subtypes. However, this also means that it is not possible to conclude that the results seen at one type of $GABA_A$R will hold true at other types of $GABA_A$Rs, leading to the necessity to test any novel drugs on

multiple subtypes of receptors. The most common $GABA_AR$ is thought to be composed of α1, β2 and γ2 subunits (Laurie *et al.*, 1992a; Laurie *et al.*, 1992b) in a stoichiometry of two α subunits, two β subunits and one γ subunit (Chang *et al.*, 1996; Tretter *et al.*, 1997). The arrangement of these subunits could vary, however, and Baumann *et al.* (2002) suggested that it is likely to be an γ-β-α-β-α arrangement in a counterclockwise configuration from their results of expressing concatamered trimers with dimers. The functionality of the above combination resembled wild type receptors and together with observations of the AChBP structure (Brejc *et al.*, 2000), this was proposed to be the likely subunit arrangement.

$GABA_AR$ Assembly and Clustering

The observation that the AChBP can assemble to form a pentamer suggests that the N-terminal domain of the cys-loop LGICs might play a role in subunit interactions independent of transmembrane helices or cytoplasmic loops. In fact, evidence shows that specific sequences within the α subunit and the β subunit N-terminal domains of the $GABA_ARs$ mediate the subunit interactions. Specifically, two tryptophan residues in the N-terminal domain of the rat α1 subunit were implicated as obligatory for pentamer formation since mutants of Trp 69 or Trp 94 did not appear to form $GABA_AR$ constructs (Srinivasan *et al.*, 1999). Taylor *et al.* (2000) extended the list of critical amino acid residues on the α subunit for oligomerization with the β3 subunit to include residues 58-67 also. By creating truncated γ2 subunits, Klausberger *et al.* (2000) determined that residues 91-104 were necessary for assembly with an α subunit, while residues 83-90 were required for assembly with a β subunit. Tretter *et al.* (1997) hypothesized that the

assembly of the $\alpha1\beta3\gamma2$ $GABA_A$Rs begins with the association of an $\alpha1$ and $\beta3$, an $\alpha1$ and $\gamma2$ and/or a $\beta3$ and $\gamma2$ subunit. In the presence of the third subunit, a pentamer receptor would form. Without the third subunit, $\alpha1\beta3$ subunits would arrange in tetramers and pentamers, while only heterodimers of $\alpha1\gamma2$ and $\beta3\gamma2$ would form. This supported the conclusions reached by Connolly *et al.* (1996) that only receptors formed from $\alpha1\beta3\gamma2$ and $\alpha1\beta3$ subunits could assemble into pentamers. This further supports the notion that the α and β subunits both play a role in pentamer formation.

The clustering of receptors in synapses has been attributed to the protein gephyrin (Kneussel *et al.*, 1999) and the $\gamma2$ subunit (Craig *et al.*, 1996). Although it is not clear whether gephyrin controls the formation of $GABA_A$R clusters or stabilizes already formed clusters, inhibiting gephyrin expression reduced the number of clustered receptors without affecting the total number of receptors expressed (Jacob *et al.*, 2005). $GABA_A$ receptor-associated protein (GABARAP) has also been shown to have a role in receptor clustering through interaction with the $\gamma2$ subunit and tubulin (Wang *et al.*, 1999). Much work has been done recently which illustrates the changes in channel behaviour when $GABA_A$Rs are expressed with GABARAP and without. $GABA_A$Rs coexpressed with GABARAP have a higher single channel conductance than receptor expressed without, and this high conductance current has a longer open duration (Everitt *et al.*, 2004; Luu *et al.*, 2006). It is clear that GABARAP does not change the kinetics of the channel directly (Boileau *et al.*, 2005), and it has been suggested that the clustering of receptors may make them open co-operatively (Everitt *et al.*, 2004). However, GABARAP knock out mice are phenotypically normal and do not show an increase in GABARAPs homologs or a decrease in $GABA_A$R expression, as determined by benzodiazepine binding (O'Sullivan

et al., 2005). This suggests that GABARAP may not be a requirement for proper $GABA_AR$ trafficking. A number of other factors have been shown to influence $GABA_AR$ trafficking. For review, see Luscher & Keller (2004).

$GABA_AR$ Binding Sites

Numerous compounds besides its endogenous ligand GABA have affinity at the $GABA_AR$. Many drugs acting at this receptor have been useful clinically in the treatment of anxiety, epilepsy, sleep disorders and alcohol withdrawal and to induce anesthesia. For example, benzodiazepines (Mohler & Okada, 1977) are often used in the treatment of general anxiety disorders, insomnia, and for the short-term management of status epilepticus (Alldredge & Lowenstein, 1999), although their use is limited by the development of tolerance and dependence. Barbiturates (Study & Barker, 1981) and neurosteroids (Harrison & Simmonds, 1984) are other modulators of $GABA_AR$ activity. A number of cations also modulate $GABA_AR$ properties, including extracellular H^+ (Takeuchi & Takeuchi, 1967), intracellular Ca^{2+} (Inoue *et al.*, 1986), Zn^{2+} (Westbrook & Mayer, 1987), La^{3+} (Zhu *et al.*, 1998) and Al^{3+} (Trombley, 1998). Some alcohols (Celentano *et al.*, 1988 and reviewed by Grobin *et al.* (1998) may also have binding sites on the $GABA_AR$ through which they can modulate GABAergic activity. The modulator binding site that is best characterized is the benzodiazepine binding site at the α-γ subunit interface (see Sigel & Buhr, 1997). For the purposes here, only the GABA binding site will be considered in detail.

$GABA_AR$ Agonists

A number of agonists, including muscimol, isoguvacine, 4,5,6,7-tetrahydroisoxazolo[5,4-c]pyridin-3-ol (THIP), isonipecotic acid, piperidine-4-sulphonic acid (P4S), imidazole-4-acetic acid (IAA), 5-(4-piperidyl)-3-isothiazolol (thio-4-PIOL), 5-(4-piperidyl)-3-isoxazolol (4-PIOL) and Z-3-[(aminoiminomethyl)thio]prop-2-enoic acid (ZAPA) have been identified for the $GABA_AR$. Both the intrinsic activity and potency of these compounds varies depending on which subunits make up the $GABA_AR$ that is being studied. These agonists can be either more or less potent than GABA and can exhibit a spectrum of intrinsic activities ranging from partial agonism to full agonism. For example, at the presumed most common $GABA_AR$ composed of $\alpha1$, $\beta2$ and $\gamma2$ subunits, isoguvacine is a full agonist with less potency than GABA. At this same receptor THIP, isonipecotic acid, P4S, IAA and 4-PIOL are partial agonists and while THIP and isonipecotic acid have similar intrinsic activity (around 70-80% of maximum GABA response), THIP is less potent than GABA but more potent than isonipecotic acid (Mortensen *et al.*, 2004). ZAPA, on the other hand, has been shown to be a full agonist with greater potency than GABA in binding experiments in rat brain membranes (Allan *et al.*, 1986).

The GABA Binding Pocket

The minimum subunit requirement for a GABA gated $GABA_AR$ is the presence of an α and β subunit (Schofield *et al.*, 1987). Therefore, it was suspected that the binding pocket must be formed by these two subunits. Similar to the nAChR, a loop model of binding has been developed (see Figure 1-7). In the $GABA_AR$, the β subunit

contributes loops A, B and C, while the α subunit contributes loops D and E (for review see Smith & Olsen, 1995).

Numerous amino acids on the α1 subunit have been implicated in having a role in agonist binding. Mutation of Phe 64 (loop D) in the rat α1 subunit (Sigel *et al.*, 1992) reduces agonist and antagonist affinities, and the equivalent position in the bovine α1 subunit (Phe 65) can be labeled with [^{3}H] muscimol (Smith & Olsen, 1994). The equivalent position in the *Torpedo* nAChR α subunit (Arg 55) is required for α-bungarotoxin activity (Wahlsten *et al.*, 1993). The substituted cysteine accessibility method (SCAM) involves substituting a series of amino acid residues to cysteines then using thiol reagents (which interact with the side chains of the cysteines) to study the effect of the mutation. Using this method, Phe 64, Arg 66, Ser 68 (loop D) (Boileau *et al.*, 1999) and Val 178, Val 180 and Asp183 (loop F) (Newell & Czajkowski, 2003) appear to line the binding site, with a mutation of only Asp 183 causing a reduction in GABA affinity. Mutating the α1 subunit amino acid residue Arg 120 (loop E) (Westh-Hansen *et al.*, 1999) to lysine significantly reduced GABA affinity, suggesting that this residue also participates in ligand binding.

Residues of the β subunit have been harder to define at the single amino acid level, although mutations of regions encompassing Trp 157-Gly 158-Tyr 159-Thr 160 (loop B) and Thr 202-Gly 203-Ser 204-Tyr 205 (loop C) reduced the binding affinity for agonists (Amin & Weiss, 1993). Amino acid residues Trp 157 to Thr 160 correspond to Trp 149 in the nAChR while Thr 202 to Tyr 205 correspond to Tyr 197 in the nAChR. Using SCAM, amino acid residues Tyr 205, Arg 207, Ser 209 (loop C) (Wagner &

Czajkowski, 2001) and Tyr 97 and Leu 99 (loop A) (Boileau *et al.*, 2002b) appear to line the binding pocket contributed by the β subunit. This is summarized in Figure 1-6.

Cation-π interactions have been shown to be involved in ACh interaction with the nAChR at α Trp 149 (Zhong *et al.*, 1998), and the analogous amino acid residue of the $5TH_3AR$, Trp 183, interacts with serotonin (Beene *et al.*, 2002). So far there has not been a residue of the $GABA_AR$ implicated in creating a cation-π interaction with GABA; however there are a number of aromatic amino acids that contribute to the GABA binding pocket. The $GABA_CR$ does not have a tryptophan at the corresponding position of α Trp 149, but the analogous position is Tyr 198. Lummis *et al.* (2005b) have shown that this tyrosine interacts with the ammonium of GABA through a cation-π interaction. It is likely that with further investigation this type of interaction may be identified between the $GABA_ARs$ and GABA.

Radioactive GABA binding studies identified three separate K_D values for GABA in the low (13 nM) and high (100 nM-1 μM) concentration range (Olsen *et al.*, 1981). Although this binding was performed on brain preparations that would contain numerous types of $GABA_ARs$, this work lead the authors to suggest that there are at least two binding sites of moderate to high affinity. This sort of behaviour has been reported with other compounds acting at $GABA_ARs$. Avermectin B_{1a} is an insecticide that is thought to mediate $GABA_AR$ activity. While studying the effects of this compound on $GABA_ARs$ in rat cerebellar granule neurons, Huang & Casida (1997) reported two K_D values for [^{3}H]-avermectin B_{1a} and determined that avermectin B_{1a} binds at both a high affinity site (K_D 5 nM) and a low affinity site (K_D 815 nM). Avermectin B_{1a} binding to the separate binding sites was proposed to lead to very different responses. Binding to the high

affinity site led to channel activation while binding to the low affinity site blocked channel activity (Huang & Casida, 1997).

Since the most common $GABA_AR$ is composed of two α subunits, two β subunits and one γ subunit, it follows that there would be at least two binding sites for GABA, one between each of the two β-α interfaces (see Figure 1-6). Baumann *et al.* (2003) hypothesized that since the subunit arrangement around the central ion pore is pseudosymmetric, the subunits forming the two binding sites would be different and that these two binding sites might display different affinities for ligands. Based on a β-α-γ-β-α counterclockwise arrangement of the subunits, they referred to the first β-α interface in the above list as site 1 and the second as site 2. In an attempt to characterize these two interfaces, the authors introduced point mutations into either the modified rat α1 subunit at Phe 65 (corresponds to Phe 64 in the unmodified rat α1 subunit) or β2 subunit at Tyr 205. Concatenated subunits were made with the mutation in one or both of the α or the β subunits and the effects on current were compared to receptors composed of wild type subunits. The authors concluded that binding site 1 had lower affinity for GABA but higher affinity for muscimol and bicuculline than binding site 2. The work suggested that first, the two binding sites could be investigated independently using the methods described and secondly that the two β-α interfaces form binding pockets for GABA that are not identical.

There is a disparity of several orders of magnitude in defining values for $GABA_AR$s in comparing binding studies with functional investigations. In both electrophysiological studies (Segal & Barker, 1984) and ion flux experiments (Cash & Subbarao, 1987a) EC_{50} and IC_{50} values are in the micromolar concentration range, while

K_D values, as mentioned earlier, are in the nanomolar to micromolar concentration range. While the appearance of two K_D values could be explained by two GABA binding sites on the $GABA_AR$ complex (one at each β-α interface), this discrepancy between K_D values and EC_{50} values has not yet been fully elucidated.

By mutating the homolog of α Phe 64 on the β subunit, i.e. β Tyr 62, Newell *et al.* (2000) abrogated [^{3}H]-muscimol binding. This led to the suggestion that the high affinity binding site might lie at the α-β interface, while the low affinity sites are at the β-α interfaces. Further work with this mutant suggested that the former site may have an additional role in stabilizing the desensitized state of the receptor (Newell *et al.*, 2000).

Channel Opening and Gating

Ligand binding to the N-terminal domain of the $GABA_AR$ is postulated to trigger a rotation of part of the extracellular domain of the subunits that leads to a rotation of the TM2 domain and causes the pore to open (Unwin, 1995), which allows ions to flow through the channel. These structural movements in the channel are referred to as 'gating', which appears to be required for receptor activation (Miyazawa *et al.*, 2003) and are the events that occur downstream from ligand binding which cause the channel to open. Some residues that are involved in the GABA binding site also appear to be involved in gating. Using SCAM analysis, Boileau *et al.* (2002a) showed that Tyr 97 and Leu 99 of the β subunit line the binding pocket of the receptor and also that mutation of Leu 99 could led to receptors that open spontaneously. This suggests a link between binding and gating, possibly through some allosteric effect. The same type of action was seen with the $GABA_CR$ ρ1 subunit when Tyr 102 was mutated (Torres & Weiss, 2002).

This residue was identified as a component of the GABA binding domain and, when mutated to serine, appeared to cause spontaneous channel openings (Torres & Weiss, 2002).

The TM2 domain has been shown to contain most of the amino acid residues lining the ion channel (Xu & Akabas, 1996). Use of SCAM confirmed that TM2 lines the channel pore of the nAChR, $5HT_3R$ and $GABA_AR$ (Xu & Akabas, 1993; Akabas *et al.*, 1994; Xu & Akabas, 1996; Reeves *et al.*, 2001) and identified that approximately every third amino acid was water accessible, which corresponds to α-helical turns of the protein. However, amino acid residues in the TM1 (Akabas & Karlin, 1995) and the cytoplasmic loop between TM1 and TM2 have also been suggested to make up part of the ion-conducting pathway (Imoto *et al.*, 1988). The channel gate would likely be located somewhere along the ion channel pore so that when closed it would inhibit the flow of ions. It has been suggested that ACh binding to the binding pocket induces changes in the conformation of the α subunits and that this change is transmitted to the TM domain by a rotation of the α subunits (Unwin *et al.*, 2002).

The 9' position of TM2 contains a highly conserved leucine ring found in nAChRs, $GABA_ARs$, glycine receptors and $5HT_3Rs$ and is postulated to be located near the middle of the pore region. If this leucine is replaced with a serine or threonine, the open state of the receptor seems to be more stable, either in the presence or absence of agonist (Revah *et al.*, 1991; Yakel *et al.*, 1993; Tierney *et al.*, 1996; Shan *et al.*, 2003). These groups have observed a decrease in the rate of desensitization and an apparent increase in ligand affinity when leucine is mutated to serine or threonine in all members of the cys-loop LGIC superfamily. Chang & Weiss (1998) showed that when this leucine

was mutated to alanine, glycine, serine, threonine, valine or tyrosine, $GABA_CRs$ had a larger resting conductance than wild type receptors, pointing to these receptors being open more often than wild type in the absence of ligand.

Unwin had suggested that these leucines make up the nAChR channel gate by interacting with each other to form a constriction in the channel when closed (Unwin, 1995). An alternative view, based on the observation of the effects of these leucines on channel desensitization, is that the leucines block the channel when it enters desensitization (Revah *et al.*, 1991) and therefore contribute to the desensitized state. While investigating another pore-domain residue, Ser 270 at the 15' position, along with the leucine at position 9', Scheller & Forman (2002) suggested that the structures that dictate gating and desensitization are distinct. This conclusion was based on the observation that mutating Ser 270 to isoleucine did not affect the desensitization rate of this receptor compared to wild type, but reduced the GABA EC_{50}. In comparison, mutating the leucine to threonine both reduced the GABA EC_{50} and reduced the rate of desensitization. Therefore, it appears that the role of the 9' leucines on channel gating may be distinct from desensitization.

Using SCAM, accessibility of the closed channel was shown to be deeper than the middle of TM2 of the nAChR (Akabas *et al.*, 1992). Gly 240, Glu 241 and Lys 242 of the TM1-TM2 loop and Met 243 and Thr 244 of the intracellular end of TM2 of the α subunit were inaccessible when the channel was closed but became accessible in the presence of ACh (Wilson & Karlin, 1998). This corresponds to the proposal of Akabas and colleagues (1992, 1994) that the channel gate is close to the intracellular end of TM2. The channel gate has been postulated to begin on the cytoplasmic side of the TM pore

and extend into the short TM1-2 cytoplasmic loop (Keramidas *et al.*, 2000; Gunthorpe & Lummis, 2001; Wilson & Karlin, 2001; Jensen *et al.*, 2002).

Regions of the TM2 and the TM2-TM3 linker are also implicated in the rate of ion transport through the $\alpha1\beta1\gamma\delta$ nAChR (Imoto *et al.*, 1988). Investigation of channel gating of neuronal AChR implicated Asp 266 of the $\alpha7$ TM2-TM3 loop and the homologous residue in $\beta4$, Asp 268, in coupling binding to gating (Campos-Caro *et al.*, 1996).

The TM2-TM3 linker has also been identified in both $GABA_AR$ and $GABA_CR$ as having a role in channel gating. An arginine residue in this loop of the $\rho1$ receptor, when mutated to an alanine, increased the open probability of the channel. This suggests that this residue may be involved in channel gating (Kusama *et al.*, 1994). Using SCAM on amino acid residues between the TM2 and TM3 of $\alpha1\beta2\gamma2s$ $GABA_ARs$ in both the presence and absence of GABA, Bera *et al.* (2002) concluded that this region undergoes a conformational change during channel activation.

Kash *et al.* (2003) further implicated the TM2-TM3 linker in ion conductance, as well as Asp 57 and Asp 149 in the extracellular loops 2 and 7 of the N-terminal ligand binding domain of the $GABA_AR$. During the process of gating, this group postulated that the positively charged lysine 279 of the TM2-TM3 linker and the negatively charged Asp 149 become closer (Kash *et al.*, 2003). This was introduced as a possible way in which ligand binding might affect the opening of the ion channel.

In the same year, Miyazawa *et al.* (2003) introduced the 'pin and socket' model of TM2-TM3 loop interaction with the extracellular N-terminal domain of the nAChR. This involves Val 44 of the $\alpha1$ subunit in loop 2 of the extracellular ligand binding domain

interacting with a hydrophobic pocket between Ser 269 and Pro 272, both of the α1 subunit, on the TM2-TM3 linker. Ligand binding is thought to cause a rotation of the TM2 domain of the receptor subunits. This interaction of Val 44 with the TM2-TM3 linker is postulated to cause the rotation in the TM2 domain that leads the channel gate opening (Miyazawa *et al.*, 2003) (see Figure 1-7). Although this appears as an unlikely interaction due to the hydrophobic side chain of valine, the authors postulated that valine interacts with a hydrophobic pocket at the N-terminal end of TM2. Lee & Sine (2005) further identified Arg 209 and Glu 45 from the N-terminal domain as residues that may play a role in linking the ligand binding domain with the channel. This was postulated as a way in which the ligand binding domain may interact with the channel to lead to the opening of the integral channel pore (Lee & Sine, 2005).

Recently, another amino acid residue on the loop between TM2 and TM3 of the $5HT_{3A}R$ has been investigated for its possible role in linking binding to gating. This residue is at the apex of this loop and is referred to as Pro 8' (Lummis *et al.*, 2005a). By replacing this proline with unnatural analogues of proline, this group showed that only the analogues that can undergo cis-trans isomerization, as proline can, produced functional receptors. The receptors composed of proline derivatives that could not undergo cis-trans isomerization could still be expressed. Replacing Pro 8' with analogues that prefer the cis conformation produced receptors that were more sensitive to serotonin than wild type receptors. This lead to the conclusion that ligand binding would cause a trans to cis isomerization of Pro 8' that could translate to a movement of TM2 and lead to channel opening (Lummis *et al.*, 2005a). However, based on the longer time scale required for a cis-trans isomerization compared to that of gating, it is unlikely that

this is a mechanism for gating. Also, while this Pro 8 is conserved in $5HT_3$Rs and nAChRs, it is not present in $GABA_A$Rs, and therefore can play no role in $GABA_A$R gating.

It appears that there is an interaction between the N-terminal ligand binding domain and the TM2-TM3 loop of both $GABA_A$Rs and nAChRs, which offers an explanation for the linkage between ligand binding and channel gating.

Multiple conductance states

Single channel recordings of a receptor capture the activity of a single receptor passing current by the opening and closing of its integral ion channel pore. Inspection of single channel recordings, however, shows current levels that fall intermediate to the channel being fully open or fully closed, suggesting that there are transitions between the full open and closed state of the receptor (see Figure 1-8). These intermediate single channel currents are often referred to as the sub-conductance states of a receptor.

Fox (1987) established a set of criteria to distinguish substates (sub-conductance currents) of a channel from currents originating in other distinct channels recorded in the same patch. This includes transitions between the states, which can often be seen during bursting activity. Furthermore, the consistent occurrence of all of the conductance states in the same patches and the observation of the lesser conductance currents only in the presence of the main conductance current supports the proposition that the two are produced by the same channel and are not the product of independent channels. Additionally, if more than one channel were present in a patch, currents would summate.

Therefore, by applying these criteria for channel substates, it should be possible to determine whether sub-conductance currents are substates of a single channel.

$GABA_AR$ single channel activity often exhibits multiple conductance currents. Miledi *et al.* (1983) suggested the existence of at least two conductance states for both the $GABA_AR$ and the nACh receptor, while Hamill *et al.* (1983) described two conductance states at 30 pS and 19 pS for the $GABA_AR$. Since then, sub-conductance states have been reported in single channel recordings from neuronal preparations (Bormann *et al.*, 1987; Bormann & Kettenmann, 1988; Mathers *et al.*, 1989; Mistry & Hablitz, 1990; Newland *et al.*, 1991) as well as in recombinant expression systems (Verdoorn *et al.*, 1990; Fisher & Macdonald, 1997), with little additional comment as to mechanism.

Some have proposed that these states may be due to the cooperative openings of additional distinct channels in the patch. Kaneda *et al.* (1995) suggested that since the proportion of openings to each conductance level varied between patches of rat granule cells, the two conductance currents of $GABA_ARs$ might be due to the presence of two separate channels. However, being that channel opening is a stochastic process, it would be unexpected to see the exact same behaviour of a channel in every patch. Eghbali *et al.* (1997) observed multiple conductance currents from $GABA_ARs$ in rat hippocampal neurons, and the conductance level appeared to increase with an increase in GABA concentration alone or with GABA and diazepam. They concluded that these multiple currents were caused by either multiple conformations of the channel or the synchronous openings of a number of channels. Eghbali *et al.* (1997) favoured the latter explanation but did not support this conclusion. Outside-out patching of dopaminergic neuron slices and dissociated neurons yielded five conductance levels from the dopaminergic neurons

and six conductance levels from the dissociated neurons (Guyon *et al.*, 1999). An increase in concentration of isoguvacine ($GABA_AR$ agonist) or zolpidem (which binds to the benzodiazepine site) in the presence of isoguvacine, increased the number of openings to the high conductance levels and decreased the number of smaller conductance level openings. The opposite was seen in the presence of Zn^{2+}. Again it was discussed that these multiple conductance levels were either the product of variable conformational states of the receptor or due to the synchronous openings of $GABA_AR$ clusters in the membrane patched. However, since direct openings to the highest conductance level were observed, the authors concluded that they could not be caused by sequential binding of the receptor and, coupled with the observation of five or six conductance levels, there are not enough conventional ligand binding sites to accommodate a model like this. Also, the conductance values Guyon *et al.* (1999) reported were multiples of 3-5 pS and the highest conductance value varied between patches. This further convinced them that they were observing the synchronous openings of multiple channels. However, the difference of 3-5 pS is close to the bandwidth of open channel noise, and one might question the validity of differentiating a level at 4 pS from a level at 7 pS. Also, in the same paper, with the use of single cell reverse transcriptase polymerase chain reaction, they reported the presence of multiple subtypes of multiple subunits. Therefore, in a heterogenous population of receptors, one would expect to record different results from different types of $GABA_ARs$.

Bormann & Clapham (1985) argued that the bursting behaviour exhibited by the channel indicates that the multiple conductance states are true states of a single channel and not multiple channels within a single patch. Bursting behaviour does satisfy one of

Fox's (1987) requirements for a channel substate in that it demonstrates transitions between conductance states. They also observed these direct transitions between conductance states with the glycine receptor and drew the same conclusion (Bormann *et al.*, 1993).

Other groups have not analysed the subconductance currents since the full-conductance current is the predominant conductance event (Newland *et al.*, 1991; Twyman & Macdonald, 1992; Mortensen *et al.*, 2004). From published sample traces, it appears as though sub-conductance currents are seen more often that the suggested 5% of the time (Mortensen *et al.* 2004), although it may be true that more than 90% of the chloride current is carried across the membrane through the main conductance state.

The presence of multiple conductance states is not just an anomaly of $GABA_A$Rs. Glycine receptors have often been reported to exhibit multiple conductance states (Bormann *et al.*, 1993; Grewer, 1999; Moorhouse *et al.*, 2002), as have nAChRs (Mathie *et al.*, 1991; Lewis *et al.*, 1997). Multiple conductance currents have also been observed in single channel recordings from receptors as diverse as acid sensing ion channels (Zhang & Canessa, 2002), serotonergic dorsal raphe potassium channels (Penington *et al.*, 1993), kainate-type glutamate receptors (Smith *et al.*, 1999; Smith & Howe, 2000), N-methyl-D aspartate (NMDA) type glutamate receptors (Cheffings & Colquhoun, 2000; Wyllie *et al.*, 2006), α-amino-3-hydroxy-5-methyl-4-isoxazolepropionic acid (AMPA) type glutamate receptors (Banke *et al.*, 2000; Smith & Howe, 2000; Smith *et al.*, 2000), vanilloid receptors (Premkumar *et al.*, 2002), ryanodine receptors (Lokuta *et al.*, 2002), P2X ATP receptors (Whitlock *et al.*, 2001) and voltage-gated drk1 potassium channels (Chapman *et al.*, 1997).

Chapman *et al.* (1997) suggested that the subconductance states they observed during drk1 potassium channel activity were related to the degree of channel activation based on the open position of the subunits making up the channel. Based on Hodgkin and Huxley's prediction, the open probability of a potassium channel would be n^4, where n is the fraction of gates open (Hodgkin & Huxley, 1952), since all four subunits of the receptor would need to be in the proper activated position to open the channel. Chapman & VanDongen (2005) tested their hypothesis with the use of two constructs of the wild type drk1 channel, one that opens at normal voltages and has a large single channel conductance (drk1-L) and one that opens at positive potentials and has the normal drk1 single channel conductance (drk1-S). After characterizing both constructs, a tandem dimer of the two constructs was created and the channel kinetics of this dimer led the authors to conclude that the sub-conductance states are a result of transient heterometric conformations of the pore where some, but not all, of the subunits are in their open, activated state (Chapman & VanDongen, 2005).

Cloues & Sather (2000) came to the same type of explanation to explain the various conductance currents observed in single channel recordings of L-type Ca^{2+} channels expressed in *Xenopus* oocytes. They investigated the conductance events using Ca^{2+}, Ba^{2+} and Li^{+} as the permeating ion and concluded that the various conductance states were caused by nonequivalent channel activation (Cloues & Sather, 2000). The multiple conductance states of ryanodine receptors have been investigated using a number of different ligands to activate the channel. Quinidine appeared to induce sub-conductance events, which led the authors to suspect that this compound was responsible for the sub-conductance currents by partially occluding the pore of the channel (Tsushima

et al., 2002). Ryanodine (Lokuta *et al.*, 2002) and 8β-amino-9α-hydroxyryanodine (Tanna *et al.*, 2005) also induce two conductances states of the ryanodine receptor, which again are thought to be the effect of different gating states of the receptor. With NMDA receptors, application of the polyamines, spermine or arcaine, to the internal or external of hippocampal neurons or *Xenopus* oocytes clamped at -60 mV resulted in an approximately 50% reduction of the main conductance state (Araneda *et al.*, 1999). Polyamines are positively charged at physiological pH, therefore it is possible that they may reduce current by open channel block, in the same manner that Mg^{2+} and Zn^{2+} are thought to block NMDA receptors (Rock & Macdonald, 1992). With fast open channel block, it may not be possible to resolve the channel openings and closings, and therefore, there is only an apparent reduction in conductance. An alternative explanation is that the association of the polyamines in the receptor vestibule changes the energy barriers around the channel, thereby reducing the rate of ion passage. Regardless of mechanism, the polyamine reduction of NMDA receptor conduction points to the ability of the receptor to be occluded but still allow the partial movement of ions and suggests that the channel can adopt partially activated states.

From the observation that bovine nAChRs had smaller conductance currents than *Torpedo* nAChRs, Imoto *et al.* (1988) were able to determine that this difference was due to the δ subunit. Chimeras of this subunit from the two species were made and the authors identified a portion of the TM2 domain and a region between TM2 and TM3 as having a role in the conductance of the nAChRs. Mutating regions near the TM2 domain have been shown to change the channel conductance and have been attributed to being a determinant in channel conductance (Imoto *et al.*, 1988). With the glycine receptor, the

mutation of a single amino acid in the TM2 domain of the α1 homo-oligomer resulted in single channel main state conductance that resembled both α2 and α3 homo-oligomers (Bormann *et al.*, 1993). The authors concluded that this amino acid of the TM2 domain was important for main state conductance. This suggests that, for the LGICs, the TM2 domain and neighbouring regions between TM1-TM2 and TM2-TM3 may be regions that influence the conductance of the channel.

Amino acid residues in the M3-M4 intracellular loops have been implicated in determining the single channel conductance of the $5HT_3$Rs (Kelley *et al.*, 2003). The homo-oligomeric $5HT_{3A}$ receptor has a much lower single channel conductance than the hetero-oligometric $5HT_{3A/B}$ receptor (Davies *et al.*, 1999). The $5HT_{3A}$ subunit shows four conserved arginine residues within this M3-M4 loop, which are not seen in the $5HT_{3B}$ subunit. Point mutations of three of the four conserved arginine residues (432, 436 and 440) to the residues aligned in the $5HT_{3B}$ receptor sequence greatly increased the single channel conductance of the channel (Kelley *et al.*, 2003). Based on the electron microscopy images of the nAChR, these residues are part of the intracellular vestibule (Miyazawa *et al.*, 1999). It is not surprising that regions of the TM3-4 intracellular loop of the $5HT_3$R play a role in determining the magnitude of conductance since the ions must flow through this structure to enter the cytoplasm of the cell from the intracellular vestibule of the receptor. The size of these portals as depicted from the electron structure (Miyazawa *et al.*, 1999) would require the ions to interact with some of the amino acid residues within this region of the protein, and thus it appears that certain amino acid residues will either facilitate or hinder the movement of ions. It might be possible that the rotation of TM2 induced by ligand binding may cause changes in the TM3 domain,

which led to changes at the level of the intracellular vestibule. However, it is still not entirely clear how the conductance of the cys-loop LGICs are regulated, nor how the multiple conductance currents are achieved.

Desensitization

If $GABA_A$Rs experience prolonged or repeated exposure to agonist, the amount of current flowing through the receptor will decrease over the time of exposure. This decay of current in the presence of agonist infers a different state of the receptor referred to as desensitization. This state was first studied on nAChR at frog muscle end plates by Katz & Thesleff (1957). They noted that desensitization occurred within seconds of applying agonist to the tissue and recovered within seconds of removing agonist. This work led the authors to propose a cyclic kinetic model where agonist can bind to either an effective or refractory form of the receptor, but the agonist's affinity for the refractory form is higher. Although highly characterized, desensitization is still not fully understood. The exponential decay of current is often multiphasic. This has been explained by some groups as distinct populations of receptors that desensitize at different rates (Cash & Subbarao, 1987b) by entering different desensitized states. Since this work was done in synaptoneurosomes, many types of $GABA_A$Rs could have been present and may explain these results. Using hippocampal neurons and designing an experiment such that saturating GABA was briefly applied to cells, then a brief second application was preceded by a short wash out period, Celentano & Wong (1994) concluded that the desensitization response was likely from a single population of receptors since a portion of the receptors would still be desensitized from the first GABA application and yet the

second application of GABA still led to multiphasic desensitization (Celentano & Wong, 1994).

As is true of agonist intrinsic activity and affinity, the specific subunits that make up a $GABA_AR$ also influence the desensitization kinetics of that receptor. $\alpha1\beta2\gamma2$ receptors show a rapid phase of desensitization followed by a slower phase which leads to a steady state response where desensitization is never complete (Tia *et al.*, 1996). In contrast, receptors constructed with a δ subunit desensitize with a single exponential of decay (Bianchi *et al.*, 2001). Using chimeras and point mutations of the γ subunit and δ subunit, Bianchi *et al.* (2001) identified the N-terminal domain and two residues in the TM1, Val 233 and Tyr 234, of the γ subunit as having a role in the fast component of desensitization. Replacing these regions with the equivalent residues in the δ subunit resulted in receptors whose desensitization resembled that of δ containing receptors. This work also suggested that the TM2 domain does not play an important role in the desensitization of the channel.

Bianchi & Macdonald (2002) compared the rates of desensitization with various application systems for GABA in both whole cells and excised patches. The perfusion systems varied in their rate of delivery of GABA, and the quicker the exchange of recording buffer with agonist, the more rapid the fast component of desensitization appeared, along with the contribution of this component. Of all the systems that were tested, excised patches achieved the quickest rise times of current and the proportion of the fast desensitization component compared to the slow desensitization component was highest (Bianchi & Macdonald, 2002). This likely corresponds to the degree of desensitization that is apparently lost within the signal rise time when drug application is

slow. Recording the desensitization of excised patches expressing $\alpha1\beta3\gamma2$ $GABA_A$Rs, Bianchi & Macdonald (2002) identified four phases of desensitization, fast, intermediate, slow and very slow. Regardless of whether two (Tia *et al.*, 1996), three (Haas & Macdonald, 1999) or four (Bianchi & Macdonald, 2002) phases of desensitization were reported, the multiphasic behaviour of desensitization suggests that there are various states of the receptor that lead to multiple desensitized states (Celentano & Wong, 1994). Whether these desensitized states are controlled at the level of the channel gate or are different conformations of the receptor is not clear at this time (Bianchi & Macdonald, 2002).

Desensitization also shows a degree of concentration-dependence. The fast phase of desensitization is not usually observed at concentrations less than the half maximal concentration for GABA activation (Dominguez-Perrot *et al.*, 1996). This points to a low affinity site on the receptor that leads to the fast phase of desensitization. However, the rate of the fast desensitization phase is not dependent on agonist concentration (Celentano & Wong, 1994; Dominguez-Perrot *et al.*, 1996). Dominguez-Perrot *et al.* (1996) postulated that this phase of desensitization might be achieved from the open fully liganded state of the receptor. Celentano & Wong (1994) showed, though, that a prepulse of a low concentration of GABA could eliminate the fast phase of desensitization of a secondary pulse of saturating GABA, suggesting that the receptor has both high and low affinity sites that mediate the desensitized states. This group also concluded that with low GABA concentrations the association of GABA to the receptor would be slow. Therefore, the fast phase of desensitization would have occurred before the peak activation response was achieved, making the fast desensitization phase immeasurable

(Celentano & Wong, 1994). Dominguez-Perrot *et al.* (1996) showed that the rate of the slow desensitization component is dependent upon agonist concentration, which led them to suggest that this state is achieved through the fully liganded but closed receptor. This is in contrast to the model published by Jones & Westbrook (1995) where so called mono-liganded receptors activate to a brief open state then desensitize to a long desensitized state while purported bi-liganded receptors enter a longer open state leading to a rapid entry into a desensitized state (Jones & Westbrook, 1995) (see Figure 1-9). Bai *et al.* (2001) also proposed a model involving both mono- and di-liganded states of the receptor to explain tonic and phasic post-synaptic currents. In this model, the mono-liganded state opens to a low conductance state which does not desensitize while the di-liganded state could desensitize with either a fast or slow entry into the desensitized states or this agonist bound state could led to an open state (Bai *et al.*, 2001) (see Figure 1-9). Therefore, the Jones & Westbrook (1995) and Bai *et al.* (2001) models differed in the origin of the state leading to desensitization.

While it appears that there are different states of receptor desensitization, the question arises as to the physiological significance of these states. Desensitization has often been considered a negative feedback mechanism that reduces the peak amplitude of inhibitory post synaptic currents (IPSCs). This was questioned by Jones & Westbrook (1995), who suggested that the fast component of desensitization may reduce the rate that GABA unbinds from the receptor and therefore may increase the duration of IPSC. The slow desensitized state is thought to have less physiological significance (Dominguez-Perrot *et al.*, 1996), although this phase may be important when the receptor is activated repetitively (Bianchi & Macdonald, 2002).

Expression Systems

Recombinant expression systems are a convenient means of expressing specific receptor subtypes. As opposed to the use of native cultures, the particular $GABA_AR$ of interest can be limited by the expression of particular subunit cDNA or RNA. Human embryonic kidney cell line number 293 (HEK293) and *Xenopus laevis* oocytes are common platforms for receptor expression. HEK293 cells have the advantage of being a resilient cell line that is easily transfected using the calcium phosphate mediated gene transfer technique. HEK293 cultures are often used for both whole cell and single channel patch clamp experiments. *Xenopus* oocytes have been used as an expression system since the early 1970s (Gurdon *et al.*, 1971). Since these oocytes have too large a space constant for single electrode clamping, two electrode voltage clamping is used to measure currents from eggs which have had their follicle cell layer removed. Also, if the vitelline membrane is removed from an oocyte, which renders the egg much more fragile, single channel recordings can be made.

One of the biggest drawbacks of these types of expression systems is the presence of endogenous channels. In oocytes that have had their follicle layer removed this is not of great concern since the *Xenopus* oocyte has few endogenous ion channels although they do express stretch receptors. This is more problematic when working with HEK293 cultures. Endogenous voltage-gated K^+ channels (Yu & Kerchner, 1998) and Ca^{2+} channels (Berjukow *et al.*, 1996) have been identified, along with a proton-gated acid sensing ion channel (Gunthorpe *et al.*, 2001). Therefore, endogenous channels must be characterized before single channel patch clamping results of channels transiently

expressed in HEK293 can be attributed to the transfected protein. Also, a holding potential can be chosen that ensures voltage-gated channel inactivation or deactivation.

Aims of the Present Study

The following studies were aimed at investigating the nature and agonist dependence of the activated states of the $GABA_AR$. Previous studies had identified multiple conductance states of the receptor, but few have investigated these states. Since $GABA_ARs$ normally require agonist binding for activation (the observation of unliganded openings has been observed), and the fact that various amplitudes of current flow through the receptor, we suggest that these sub-conductance states are achieved through differentially bound and activated forms of the receptor. Chapter 3 investigates all of the conductance states of the most common $GABA_AR$ ($\alpha1\beta2\gamma2$) using single channel inside-out patch clamping. The goal was to determine the number of conductance states that could be differentiated, and how they were influenced by the concentration of GABA. We investigated the changes in the frequency and proportion of the conductance states and the open time duration at different concentrations of GABA in an effort to understand the concentration-dependent differences in the behaviour of a single channel with its endogenous ligand.

This work was extended in Chapter 4 to consider how these parameters change when the $GABA_AR$ is activated by partial agonists. The two compounds we chose to investigate were THIP and P4S. Both of these drugs are partial agonists at this particular $GABA_AR$ construct and have more rigid chemical structures compared to GABA. It was hypothesized that a compound with a rigid structure would inhibit the conformational

changes required within the receptor to achieve the fully activated state compared to GABA, and this could explain why these compounds have less intrinsic activity than GABA. Inside-out single channel recordings were made as described in Chapter 3, this time using THIP or P4S as the agonist. Frequency of opening to each conductance state was measured in the same way as above, as was the open duration. These parameters were compared to those which were obtained when the receptor was activated by GABA.

If the results we observed with the single channel studies can be explained by differential binding of agonists to multiple binding sites on the receptor, then by simultaneously occupying two binding sites, we may expect to observe a change in the channel activity. In an attempt to achieve this situation, we employed the use of polymethylene digabamides. These are compounds composed of two GABA moieties separated by a variable chain length. Since both ends of these compounds could potentially bind to distinct sites on the $GABA_AR$, they are referred to as bisfunctional ligands. It may be possible to determine the optimal chain length separating the two functional groups by considering changes in the activity of $GABA_ARs$ in the presence of the various compounds and therefore postulate the relative distance between two binding sites. Of most interest initially was butylene digabamide, since ion flux experiments of mouse synaptosomes suggested that this compound was a "superagonist" compared to GABA (Carlier *et al.*, 2002). A series of polymethlyene digabamide compounds was investigated using the whole cell patch clamp configuration. All of these compounds were partial agonists at the $\alpha1\beta2\gamma2$ $GABA_AR$ and showed lower potency than GABA. However, a dramatic change in the desensitization kinetics was observed. Since

desensitization is a behaviour of bound receptors, this was further investigated in an attempt to correlate agonist chain length with binding and binding with desensitization.

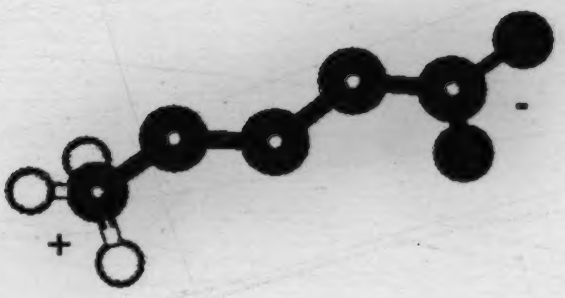

Figure 1-1: The structure of GABA. GABA is zwitterionic (having both a positive and negative charge) with an isoelectric point at physiological pH. At physiological pH, GABA is electroneutral.

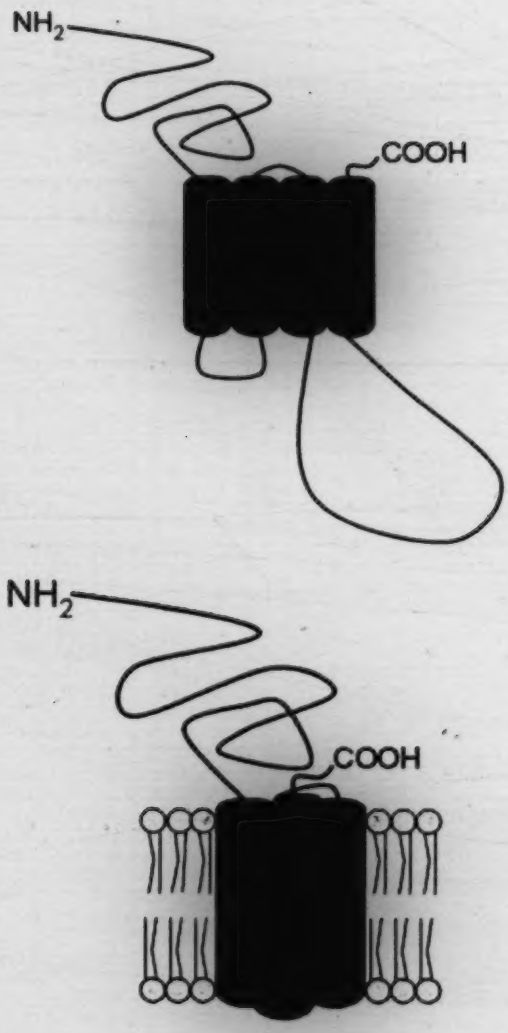

Figure 1-2: Model of a $GABA_AR$ subunit. Each subunit is composed of an extracellular amino-terminal domain, four membrane spanning regions (numbered above 1-4) and a short carboxy-terminal domain. Short loops connect the adjacent membrane spanning regions to each other. Between the third and four transmembrane domains this region is longer. The top image shows the transmembrane domains side by side, while the bottom image depicts their arrangement in a lipid membrane.

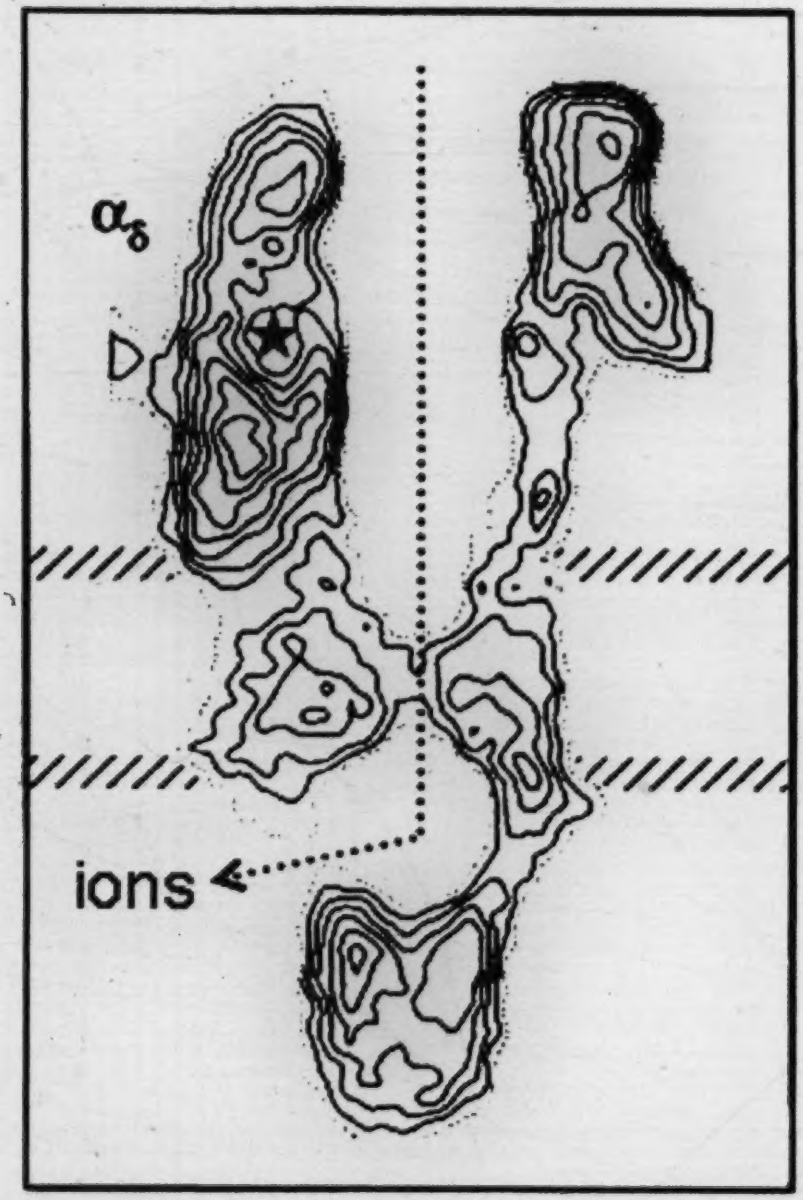

Figure 1-3: Cross section of a nAChR. The cryo-electron microscopy at 4.6 Å resolution of the *Torpedo* nAChR illustrates the large extracellular vestibule and smaller intracellular vestibule. The putative ACh binding pocket is shown with a red star. The postulated route of ion flow is depicted with a dashed line. Image modified from Miyazawa et al. (1999).

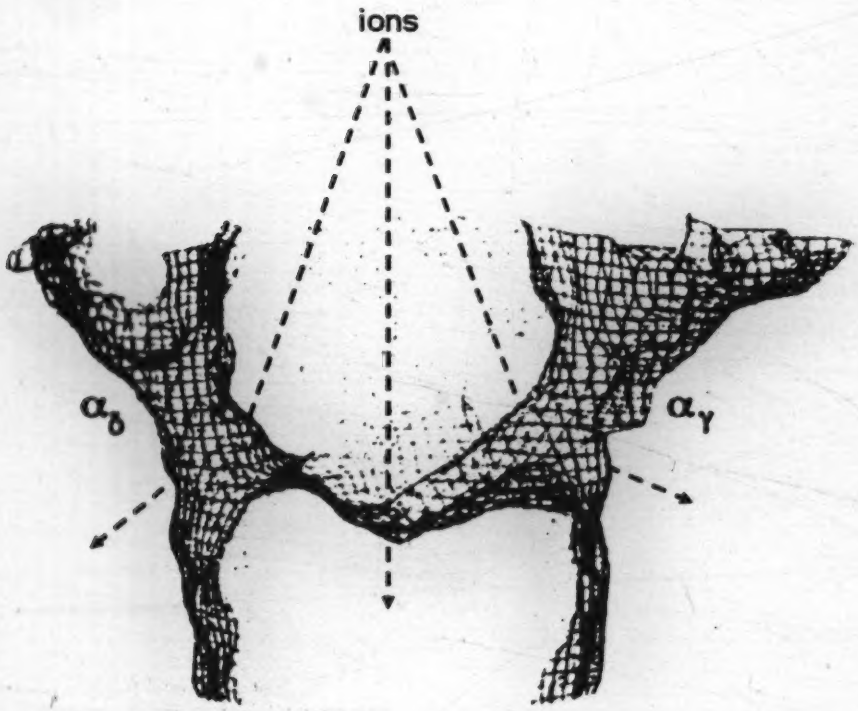

Figure 1-4: View of the cytoplasmic section of a nAChR achieved through cryo-electron microscopy. Image modified from Miyazawa et al. (1999). The section in blue illustrates the inverted cone formed by the cytoplasmic regions of the subunits coming together at the intracellular surface of the receptor. The dashed line represents the paths ions could travel to exit the internal vestibule.

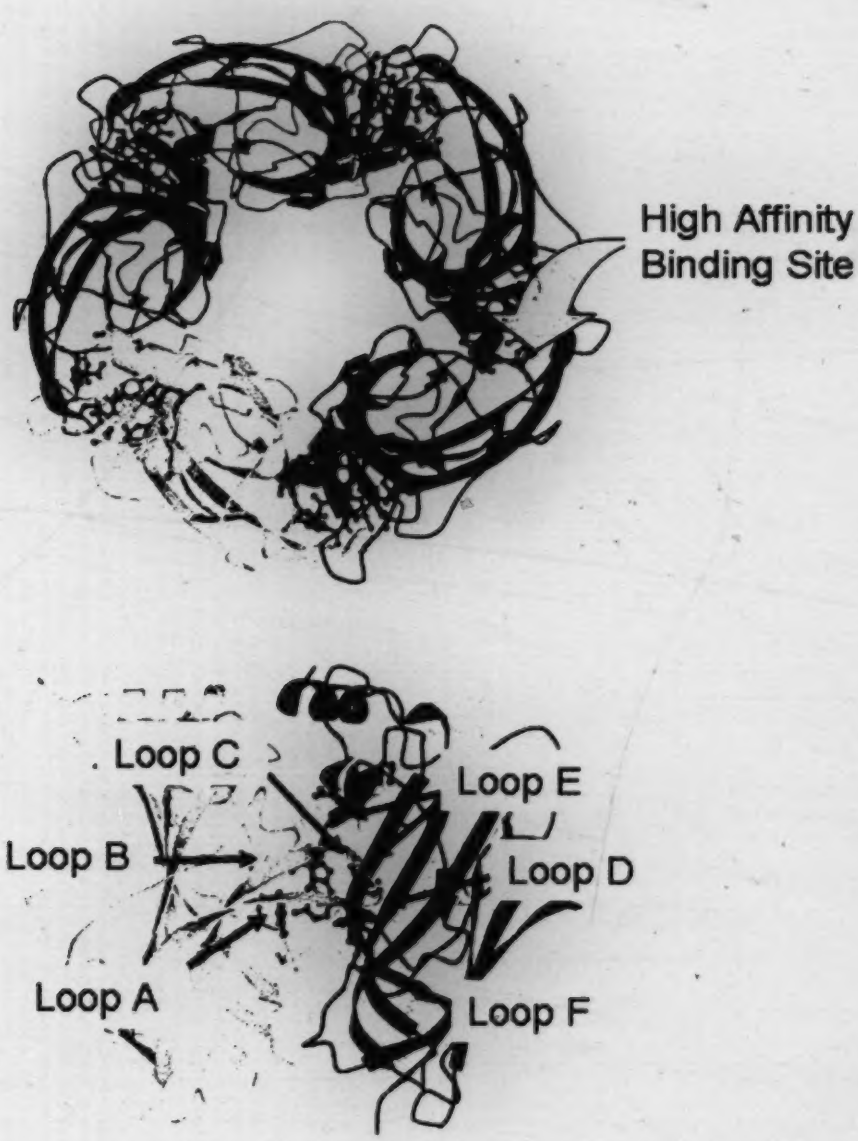

Figure 1-5: Crystal structure of AChBP at 2.7 Å. Top: View looking down on the protein shows the arrangement of five subunits with ligand binding occurring at each of the subunit interfaces. The blue arrow depicts one of these sites. Bottom: Cross sectional view of the protein illustrating one subunit in yellow and a second in blue. This depicts the ligand interaction with the two subunit interfaces. Image modified from Brejc et al. (2001).

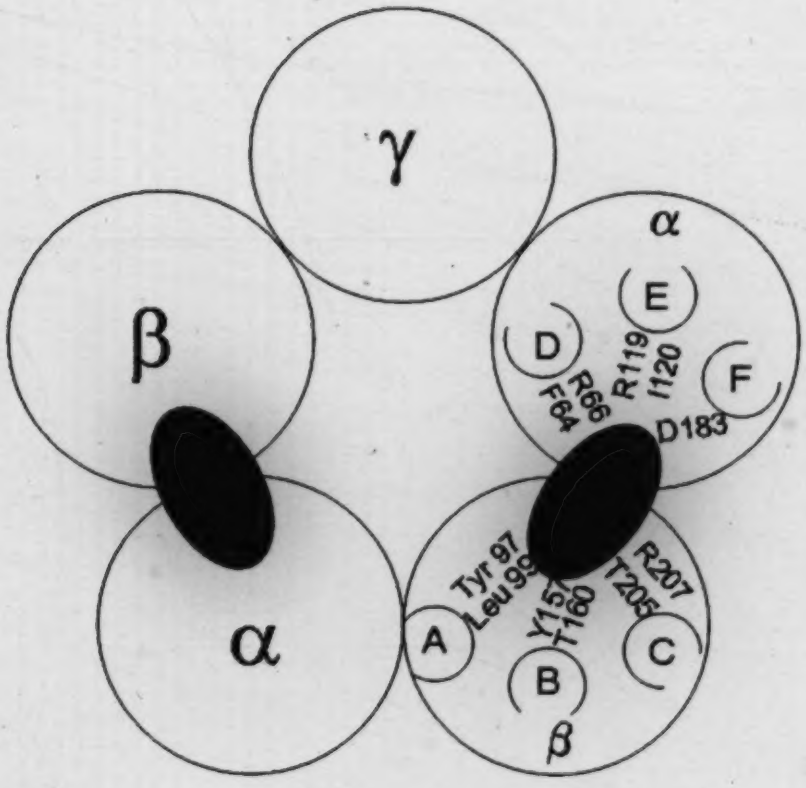

Figure 1-6: A model of the five subunits in the most common type of $GABA_AR$. The classical GABA binding pockets are located at the β-α interfaces. Specific amino acid residues thought to contribute to the binding pocket are highlighted above. References to each are available in the text (see Chapter 1). The β subunit contributes residues from loops A, B and C while the α subunit contributes residues from loops D, E and F.

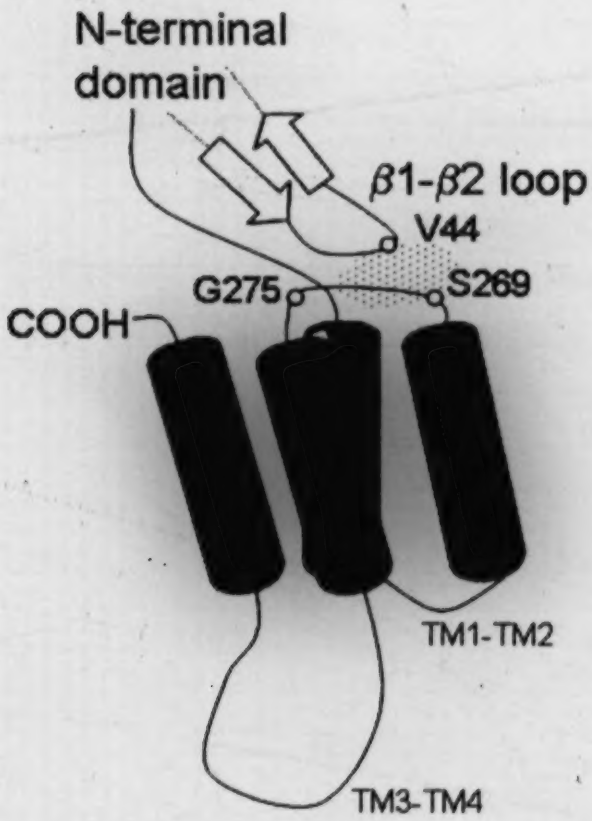

Figure 1-7: Model of nAChR gating. Cartoon version of the 'pin and socket' model of nAChR gating proposed by Miyazawa et al. (2003). This model involves Val 44 from an extracellular domain loop, the β1-β2 loop (also called loop 2) interacting with a hydrophobic region between Ser 269 and Pro 272 on the TM2-TM3 linker. This interaction is thought to cause a rotation of the subunit that leads to the central ion pore opening.

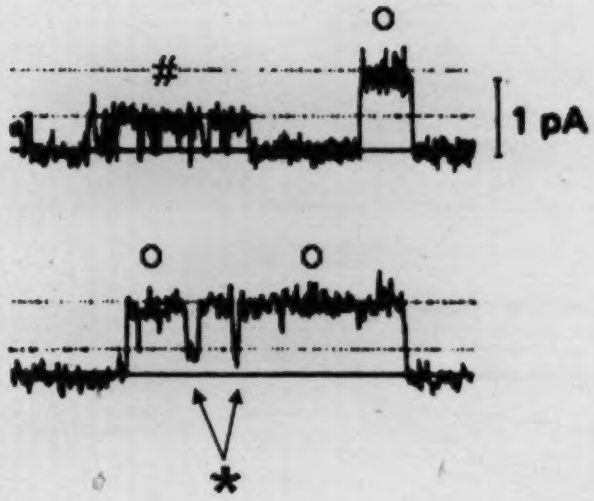

Figure 1-8: Multiple conductance states of $GABA_AR$. Modified from Bormann et al. (1987). Single channel recordings from cell attached patches of mouse spinal cord neuron soma illustrate two conductance levels of a GABA activated channel. Openings to the full-conductance level (o) and sub-conductance level (#) are evident in the top panel, while openings to the full-conductance level with closures to the sub-conductance level (*) are evident at the bottom.

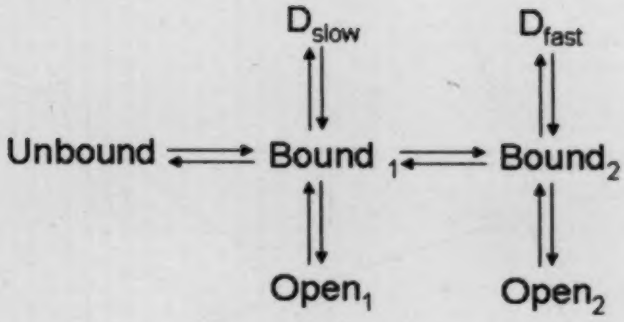

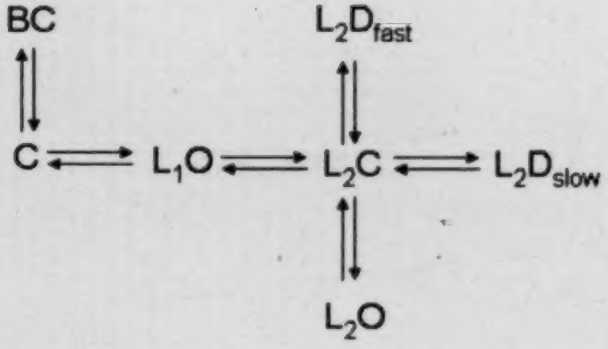

Figure 1-9: Models of channel activation and desensitization. Top panel is the Jones and Westbrook (1995) model and the bottom panel is the model proposed by Bai et al. (2001). Both describe a mono-liganded form of the receptor, denoted by the subscript 1, and a di-liganded states of the receptor, subscript 2. D refers to desensitized states of the receptor while open and closed states of the receptor are denoted O and C respectively. Ligand bound states are identified by L and Bound. BC refers to a bicuculline bound state of the receptor. These models are described in further detail in the text (see Chapter 1).

Bibliography

Abramson SN, Culver P, Kline T, Li Y, Guest P, Gutman L & Taylor P. (1988). Lophotoxin and related coral toxins covalently label the alpha-subunit of the nicotinic acetylcholine receptor. *J Biol Chem* **263,** 18568-18573.

Akabas MH & Karlin A. (1995). Identification of acetylcholine receptor channel-lining residues in the M1 segment of the alpha-subunit. *Biochemistry* **34,** 12496-12500.

Akabas MH, Kaufmann C, Archdeacon P & Karlin A. (1994). Identification of acetylcholine receptor channel-lining residues in the entire M2 segment of the alpha subunit. *Neuron* **13,** 919-927.

Akabas MH, Stauffer DA, Xu M, Karlin A. (1992). Acetylcholine receptor channel structure probed in cysteine-substituted mutants. *Science* **258**, 307-310.

Allan RD, Dickenson HW, Hiern BP, Johnston GA & Kazlauskas R. (1986). Isothiouronium compounds as gamma-aminobutyric acid agonists. *Br J Pharmacol* **88,** 379-387.

Alldredge BK & Lowenstein DH. (1999). Status epilepticus: new concepts. *Curr Opin Neurol* **12,** 183-190.

Amin J & Weiss DS. (1993). GABAA receptor needs two homologous domains of the beta-subunit for activation by GABA but not by pentobarbital. *Nature* **366,** 565-569.

Angelotti TP & Macdonald RL. (1993). Assembly of GABAA receptor subunits: alpha 1 beta 1 and alpha 1 beta 1 gamma 2S subunits produce unique ion channels with dissimilar single-channel properties. *J Neurosci* **13,** 1429-1440.

Araneda RC, Lan JY, Zheng X, Zukin RS & Bennett MV. (1999). Spermine and arcaine block and permeate N-methyl-D-aspartate receptor channels. *Biophys J* **76,** 2899-2911.

Arias HR. (1997). Topology of ligand binding sites on the nicotinic acetylcholine receptor. *Brain Res Brain Res Rev* **25,** 133-191.

Bai D, Zhu G, Pennefather P, Jackson MF, MacDonald JF & Orser BA. (2001). Distinct functional and pharmacological properties of tonic and quantal inhibitory postsynaptic currents mediated by gamma-aminobutyric acid(A) receptors in hippocampal neurons. *Mol Pharmacol* **59,** 814-824.

Banke TG, Bowie D, Lee H, Huganir RL, Schousboe A & Traynelis SF. (2000). Control of GluR1 AMPA receptor function by cAMP-dependent protein kinase. *J Neurosci* **20,** 89-102.

Barnard EA, Skolnick P, Olsen RW, Mohler H, Sieghart W, Biggio G, Braestrup C, Bateson AN & Langer SZ. (1998). International Union of Pharmacology. XV. Subtypes of gamma-aminobutyric acidA receptors: classification on the basis of subunit structure and receptor function. *Pharmacol Rev* **50,** 291-313.

Baumann SW, Baur R & Sigel E. (2002). Forced subunit assembly in alpha1beta2gamma2 GABAA receptors. Insight into the absolute arrangement. *J Biol Chem* **277,** 46020-46025.

Baumann SW, Baur R & Sigel E. (2003). Individual properties of the two functional agonist sites in GABA(A) receptors. *J Neurosci* **23,** 11158-11166.

Baur R & Sigel E. (2003). On high- and low-affinity agonist sites in GABAA receptors. *J Neurochem* **87,** 325-332.

Beene DL, Brandt GS, Zhong W, Zacharias NM, Lester HA & Dougherty DA. (2002). Cation-pi interactions in ligand recognition by serotonergic (5-HT3A) and nicotinic acetylcholine receptors: the anomalous binding properties of nicotine. *Biochemistry* **41,** 10262-10269.

Ben-Ari Y, Khazipov R, Leinekugel X, Caillard O & Gaiarsa JL. (1997). GABAA, NMDA and AMPA receptors: a developmentally regulated 'menage a trois'. *Trends Neurosci* **20,** 523-529.

Bera AK, Chatav M & Akabas MH. (2002). GABA(A) receptor M2-M3 loop secondary structure and changes in accessibility during channel gating. *J Biol Chem* **277,** 43002-43010.

Berjukow S, Doring F, Froschmayr M, Grabner M, Glossmann H & Hering S. (1996). Endogenous calcium channels in human embryonic kidney (HEK293) cells. *Br J Pharmacol* **118,** 748-754.

Bianchi MT, Haas KF & Macdonald RL. (2001). Structural determinants of fast desensitization and desensitization-deactivation coupling in GABAa receptors. *J Neurosci* **21,** 1127-1136.

Bianchi MT & Macdonald RL. (2002). Slow phases of GABA(A) receptor desensitization: structural determinants and possible relevance for synaptic function. *J Physiol* **544,** 3-18.

Blount P & Merlie JP. (1989). Molecular basis of the two nonequivalent ligand binding sites of the muscle nicotinic acetylcholine receptor. *Neuron* **3,** 349-357.

Boileau AJ, Baur R, Sharkey LM, Sigel E & Czajkowski C. (2002a). The relative amount of cRNA coding for gamma2 subunits affects stimulation by benzodiazepines in GABA(A) receptors expressed in Xenopus oocytes. *Neuropharmacology* **43,** 695-700.

Boileau AJ, Evers AR, Davis AF & Czajkowski C. (1999). Mapping the agonist binding site of the GABAA receptor: evidence for a beta-strand. *J Neurosci* **19,** 4847-4854.

Boileau AJ, Newell JG & Czajkowski C. (2002b). GABA(A) receptor beta 2 Tyr97 and Leu99 line the GABA-binding site. Insights into mechanisms of agonist and antagonist actions. *J Biol Chem* **277,** 2931-2937.

Boileau AJ, Pearce RA & Czajkowski C. (2005). Tandem subunits effectively constrain GABAA receptor stoichiometry and recapitulate receptor kinetics but are insensitive to GABAA receptor-associated protein. *J Neurosci* **25,** 11219-11230.

Bormann J & Clapham DE. (1985). gamma-Aminobutyric acid receptor channels in adrenal chromaffin cells: a patch-clamp study. *Proc Natl Acad Sci U S A* **82,** 2168-2172.

Bormann J, Hamill OP & Sakmann B. (1987). Mechanism of anion permeation through channels gated by glycine and gamma-aminobutyric acid in mouse cultured spinal neurones. *J Physiol* **385,** 243-286.

Bormann J & Kettenmann H. (1988). Patch-clamp study of gamma-aminobutyric acid receptor Cl- channels in cultured astrocytes. *Proc Natl Acad Sci U S A* **85,** 9336-9340.

Bormann J, Rundstrom N, Betz H & Langosch D. (1993). Residues within transmembrane segment M2 determine chloride conductance of glycine receptor homo- and hetero-oligomers. *Embo J* **12,** 3729-3737.

Bowery NG. (1993). GABAB receptor pharmacology. *Annu Rev Pharmacol Toxicol* **33,** 109-147.

Brejc K, van Dijk WJ, Klaassen RV, Schuurmans M, van Der Oost J, Smit AB & Sixma TK. (2001). Crystal structure of an ACh-binding protein reveals the ligand-binding domain of nicotinic receptors. *Nature* **411,** 269-276.

Bren N & Sine SM. (1997). Identification of residues in the adult nicotinic acetylcholine receptor that confer selectivity for curariform antagonists. *J Biol Chem* **272,** 30793-30798.

Campos-Caro A, Sala S, Ballesta JJ, Vicente-Agullo F, Criado M & Sala F. (1996). A single residue in the M2-M3 loop is a major determinant of coupling between

binding and gating in neuronal nicotinic receptors. *Proc Natl Acad Sci U S A* **93,** 6118-6123.

Carlier PR, Chow ES, Barlow RL & Bloomquist JR. (2002). Discovery of non-zwitterionic GABA(A) receptor full agonists and a superagonist. *Bioorg Med Chem Lett* **12,** 1985-1988.

Cash DJ & Subbarao K. (1987a). Channel opening of gamma-aminobutyric acid receptor from rat brain: molecular mechanisms of the receptor responses. *Biochemistry* **26,** 7562-7570.

Cash DJ & Subbarao K. (1987b). Desensitization of gamma-aminobutyric acid receptor from rat brain: two distinguishable receptors on the same membrane. *Biochemistry* **26,** 7556-7562.

Celentano JJ, Gibbs TT & Farb DH. (1988). Ethanol potentiates GABA- and glycine-induced chloride currents in chick spinal cord neurons. *Brain Res* **455,** 377-380.

Celentano JJ & Wong RK. (1994). Multiphasic desensitization of the GABAA receptor in outside-out patches. *Biophys J* **66,** 1039-1050.

Chang Y, Wang R, Barot S & Weiss DS. (1996). Stoichiometry of a recombinant GABAA receptor. *J Neurosci* **16,** 5415-5424.

Chang Y & Weiss DS. (1998). Substitutions of the highly conserved M2 leucine create spontaneously opening rho1 gamma-aminobutyric acid receptors. *Mol Pharmacol* **53,** 511-523.

Chapman ML & VanDongen AM. (2005). K channel subconductance levels result from heteromeric pore conformations. *J Gen Physiol* **126,** 87-103.

Chapman ML, VanDongen HM & VanDongen AM. (1997). Activation-dependent subconductance levels in the drk1 K channel suggest a subunit basis for ion permeation and gating. *Biophys J* **72,** 708-719.

Cheffings CM & Colquhoun D. (2000). Single channel analysis of a novel NMDA channel from Xenopus oocytes expressing recombinant NR1a, NR2A and NR2D subunits. *J Physiol* **526 Pt 3,** 481-491.

Cherubini E, Gaiarsa JL & Ben-Ari Y. (1991). GABA: an excitatory transmitter in early postnatal life. *Trends Neurosci* **14,** 515-519.

Chiara DC & Cohen JB. (1997). Identification of amino acids contributing to high and low affinity d-tubocurarine sites in the Torpedo nicotinic acetylcholine receptor. *J Biol Chem* **272,** 32940-32950.

Chiara DC, Middleton RE & Cohen JB. (1998). Identification of tryptophan 55 as the primary site of [^{3}H]nicotine photoincorporation in the gamma-subunit of the Torpedo nicotinic acetylcholine receptor. *FEBS Lett* **423,** 223-226.

Chiara DC, Xie Y & Cohen JB. (1999). Structure of the agonist-binding sites of the Torpedo nicotinic acetylcholine receptor: affinity-labeling and mutational analyses identify gamma Tyr-111/delta Arg-113 as antagonist affinity determinants. *Biochemistry* **38,** 6689-6698.

Cloues RK & Sather WA. (2000). Permeant ion binding affinity in subconductance states of an L-type Ca^{2+} channel expressed in Xenopus laevis oocytes. *J Physiol* **524 Pt 1,** 19-36.

Cohen JB, Sharp SD & Liu WS. (1991). Structure of the agonist-binding site of the nicotinic acetylcholine receptor. [^{3}H]acetylcholine mustard identifies residues in the cation-binding subsite. *J Biol Chem* **266,** 23354-23364.

Connolly CN, Krishek BJ, McDonald BJ, Smart TG & Moss SJ. (1996). Assembly and cell surface expression of heteromeric and homomeric gamma-aminobutyric acid type A receptors. *J Biol Chem* **271,** 89-96.

Craig AM, Banker G, Chang W, McGrath ME & Serpinskaya AS. (1996). Clustering of gephyrin at GABAergic but not glutamatergic synapses in cultured rat hippocampal neurons. *J Neurosci* **16,** 3166-3177.

Cromer BA, Morton CJ & Parker MW. (2002). Anxiety over GABA(A) receptor structure relieved by AChBP. *Trends Biochem Sci* **27,** 280-287.

Czajkowski C, Kaufmann C & Karlin A. (1993). Negatively charged amino acid residues in the nicotinic receptor delta subunit that contribute to the binding of acetylcholine. *Proc Natl Acad Sci U S A* **90,** 6285-6289.

Davidson, N. (1976). *Neurotransmitter amino acids*. Academic Press Inc., London.

Davies PA, Pistis M, Hanna MC, Peters JA, Lambert JJ, Hales TG & Kirkness EF. (1999). The 5-HT3B subunit is a major determinant of serotonin-receptor function. *Nature* **397,** 359-363.

Dennis M, Giraudat J, Kotzyba-Hibert F, Goeldner M, Hirth C, Chang JY, Lazure C, Chretien M & Changeux JP. (1988). Amino acids of the Torpedo marmorata acetylcholine receptor alpha subunit labeled by a photoaffinity ligand for the acetylcholine binding site. *Biochemistry* **27,** 2346-2357.

Dominguez-Perrot C, Feltz P & Poulter MO. (1996). Recombinant GABAA receptor desensitization: the role of the gamma 2 subunit and its physiological significance. *J Physiol* **497 (Pt 1),** 145-159.

Dougherty DA & Stauffer DA. (1990). Acetylcholine binding by a synthetic receptor: implications for biological recognition. *Science* **250,** 1558-1560.

Dunn SM & Raftery MA. (1997a). Agonist binding to the Torpedo acetylcholine receptor. 1. Complexities revealed by dissociation kinetics. *Biochemistry* **36,** 3846-3853.

Dunn SM & Raftery MA. (1997b). Agonist binding to the Torpedo acetylcholine receptor. 2. Complexities revealed by association kinetics. *Biochemistry* **36,** 3854-3863.

Eghbali M, Curmi JP, Birnir B & Gage PW. (1997). Hippocampal GABA(A) channel conductance increased by diazepam. *Nature* **388,** 71-75.

Ernst M, Bruckner S, Boresch S & Sieghart W. (2005). Comparative models of GABAA receptor extracellular and transmembrane domains: important insights in pharmacology and function. *Mol Pharmacol* **68,** 1291-1300.

Everitt AB, Luu T, Cromer B, Tierney ML, Birnir B, Olsen RW & Gage PW. (2004). Conductance of recombinant GABA (A) channels is increased in cells co-expressing GABA(A) receptor-associated protein. *J Biol Chem* **279,** 21701-21706.

Fisher JL & Macdonald RL. (1997). Single channel properties of recombinant GABAA receptors containing gamma 2 or delta subtypes expressed with alpha 1 and beta 3 subtypes in mouse L929 cells. *J Physiol* **505,** 283-297.

Fox JA. (1987). Ion channel subconductance states. *J Membr Biol* **97,** 1-8.

Galzi JL, Revah F, Black D, Goeldner M, Hirth C & Changeux JP. (1990). Identification of a novel amino acid alpha-tyrosine 93 within the cholinergic ligands-binding sites of the acetylcholine receptor by photoaffinity labeling. Additional evidence for a three-loop model of the cholinergic ligands-binding sites. *J Biol Chem* **265,** 10430-10437.

Grewer C. (1999). Investigation of the alpha(1)-glycine receptor channel-opening kinetics in the submillisecond time domain. *Biophys J* **77,** 727-738.

Grobin AC, Matthews DB, Devaud LL & Morrow AL. (1998). The role of GABA(A) receptors in the acute and chronic effects of ethanol. *Psychopharmacology (Berl)* **139,** 2-19.

Gunthorpe MJ & Lummis SC. (2001). Conversion of the ion selectivity of the 5-HT(3a) receptor from cationic to anionic reveals a conserved feature of the ligand-gated ion channel superfamily. *J Biol Chem* **276,** 10977-10983.

Gunthorpe MJ, Smith GD, Davis JB & Randall AD. (2001). Characterisation of a human acid-sensing ion channel (hASIC1a) endogenously expressed in HEK293 cells. *Pflugers Arch* **442,** 668-674.

Gurdon JB, Lane CD, Woodland HR & Marbaix G. (1971). Use of frog eggs and oocytes for the study of messenger RNA and its translation in living cells. *Nature* **233,** 177-182.

Guyon A, Laurent S, Paupardin-Tritsch D, Rossier J & Eugene D. (1999). Incremental conductance levels of GABAA receptors in dopaminergic neurones of the rat substantia nigra pars compacta. *J Physiol* **516 (Pt 3),** 719-737.

Haas KF & Macdonald RL. (1999). GABAA receptor subunit gamma2 and delta subtypes confer unique kinetic properties on recombinant GABAA receptor currents in mouse fibroblasts. *J Physiol* **514 (Pt 1),** 27-45.

Hamill OP, Bormann J & Sakmann B. (1983). Activation of multiple-conductance state chloride channels in spinal neurones by glycine and GABA. *Nature* **305,** 805-808.

Harrison NL & Simmonds MA. (1984). Modulation of the GABA receptor complex by a steroid anaesthetic. *Brain Res* **323,** 287-292.

Hedblom E & Kirkness EF. (1997). A novel class of GABAA receptor subunit in tissues of the reproductive system. *J Biol Chem* **272,** 15346-15350.

Hodgkin AL & Huxley AF. (1952). Currents carried by sodium and potassium ions through the membrane of the giant axon of Loligo. *J Physiol* **116,** 449-472.

Huang J & Casida JE. (1997). Avermectin B1a binds to high- and low-affinity sites with dual effects on the gamma-aminobutyric acid-gated chloride channel of cultured cerebellar granule neurons. *J Pharmacol Exp Ther* **281,** 261-266.

Imoto K, Busch C, Sakmann B, Mishina M, Konno T, Nakai J, Bujo H, Mori Y, Fukuda K & Numa S. (1988). Rings of negatively charged amino acids determine the acetylcholine receptor channel conductance. *Nature* **335,** 645-648.

Inoue M, Oomura Y, Yakushiji T & Akaike N. (1986). Intracellular calcium ions decrease the affinity of the GABA receptor. *Nature* **324,** 156-158.

Jacob TC, Bogdanov YD, Magnus C, Saliba RS, Kittler JT, Haydon PG & Moss SJ. (2005). Gephyrin regulates the cell surface dynamics of synaptic GABAA receptors. *J Neurosci* **25,** 10469-10478.

Jensen ML, Timmermann DB, Johansen TH, Schousboe A, Varming T & Ahring PK. (2002). The beta subunit determines the ion selectivity of the GABAA receptor. *J Biol Chem* **277,** 41438-41447.

Jones MV & Westbrook GL. (1995). Desensitized states prolong GABAA channel responses to brief agonist pulses. *Neuron* **15,** 181-191.

Kaneda M, Farrant M & Cull-Candy SG. (1995). Whole-cell and single-channel currents activated by GABA and glycine in granule cells of the rat cerebellum. *J Physiol* **485 (Pt 2),** 419-435.

Kao PN, Dwork AJ, Kaldany RR, Silver ML, Wideman J, Stein S & Karlin A. (1984). Identification of the alpha subunit half-cystine specifically labeled by an affinity reagent for the acetylcholine receptor binding site. *J Biol Chem* **259,** 11662-11665.

Kash TL, Jenkins A, Kelley JC, Trudell JR & Harrison NL. (2003). Coupling of agonist binding to channel gating in the GABA(A) receptor. *Nature* **421,** 272-275.

Katz B, Thesleff S. (1957). A study of the 'desensitization' produced by acetylcholine at the motor end-plate. *J Physiol* **138,** 63-80.

Kelley SP, Dunlop JI, Kirkness EF, Lambert JJ & Peters JA. (2003). A cytoplasmic region determines single-channel conductance in 5-HT3 receptors. *Nature* **424,** 321-324.

Keramidas A, Moorhouse AJ, French CR, Schofield PR & Barry PH. (2000). M2 pore mutations convert the glycine receptor channel from being anion- to cation-selective. *Biophys J* **79,** 247-259.

Klausberger T, Fuchs K, Mayer B, Ehya N & Sieghart W. (2000). GABA(A) receptor assembly. Identification and structure of gamma(2) sequences forming the intersubunit contacts with alpha(1) and beta(3) subunits. *J Biol Chem* **275,** 8921-8928.

Kneussel M, Brandstatter JH, Laube B, Stahl S, Muller U & Betz H. (1999). Loss of postsynaptic GABA(A) receptor clustering in gephyrin-deficient mice. *J Neurosci* **19,** 9289-9297.

Kusama T, Wang JB, Spivak CE & Uhl GR. (1994). Mutagenesis of the GABA rho 1 receptor alters agonist affinity and channel gating. *Neuroreport* **5,** 1209-1212.

Laurie DJ, Seeburg PH & Wisden W. (1992a). The distribution of 13 GABAA receptor subunit mRNAs in the rat brain. II. Olfactory bulb and cerebellum. *J Neurosci* **12,** 1063-1076.

Laurie DJ, Wisden W & Seeburg PH. (1992b). The distribution of thirteen GABAA receptor subunit mRNAs in the rat brain. III. Embryonic and postnatal development. *J Neurosci* **12,** 4151-4172.

Lee WY & Sine SM. (2005). Principal pathway coupling agonist binding to channel gating in nicotinic receptors. *Nature* **438,** 243-247.

Le Van Quyen M, Khalilov I, Ben-Ari Y. (2006). The dark side of high-frequency oscillations in the developing brain. *TRENDS* **29,** 419-427.

Lewis TM, Harkness PC, Sivilotti LG, Colquhoun D & Millar NS. (1997). The ion channel properties of a rat recombinant neuronal nicotinic receptor are dependent on the host cell type. *J Physiol* **505 (Pt 2),** 299-306.

Lokuta AJ, Komai H, McDowell TS & Valdivia HH. (2002). Functional properties of ryanodine receptors from rat dorsal root ganglia. *FEBS Lett* **511,** 90-96.

Lummis SC, Beene DL, Lee LW, Lester HA, Broadhurst RW & Dougherty DA. (2005a). Cis-trans isomerization at a proline opens the pore of a neurotransmitter-gated ion channel. *Nature* **438,** 248-252.

Lummis SC, D LB, Harrison NJ, Lester HA & Dougherty DA. (2005b). A cation-pi binding interaction with a tyrosine in the binding site of the GABAC receptor. *Chem Biol* **12,** 993-997.

Luscher B & Keller CA. (2004). Regulation of GABAA receptor trafficking, channel activity, and functional plasticity of inhibitory synapses. *Pharmacol Ther* **102,** 195-221.

Luu T, Gage PW & Tierney ML. (2006). GABA increases both the conductance and mean open time of recombinant GABAA channels co-expressed with GABARAP. *J Biol Chem* **281,** 35699-35708.

Mathers DA, Grewal A & Wang YH. (1989). Membrane channels activated by taurine in cultured mouse spinal cord neurons. *Neurosci Lett* **98,** 229-233.

Mathie A, Cull-Candy SG & Colquhoun D. (1991). Conductance and kinetic properties of single nicotinic acetylcholine receptor channels in rat sympathetic neurones. *J Physiol* **439,** 717-750.

McKernan RM & Whiting PJ. (1996). Which GABAA-receptor subtypes really occur in the brain? *Trends Neurosci* **19,** 139-143.

Michelson HB & Wong RK. (1991). Excitatory synaptic responses mediated by GABAA receptors in the hippocampus. *Science* **253,** 1420-1423.

Middleton RE & Cohen JB. (1991). Mapping of the acetylcholine binding site of the nicotinic acetylcholine receptor: [^{3}H]nicotine as an agonist photoaffinity label. *Biochemistry* **30,** 6987-6997.

Miledi R, Parker I & Sumikawa K. (1983). Recording of single gamma-aminobutyrate- and acetylcholine-activated receptor channels translated by exogenous mRNA in Xenopus oocytes. *Proc R Soc Lond B Biol Sci* **218,** 481-484.

Mistry DK & Hablitz JJ. (1990). Activation of subconductance states by gamma-aminobutyric acid and its analogs in chick cerebral neurons. *Pflugers Arch* **416,** 454-461.

Miyazawa A, Fujiyoshi Y, Stowell M & Unwin N. (1999). Nicotinic acetylcholine receptor at 4.6 A resolution: transverse tunnels in the channel wall. *J Mol Biol* **288,** 765-786.

Miyazawa A, Fujiyoshi Y & Unwin N. (2003). Structure and gating mechanism of the acetylcholine receptor pore. *Nature* **423,** 949-955.

Mohler H & Okada T. (1977). Benzodiazepine receptor: demonstration in the central nervous system. *Science* **198,** 849-851.

Moorhouse AJ, Keramidas A, Zaykin A, Schofield PR & Barry PH. (2002). Single channel analysis of conductance and rectification in cation-selective, mutant glycine receptor channels. *J Gen Physiol* **119,** 411-425.

Mortensen M, Kristiansen U, Ebert B, Frolund B, Krogsgaard-Larsen P & Smart TG. (2004). Activation of single heteromeric GABA(A) receptor ion channels by full and partial agonists. *J Physiol* **557,** 389-413.

Nayeem N, Green TP, Martin IL & Barnard EA. (1994). Quaternary structure of the native GABAA receptor determined by electron microscopic image analysis. *J Neurochem* **62,** 815-818.

Neubig RR & Cohen JB. (1979). Equilibrium binding of [3H]tubocurarine and [^{3}H]acetylcholine by Torpedo postsynaptic membranes: stoichiometry and ligand interactions. *Biochemistry* **18,** 5464-5475.

Newell JG & Czajkowski C. (2003). The GABAA receptor alpha 1 subunit Pro174-Asp191 segment is involved in GABA binding and channel gating. *J Biol Chem* **278,** 13166-13172.

Newell JG, Davies M, Bateson AN & Dunn SM. (2000). Tyrosine 62 of the gamma-aminobutyric acid type A receptor beta 2 subunit is an important determinant of high affinity agonist binding. *J Biol Chem* **275,** 14198-14204.

Newland CF, Colquhoun D & Cull-Candy SG. (1991). Single channels activated by high concentrations of GABA in superior cervical ganglion neurones of the rat. *J Physiol* **432,** 203-233.

O'Sullivan GA, Kneussel M, Elazar Z & Betz H. (2005). GABARAP is not essential for GABA receptor targeting to the synapse. *Eur J Neurosci* **22,** 2644-2648.

Obata K, Oide M & Tanaka H. (1978). Excitatory and inhibitory actions of GABA and glycine on embryonic chick spinal neurons in culture. *Brain Res* **144,** 179-184.

Olsen RW, Bergman MO, Van Ness PC, Lummis SC, Watkins AE, Napias C & Greenlee DV. (1981). gamma-Aminobutyric acid receptor binding in mammalian brain. Heterogeneity of binding sites. *Mol Pharmacol* **19,** 217-227.

Pedersen SE & Cohen JB. (1990). d-Tubocurarine binding sites are located at alpha-gamma and alpha-delta subunit interfaces of the nicotinic acetylcholine receptor. *Proc Natl Acad Sci U S A* **87,** 2785-2789.

Penington NJ, Kelly JS & Fox AP. (1993). Unitary properties of potassium channels activated by 5-HT in acutely isolated rat dorsal raphe neurones. *J Physiol* **469,** 407-426.

Popot JL & Changeux JP. (1984). Nicotinic receptor of acetylcholine: structure of an oligomeric integral membrane protein. *Physiol Rev* **64,** 1162-1239.

Premkumar LS, Agarwal S & Steffen D. (2002). Single-channel properties of native and cloned rat vanilloid receptors. *J Physiol* **545,** 107-117.

Prince RJ & Sine SM. (1996). Molecular dissection of subunit interfaces in the acetylcholine receptor. Identification of residues that determine agonist selectivity. *J Biol Chem* **271,** 25770-25777.

Raftery MA, Hunkapiller MW, Strader CD, Hood LE. (1980). Acetylcholine receptor: complex of homologous subunits. *Science* **208,** 1454-1456.

Reeves DC, Goren EN, Akabas MH & Lummis SC. (2001). Structural and electrostatic properties of the 5-HT3 receptor pore revealed by substituted cysteine accessibility mutagenesis. *J Biol Chem* **276,** 42035-42042.

Revah F, Bertrand D, Galzi JL, Devillers-Thiery A, Mulle C, Hussy N, Bertrand S, Ballivet M & Changeux JP. (1991). Mutations in the channel domain alter desensitization of a neuronal nicotinic receptor. *Nature* **353,** 846-849.

Rock DM & Macdonald RL. (1992). The polyamine spermine has multiple actions on N-methyl-D-aspartate receptor single-channel currents in cultured cortical neurons. *Mol Pharmacol* **41,** 83-88.

Scheller M & Forman SA. (2002). Coupled and uncoupled gating and desensitization effects by pore domain mutations in GABA(A) receptors. *J Neurosci* **22,** 8411-8421.

Schofield PR, Darlison MG, Fujita N, Burt DR, Stephenson FA, Rodriguez H, Rhee LM, Ramachandran J, Reale V, Glencorse TA & et al. (1987). Sequence and functional expression of the GABA A receptor shows a ligand-gated receptor super-family. *Nature* **328,** 221-227.

Seeburg PH, Wisden W, Verdoorn TA, Pritchett DB, Werner P, Herb A, Luddens H, Sprengel R & Sakmann B. (1990). The GABAA receptor family: molecular and functional diversity. *Cold Spring Harb Symp Quant Biol* **55,** 29-40.

Segal M & Barker JL. (1984). Rat hippocampal neurons in culture: properties of GABA-activated Cl- ion conductance. *J Neurophysiol* **51,** 500-515.

Shan Q, Nevin ST, Haddrill JL & Lynch JW. (2003). Asymmetric contribution of alpha and beta subunits to the activation of alphabeta heteromeric glycine receptors. *J Neurochem* **86,** 498-507.

Sieghart W. (1988). Comparison of two different benzodiazepine binding proteins by peptide mapping after limited proteolysis. *Brain Res* **450,** 387-391.

Sieghart W & Sperk G. (2002). Subunit composition, distribution and function of GABA(A) receptor subtypes. *Curr Top Med Chem* **2,** 795-816.

Sigel E, Baur R, Kellenberger S & Malherbe P. (1992). Point mutations affecting antagonist affinity and agonist dependent gating of GABAA receptor channels. *Embo J* **11,** 2017-2023.

Sigel E & Buhr A. (1997). The benzodiazepine binding site of GABAA receptors. *Trends Pharmacol Sci* **18,** 425-429.

Simeone TA, Donevan SD & Rho JM. (2003). Molecular biology and ontogeny of gamma-aminobutyric acid (GABA) receptors in the mammalian central nervous system. *J Child Neurol* **18,** 39-48; discussion 49.

Sine SM, Kreienkamp HJ, Bren N, Maeda R & Taylor P. (1995). Molecular dissection of subunit interfaces in the acetylcholine receptor: identification of determinants of alpha-conotoxin M1 selectivity. *Neuron* **15,** 205-211.

Smit AB, Syed NI, Schaap D, van Minnen J, Klumperman J, Kits KS, Lodder H, van der Schors RC, van Elk R, Sorgedrager B, Brejc K, Sixma TK & Geraerts WP. (2001). A glia-derived acetylcholine-binding protein that modulates synaptic transmission. *Nature* **411,** 261-268.

Smith GB & Olsen RW. (1994). Identification of a [^{3}H]muscimol photoaffinity substrate in the bovine gamma-aminobutyric acidA receptor alpha subunit. *J Biol Chem* **269,** 20380-20387.

Smith GB & Olsen RW. (1995). Functional domains of GABAA receptors. *Trends Pharmacol Sci* **16,** 162-168.

Smith TC & Howe JR. (2000). Concentration-dependent substate behavior of native AMPA receptors. *Nat Neurosci* **3,** 992-997.

Smith TC, Wang LY & Howe JR. (1999). Distinct kainate receptor phenotypes in immature and mature mouse cerebellar granule cells. *J Physiol* **517 (Pt 1),** 51-58.

Smith TC, Wang LY & Howe JR. (2000). Heterogeneous conductance levels of native AMPA receptors. *J Neurosci* **20,** 2073-2085.

Srinivasan S, Nichols CJ, Lawless GM, Olsen RW & Tobin AJ. (1999). Two invariant tryptophans on the alpha1 subunit define domains necessary for GABA(A) receptor assembly. *J Biol Chem* **274,** 26633-26638.

Staley KJ, Soldo BL & Proctor WR. (1995). Ionic mechanisms of neuronal excitation by inhibitory GABAA receptors. *Science* **269,** 977-981.

Stauffer DA & Karlin A. (1994). Electrostatic potential of the acetylcholine binding sites in the nicotinic receptor probed by reactions of binding-site cysteines with charged methanethiosulfonates. *Biochemistry* **33,** 6840-6849.

Study RE & Barker JL. (1981). Diazepam and (-)-pentobarbital: fluctuation analysis reveals different mechanisms for potentiation of gamma-aminobutyric acid responses in cultured central neurons. *Proc Natl Acad Sci U S A* **78,** 7180-7184.

Takeuchi A & Takeuchi N. (1967). Electrophysiological studies of the action of GABA on the synaptic membrane. *Fed Proc* **26,** 1633-1638.

Tanna B, Welch W, Ruest L, Sutko JL & Williams AJ. (2005). Voltage-sensitive equilibrium between two states within a ryanoid-modified conductance state of the ryanodine receptor channel. *Biophys J* **88,** 2585-2596.

Taylor PM, Connolly CN, Kittler JT, Gorrie GH, Hosie A, Smart TG & Moss SJ. (2000). Identification of residues within GABA(A) receptor alpha subunits that mediate specific assembly with receptor beta subunits. *J Neurosci* **20,** 1297-1306.

Thomäs P & Smart TG. (2005). HEK293 cell line: a vehicle for the expression of recombinant proteins. *J Pharmacol Toxicol Methods* **51,** 187-200.

Tia S, Wang JF, Kotchabhakdi N & Vicini S. (1996). Distinct deactivation and desensitization kinetics of recombinant GABAA receptors. *Neuropharmacology* **35,** 1375-1382.

Tierney ML, Birnir B, Pillai NP, Clements JD, Howitt SM, Cox GB & Gage PW. (1996). Effects of mutating leucine to threonine in the M2 segment of alpha1 and beta1 subunits of GABAA alpha1beta1 receptors. *J Membr Biol* **154,** 11-21.

Torres VI & Weiss DS. (2002). Identification of a tyrosine in the agonist binding site of the homomeric rho1 gamma-aminobutyric acid (GABA) receptor that, when mutated, produces spontaneous opening. *J Biol Chem* **277,** 43741-43748.

Toyoshima C & Unwin N. (1988). Contrast transfer for frozen-hydrated specimens: determination from pairs of defocused images. *Ultramicroscopy* **25,** 279-291.

Tretter V, Ehya N, Fuchs K & Sieghart W. (1997). Stoichiometry and assembly of a recombinant GABAA receptor subtype. *J Neurosci* **17,** 2728-2737.

Trombley PQ. (1998). Selective modulation of GABAA receptors by aluminum. *J Neurophysiol* **80,** 755-761.

Trudell J. (2002). Unique assignment of inter-subunit association in GABA(A) alpha 1 beta 3 gamma 2 receptors determined by molecular modeling. *Biochim Biophys Acta* **1565,** 91-96.

Tsushima RG, Kelly JE & Wasserstrom JA. (2002). Subconductance activity induced by quinidine and quinidinium in purified cardiac sarcoplasmic reticulum calcium release channels. *J Pharmacol Exp Ther* **301,** 729-737.

Twyman RE & Macdonald RL. (1992). Neurosteroid regulation of GABAA receptor single-channel kinetic properties of mouse spinal cord neurons in culture. *J Physiol* **456,** 215-245.

Unwin N. (1989). The structure of ion channels in membranes of excitable cells. *Neuron* **3,** 665-676.

Unwin N. (1993). Nicotinic acetylcholine receptor at 9 A resolution. *J Mol Biol* **229,** 1101-1124.

Unwin N. (1995). Acetylcholine receptor channel imaged in the open state. *Nature* **373,** 37-43.

Unwin N, Miyazawa A, Li J, Fujiyoshi. (2002) Activation of the nicotinic acetylcholine receptor involves a switch in conformation of the α subunit. *J Mol Biol* **319,** 1165-1176.

Verdoorn TA, Draguhn A, Ymer S, Seeburg PH & Sakmann B. (1990). Functional properties of recombinant rat GABAA receptors depend upon subunit composition. *Neuron* **4,** 919-928.

Wagner DA & Czajkowski C. (2001). Structure and dynamics of the GABA binding pocket: A narrowing cleft that constricts during activation. *J Neurosci* **21,** 67-74.

Wahlsten JL, Lindstrom JM & Conti-Tronconi BM. (1993). Amino acid residues within the sequence region alpha 55-74 of Torpedo nicotinic acetylcholine receptor interacting with antibodies to the main immunogenic region and with snake alpha-neurotoxins. *J Recept Res* **13,** 989-1008.

Wang H, Bedford FK, Brandon NJ, Moss SJ & Olsen RW. (1999). GABA(A)-receptor-associated protein links GABA(A) receptors and the cytoskeleton. *Nature* **397,** 69-72.

Weill CL, McNamee MG & Karlin A. (1974). Affinity-labeling of purified acetylcholine receptor from Torpedo californica. *Biochem Biophys Res Commun* **61,** 997-1003.

Westbrook GL & Mayer ML. (1987). Micromolar concentrations of Zn^{2+} antagonize NMDA and GABA responses of hippocampal neurons. *Nature* **328,** 640-643.

Westh-Hansen SE, Witt MR, Dekermendjian K, Liljefors T, Rasmussen PB & Nielsen M. (1999). Arginine residue 120 of the human GABAA receptor alpha 1, subunit is essential for GABA binding and chloride ion current gating. *Neuroreport* **10,** 2417-2421.

Whiting P, McKernan RM & Iversen LL. (1990). Another mechanism for creating diversity in gamma-aminobutyrate type A receptors: RNA splicing directs expression of two forms of gamma 2 phosphorylation site. *Proc Natl Acad Sci U S A* **87,** 9966-9970.

Whitlock A, Burnstock G & Gibb AJ. (2001). The single-channel properties of purinergic P2X ATP receptors in outside-out patches from rat hypothalamic paraventricular parvocells. *Pflugers Arch* **443,** 115-122.

Wilson G & Karlin A. (2001). Acetylcholine receptor channel structure in the resting, open, and desensitized states probed with the substituted-cysteine-accessibility method. *Proc Natl Acad Sci U S A* **98,** 1241-1248.

Wilson GG & Karlin A. (1998). The location of the gate in the acetylcholine receptor channel. *Neuron* **20,** 1269-1281.

Wisden W, Laurie DJ, Monyer H & Seeburg PH. (1992). The distribution of 13 GABAA receptor subunit mRNAs in the rat brain. I. Telencephalon, diencephalon, mesencephalon. *J Neurosci* **12,** 1040-1062.

Wisden W & Seeburg PH. (1992). GABAA receptor channels: from subunits to functional entities. *Curr Opin Neurobiol* **2,** 263-269.

Wyllie DJ, Johnston AR, Lipscombe D & Chen PE. (2006). Single-channel analysis of a point mutation of a conserved serine residue in the S2 ligand-binding domain of the NR2A NMDA receptor subunit. *J Physiol* **574,** 477-489.

Xu M & Akabas MH. (1993). Amino acids lining the channel of the gamma-aminobutyric acid type A receptor identified by cysteine substitution. *J Biol Chem* **268,** 21505-21508.

Xu M & Akabas MH. (1996). Identification of channel-lining residues in the M2 membrane-spanning segment of the GABA(A) receptor alpha1 subunit. *J Gen Physiol* **107,** 195-205.

Yakel JL, Lagrutta A, Adelman JP & North RA. (1993). Single amino acid substitution affects desensitization of the 5-hydroxytryptamine type 3 receptor expressed in Xenopus oocytes. *Proc Natl Acad Sci U S A* **90,** 5030-5033.

Yu SP & Kerchner GA. (1998). Endogenous voltage-gated potassium channels in human embryonic kidney (HEK293) cells. *J Neurosci Res* **52,** 612-617.

Zhang P & Canessa CM. (2002). Single channel properties of rat acid-sensitive ion channel-1alpha, -2a, and -3 expressed in Xenopus oocytes. *J Gen Physiol* **120,** 553-566.

Zhong W, Gallivan JP, Zhang Y, Li L, Lester HA & Dougherty DA. (1998). From ab initio quantum mechanics to molecular neurobiology: a cation-pi binding site in the nicotinic receptor. *Proc Natl Acad Sci U S A* **95,** 12088-12093.

Zhu WJ, Wang JF, Corsi L & Vicini S. (1998). Lanthanum-mediated modification of GABAA receptor deactivation, desensitization and inhibitory synaptic currents in rat cerebellar neurons. *J Physiol* **511 (Pt 3),** 647-661.

CHAPTER 2

METHODS

Cell culture and expression of recombinant receptors in cultures

Human Embryonic Kidney 293 (HEK293) cells were maintained in Dulbecco's Modified Eagle's Medium (Sigma) supplemented with 10% Bovine Growth Serum (Hyclone) at 37°C in 5% $C0_2$/95% air. HEK293 cells were transiently transfected with human $GABA_AR$ α1, β2, and γ2L subunit cDNAs in the pcDNA 3.1 (+) vector. After subculture, cells were grown on 35 mm plates for a minimum of four hours to approximately 20-30% confluency. The growth medium was exchanged with 1.5 mL of fresh medium at the start of the transfection procedure. Cultures were transfected with 0.38 μg of each of the human $GABA_A$ receptor subunits, α1, β2, and γ2L, using a modified calcium phosphate-mediated gene transfer technique first described by Chen & Okayama (1988). Briefly, 3.2 μg of each subunit cDNA in a 1:1:1 ratio in 507 μl autoclaved water and 72 μl 2M calcium chloride were added dropwise to 590 μl of concentrated HEPES buffered solution (in mM: 273 NaCl, 1.48 Na_2HPO_4, 55.6 HEPES, pH 7.4). Increasing the ratio of the γ subunit to the α and β subunits did not appear to change the efficiency of transfections nor the amplitude of current of the resulting receptors (not shown). An aliquot of green fluorescence protein (GFP) cDNA was also transfected at the same time so that transfected cells could be easily identified when excited with 470 nm blue light and emissions filtered at 510 nm (see Figure 2-1). Transfections performed in the absence of GFP yielded receptors with the same current amplitude as receptors from tranfections where GFP was added (results not shown). The transfection reagent was allowed to sit at room temperature (approximately 21°C) for 10-15 minutes before 136 μl was added dropwise with a 200 μl pipette to each 35 mm plate

of cultured cells. Whole cell and excised inside-out single channel recordings were made from these cells at room temperature, 24-72 hours after transfection.

Patch Clamp Electrophysiology

Single channel and whole cell GABA-activated membrane currents were recorded from single cells using an Axopatch 200B amplifier. Currents were filtered, usually at 3 kHz, by an npi LPBF-48DG Bessel filter and converted to a digital signal by a Digidata 1322A before being stored on hard drive. Strathclyde electrophysiology software (John Dempster, WinEDR 2.4.9 (single channel) and WinWCP 2.4.9 (whole cell)) were used in acquisition and analysis of the recorded currents. Single channel acquisition digitization frequency was set at 100 KHz. Patch electrodes were pulled with a Flaming Brown P-87 micropipette puller (Sutter Instrument Company, Novato, CA) to a resistance of 10-15 MΩ for single channel and 3-5 MΩ for whole cell. Thick walled (1.7 mm OD, 0.75 mm ID) 22% PbO glass #0010 (World Precision Instruments, Inc., Sarasota, FL., USA) was used for single channel electrodes, while thin walled glass (1.2 mm OD, 0.68 mm ID) (A-M Systems, Inc., Everett, WA., USA. Item No. 7052) was used for whole cell recordings. Electrodes for single channel recordings were coated with Sylgard®-184 at the tip to reduce capacitance. In single channel recordings, drugs were dissolved directly in a solution containing (mM): 135 NaCl, 5.4 KCl, 1.0 $MgCl_2$, 1.8 $CaCl_2$ and 10 HEPES, pH 7.4 and filled into the recording electrode. The same solution without drug was used as the bath solution. Voltage across the membrane was thus wholly determined by the patch amplifier setting.

The intracellular solution used for whole cell recordings was composed of (mM): 140 KCl, 2.0 $MgCl_2$, 5.0 EGTA, 10 HEPES and 3 Mg-ATP, pH 7.4 and the extracellular solution was composed of (mM): 140 NaCl, 4.7 KCl, 1.2 $MgCl_2$, 2.5 $CaCl_2$, 11 glucose and 10 HEPES, pH 7.4.

Analysis of Whole-Cell Currents

The amplitude of membrane currents activated by ligand was determined at a holding potential of -50 mV. GABA was applied by gravity flow from a micropipette at a distance of approximately 500 μm from the clamped cell. The rate of perfusion was approximately 500 μl/minute or 1 ml/min, as specified. Since the clamped cell was directly in the stream of fluid emitting from the pipette, concentration change was virtually instantaneous in terms of the recording time frame, once the changed solution cleared the delivery pipette. The amplitude of the current at the peak response, before observable desensitization occurred, was reported as the current response. Concentration-effect curves were fitted in GraphPad Prism 4 software using the following equation:

$$I = \frac{I_{max}[X]^n}{EC_{50}^n + [X]^n}$$

where I = measured current, [X] = agonist concentration, EC_{50} = agonist concentration producing 50% of the maximum response (I_{max}) and n = Hill coefficient. In each experiment, the current was normalized to the maximum current evoked by GABA, and the normalized data were reported as the percent of the maximum GABA response in the concentration-effect curves.

Analysis of Single-Channel Currents

Recordings of single-channel currents from excised inside-out patches were made at an electrode holding potential of +70 mV ie. The "inside" of the membrane patch was negative with respect to the "outside". Three conductance states were seen in all recordings that were made of currents identified as $GABA_AR$ currents. Other channel types were occasionally identified, all of which could be seen in the absence of GABA, the presence of bicuculline and without $GABA_AR$ transfection. Specifically, single channel currents with an amplitude of 1.8 pA were observed displaying channel open durations of multiple seconds. Another channel displayed single channel currents with an amplitude of 4-5 pA. Patches manifesting these currents were excluded from analysis since such currents are apparently endogenous to the HEK293 cells. Patches that yielded current patterns indicative of more than one receptor were also excluded from the analysis. The results shown in Chapters 3 and 4 are from at least 3 different patches at each agonist concentration. Results are reported as mean ± S.E.M., unless otherwise stated, from a minimum of three patches derived from a minimum of two separate transfections.

Amplitude Analysis

Current amplitudes were measured using the single channel analysis function of the WinEDR software. The threshold of event detection was set at twice the peak baseline noise amplitude to capture the smallest current events. By filtering at 3 KHz, the shortest events that can be completely resolved in amplitude are 150 μs in duration. Events shorter than this were, therefore, excluded from analysis.

Amplitude histograms were generated using Clampfit 9.0. The events from three different patches at each GABA concentration of 1nM, 10 nM, 100 nM, 1 μM, 10 μM, 30 μM and 500 μM were fitted by Gaussian populations. With channels activated by THIP or P4S, amplitude histograms were created from three patches each for 10 μM, 100 μM and 1mM THIP and 1 μM, 10 μM and 100 μM P4S. Except when agonist concentration was too low to evoke a large enough proportion of full-conductance events, these histograms were fitted best by three Gaussian populations using the following formula:

$$n(I)=\sum_{i=1}^{n}\frac{A_i}{\sqrt{2\pi}\sigma_i}\exp\left(\frac{-(I_i-I_{oi})^2}{2\sigma_i^2}\right)$$

where I_o= mean value, σ^2= variance and A= amplitude.

Amplitude values for currents evoked by each agonist are reported as the average amplitude determined from all agonist concentration in which histograms were created ± S.D. Single channel conductance was calculated from the average chord conductance.

Frequency Analysis

Using the single channel analysis function of the WinEDR software, the threshold for event detection was set separately for each current amplitude. For the mini- and sub-conductance currents, amplitudes of current greater than that being studied were excluded. Open events were counted in 500 ms time frames for each current amplitude. 500 ms was chosen as being of sufficient duration to encompass several receptor occupation cycles if the concentration of ligand warranted (Mortensen *et al.*, 2004). Sections of time in which the channel was predominantly closed were excluded from the analysis so that events represent periods of channel activity. Again, events shorter than

150 μs were excluded. At least 25 bins composed of approximately the same number of bins from 3-4 different patches were counted for each concentration. The average number of events per bin ± S.E.M. were plotted against agonist concentration to generate frequency concentration curves for each current amplitude.

Open Duration Analysis

Open events were detected using the WinEDR single channel analysis function. As before, the event threshold was set to detect each current amplitude separately and exclude larger current amplitudes where applicable (i.e. when investigating mini- and sub-conductance currents). Events shorter than 150 μs were excluded from the analysis. The open duration for each current amplitude was measured and placed into Sigworth-Sine plots using logarithmic binning. Curves were fitted using the probability function:

$$p(t)= \sum_{i=1}^{n_{exp}} \frac{A_i}{\tau_i} * \exp\left(\frac{-t}{\tau_i}\right)$$

where n^{exp}= number of exponential components, A_i= fraction of total number of dwell times associated with component, i= component and τ_i= mean dwell time. Tau values and the fraction of total dwell times with each component were solved using this equation.

To verify these results, the open duration for each current amplitude at a single concentration of each agonist close to its EC_{50} was binned arithmetically and plotted on a linear time scale in GraphPad Prism 4 (1 μM GABA, 10 μM P4S, 100 μM THIP). One, two and three phase exponential decays were fitted to these graphs using the following formulae for exponential decay to determine the best fit:

$$y = \text{span } 1 * \exp(-K1 * X) + \text{plateau}$$

$$y = \text{span } 1 * \exp(-K1 * X) + \text{span } 2 * \exp(-K2 * X) + \text{plateau}$$

$$y = \text{span } 1 * \exp(-K1 * X) + \text{span } 2 * \exp(-K2 * X) + \text{span } 3 * \exp(-K3 * X) \text{ plateau}$$

K1, K2 and K3 are rate constants. Tau values (half lives) are calculated by dividing 0.69 by the rate constant. The resulting tau values measured by exponential decay agreed closely to those measured using the probability function.

Expression in *Xenopus laevis* Oocytes

Mature (stage V-VI) *Xenopus laevis* oocytes were prepared and supplied by the laboratory of James Young (Department of Physiology, University of Alberta). Oocytes of this stage are approximately 1-1.2 mm in diameter and feature a dark coloured hemisphere termed the animal pole and a light coloured hemisphere referred to as the vegetal pole. Preparation was performed as described by Goldin (1992). Briefly, a portion of the ovary lobe was removed from the *Xenopus* caudal coelom through a lateral incision. Lobes were broken up with forceps while immersed in ND96 solution (in mM): 96 NaCl, 2 KCl, 1.8 $CaCl_2$ and 5 HEPES, pH 7.4, to expose the oocytes. The oocytes are transferred to Ca^{2+}- and Mg^{2+}- free ND96 solution containing 0.25 mg/ml collagenase P and 0.25 mg/ml trypsin inhibitor and shaken in this solution, which is replaced as necessary as it gets cloudy, to remove the follicle layer from the oocytes.

Plasmids containing the cDNA encoding the above mentioned individual $GABA_AR$ subunits were linearized with XBaI (α1 and γ2) or BspMI (β2) and used as a

template for *in vitro* transcription with T7 RNA polymerase (Invitrogen) to generate RNA transcripts. Each oocyte was injected in the vegetal pole with α1, β2 and γ2L RNA in a 1:1:1 ratio (final RNA concentration of 1 μg/μl in diethylpyrocarbonate-treated water) to a final volume of 30-50 nl of total RNA. Injected oocytes were maintained in ND96 solution supplemented with 10% gentamicin antibiotic solution (10 mg/ml) (Gibco). After 2-8 days maintained at 14°C, oocytes were used for desensitization experiments.

Two-Electrode Voltage Clamp

Oocytes were maintained under two electrode voltage clamp at a holding potential of -60 mV (see Figure 2-2). Both electrodes penetrated the oocyte at the vegetal pole. Electrodes were pulled from glass capillary tubing (OD=1.5mm, ID=0.86mm) Warner Instruments Inc. Cat# 64-0794 using a two stage electrode puller (Narishige model pp-830) and filled with 3M KCl. In recording solution, electrodes had resistances of 0.5-1.5 MΩ. Frog Ringer's solution (in mM): 120 NaCl, 5 HEPES, 2 KCl, 1.8 $CaCl_2$, pH 7.4, was continuously perfused over the clamped oocyte, in a recording chamber approximately 2 ml in volume. Bath solution was replenished at a rate of 8 ml/min and drugs were added to the bath perfusate. The bath exchange time is approximately 15 seconds. Currents were recorded using a GeneClamp 500B amplifier and stored using Axoscope 9 (Axon Instruments) software.

Two-Electrode Voltage Clamp Analysis

Analysis of desensitization was performed using Clampfit 9 to determine the time constant(s) of current decay by best fit iteration. Mono-, bi- and tri- exponentials of decay were applied to each current decay to determine the best fit.

The formula for exponential decay used is:

$$f(t)= \sum_{i=1}^{n} A_i e^{-t/\tau_i} + C$$

where A_i= amplitude, τ_i= rate constant and C= residual current.

Drugs Investigated

γ-Aminobutyric acid (GABA), 4,5,6,7-tetrahydroisoxazolo-[5,4-c]pyridin-3-ol (THIP) and piperidine-4-sulphonic acid (P4S) were purchased from Sigma. ZAPA and the polymethylene digabamide compounds were synthesized in the laboratory of Dr. Paul R. Carlier (Department of Chemistry, Virginia Tech) as described in Carlier *et al.* (2002) and generously supplied to our laboratory. All of these compounds are water soluble and could be dissolved directly into water or a water based solution.

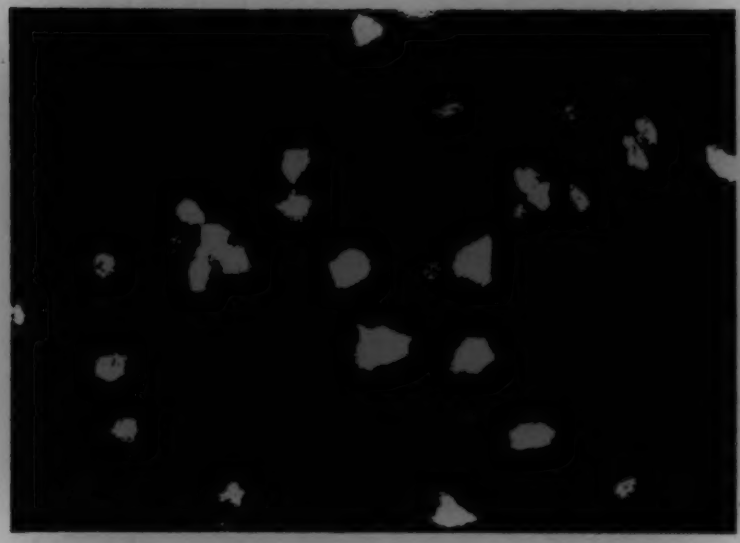

Figure 2-1: Transfected HEK293 cells. HEK293 cells transfected with the cDNA for GFP and human α1, β2 and γ2L $GABA_AR$ subunits. In this photo, excitation was achieved with ultraviolet light and emissions were filtered at 510nm. Patching round (unhealthy-looking) cells expressing GFP achieved a high degree of success as

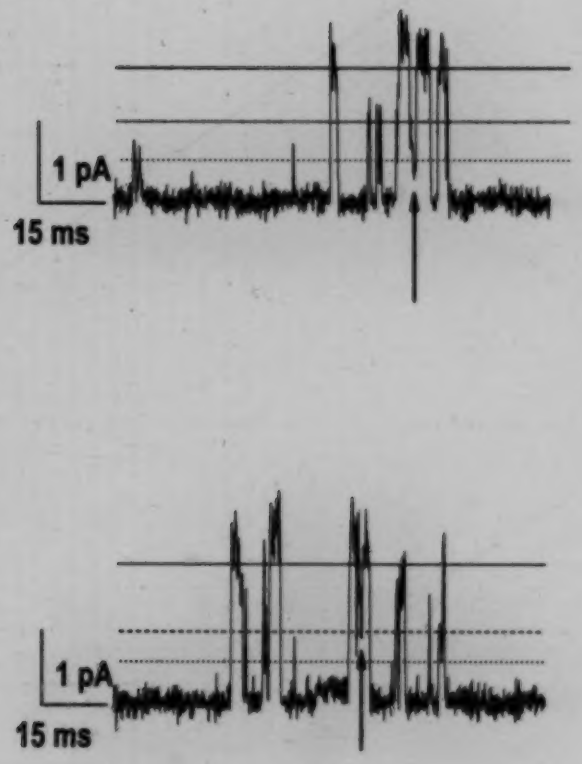

Figure 2-2: Examples of channel closures. An open channel can close not only to baseline but also to lower conductance levels. The arrow in the top panel points to a full-conductance current closing to the mini-conductance current level. In the bottom panel the arrow points to a closure from the full-conductance level to the sub-conductance current level. In all cases, channel closure to a lesser current level was considered the end of the open duration of the original opening.

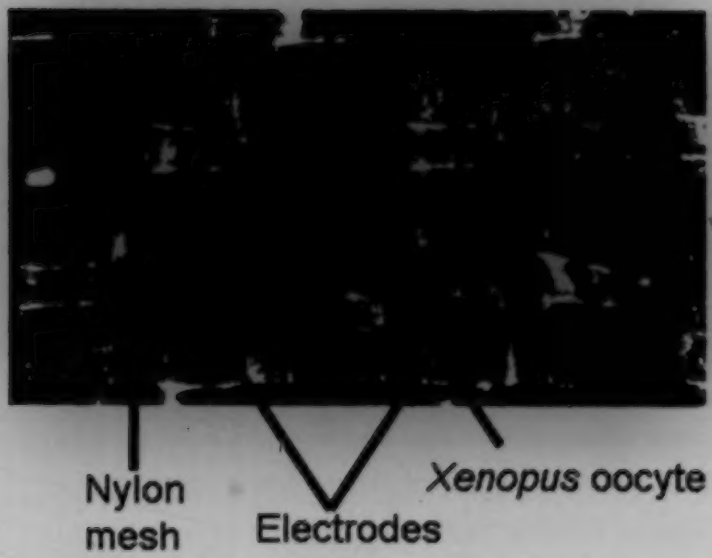

Figure 2-3: *Xenopus* oocyte under two-electrode voltage-clamp. Image modified from a picture taken by Erwin Sigel (http://www.cx.unibe.ch/~sigel/). This view shows predominantly the white (vegetal pole) side of the oocyte, while an edge of the black (animal pole) aide can be seen on the left-hand side. RNA is injected and the electrodes are impaled into the vegetal pole of the oocyte.

Bibliography

Carlier PR, Chow ES, Barlow RL & Bloomquist JR. (2002). Discovery of non-zwitterionic GABA(A) receptor full agonists and a superagonist. *Bioorg Med Chem Lett* **12,** 1985-1988.

Chen CA & Okayama H. (1988). Calcium phosphate-mediated gene transfer: a highly efficient transfection system for stably transforming cells with plasmid DNA. *Biotechniques* **6,** 632-638.

Dempster, John. Electrophysiology software available at: http://spider.science.strath.ac.uk/PhysPharm/showPage.php?pageName=software

Goldin AL. (1992). Maintenance of Xenopus laevis and oocyte injection. *Methods Enzymol* **207,** 266-279.

Mortensen M, Kristiansen U, Ebert B, Frolund B, Krogsgaard-Larsen P & Smart TG. (2004). Activation of single heteromeric GABA(A) receptor ion channels by full and partial agonists. *J Physiol* **557,** 389-413.

CHAPTER 3

THE ACTIVATED STATES OF THE $\alpha1\beta2\gamma2L$ $GABA_A$ RECEPTOR

A version this chapter has been submitted for publication

Introduction

In single channel recordings from $GABA_AR$, it has long been observed that the channel can pass current at levels intermediate to the full-conductance current (Hamill *et al.*, 1983; Miledi *et al.*, 1983). Such sub-conductance currents are regularly disregarded for several reasons. Some have suggested the possibility that they could be manifestations of multiple cooperative channels within the recording patch (Kaneda *et al.*, 1995; Gage, 1998; Guyon *et al.*, 1999). Others accept the sub-conductance currents as being indicative of substates of the receptor but have dismissed them since they are rare in comparison with the predominant full-conductance currents (Newland *et al.*, 1991; Twyman & Macdonald, 1992; Mortensen *et al.*, 2004). As no resolution has been reached in defining the sub-conductance currents, the current work was undertaken to determine the validity of the sub-conductance currents as representing additional activated states of the receptor. To accomplish this, single channel recordings were made from HEK293 cells transiently expressing the $\alpha1\beta2\gamma2L$ $GABA_AR$. The channel activity of all the conductance states was investigated at various concentrations of GABA to determine if these currents demonstrate concentration dependence.

Methods

Single channel and whole cell electrophysiological experiments were performed on HEK293 cells transiently transfected with the human $\alpha1\beta2\gamma2L$ $GABA_AR$ constructs as described in the previous chapter. In this chapter, whole cell experiments were performed using a perfusion rate of 500 µl/min through a 2 ml recording dish.

Results

Activation of $GABA_AR$ by GABA: whole cell recordings

GABA was applied over a concentration range of 0.1 – 300 μM to HEK 293 cells expressing $GABA_AR$ (α1β2γ2L) and the resulting whole cell currents were recorded. Samples of these currents are shown in Figure 3-1. The resulting concentration-response curve is also illustrated in Figure 3-1. The whole cell responses were used as a reference for determining the range of GABA concentrations to be tested at the single channel level. The concentration-response curve has an EC_{50} of 1.94 μM and maximum response was achieved between 30 and 100 μM. The mean Hill slope of this curve is 1.59 ± 0.31. Using similar expression protocols and systems, Hales *et al.* (2005) reported an EC_{50} of around 6.6 μM. While the EC_{50} value for GABA in our system is lower than is usually reported, this may be explained by the differences in perfusion systems. Due to the slow rate of our perfusion system, the peak current responses may be reduced by the desensitization of receptors and thereby shift the concentration-effect curve to lower concentration values. Although not the focus of this study, desensitization is increasingly seen at concentrations of GABA 3 μM and above, while it is not seen at 0.1 or 1 μM GABA.

Single Channel Conductance

Single channel recordings were made from excised inside-out patches at a transmembrane holding potential of 70 mV with the inside negative to the outside. The single channel properties of the $GABA_AR$ were investigated at nine concentrations of GABA between 100 pM and 500 μM. At all concentrations of GABA considered the

plots were fitted best with three Gaussian populations (see Figure 3-2) which indicate that three distinct amplitudes of current were present, the lowest of which was at least three times the value of baseline noise. The mean current amplitudes were determined and the chord conductance calculated. We identified these amplitude states as the mini-conductance state at 7 pS, the sub-conductance state at 16 pS and the full-conductance state at 29 pS. Examples of currents at these amplitudes can be seen in Figure 3-3a and b. These same three amplitude states in inverted form were also present when the holding potential was reversed (results not shown). Open channel noise of the LGICs is a problem for single channel analysis. Sigworth (1985) expected an increase in open channel noise due to conformational changes in the channel. Open channel noise was described by Colmenares (1993) as the non-uniform movement of ions through the open channel pore as a result of, among other sources, the channel protein changing conformation. GFP did not influence these states (results not shown). Channels closed not only to baseline, but also from full-conductance openings to the sub-, or mini-conductance state, or from sub-conductance openings to the mini-conductance state. These types of closures were quite frequent and the closure from one current level to another was always regarded as a closure of the initial opening. The frequency of open channel events increased with increasing GABA concentration.

Frequency of Events

The frequency of channel openings to each of the three amplitude states was used as a consistent means of comparing activity at various concentrations of agonist. During episodes of $GABA_AR$ activity the number of mini-, sub-, and full- conductance events

that occurred in sequential periods of 500 ms were counted and averaged at each concentration of GABA. While an accurate determination of EC_{50} for the resulting frequency-concentration curves is not possible, an approximate value is provided for each curve from an estimate of the delineation of the curves. The mean frequency of mini-conductance events rose to around 11 events/bin at 100 pM GABA and to around 22 events/bin at 1 nM. Thereafter, the frequency of the mini-conductance currents appeared nearly constant at around 20 events/bin over the rest of the concentration range (top panel of Figure 3-4). The frequency-concentration curve for the mini-conductance events has an estimated EC_{50} of approximately 100 pM. The mean frequency curves of both the sub- and full-conductance currents rose in a biphasic manner (middle and bottom panels of Figure 3-4). The initial rise of the sub-conductance frequency curve increased over the concentration range of 100 pM to 1 nM to about 12 events/bin and remained constant over the concentration range 1 nM to 100 μM to around 15 events/bin until showing a late abrupt rise at 500 μM to around 30 events/bin. This curve would generate two EC_{50} values, one of approximately 200 pM and one greater than 100 μM. The first rise in full-conductance frequency increased over the concentration range of 100 nM and 1 μM to around 10 events/bin then increased further between 1 μM and 500 μM to a maximum of around 40 events/bin. The EC_{50} values for this curve are estimated at approximately 100 nM and 30 μM.

Open Duration Analysis of $GABA_AR$

The open duration of the mini-conductance state was determined at three concentrations of GABA between 1 μM and 30 μM. When plotted on a Sigworth-Sine

plot (Sigworth & Sine 1987), the distribution of the mini-conductance currents durations, though truncated by the lower limit of detection, apparently conforms to a single exponential and could not be fitted with two exponentials using the WinEDR software (top panel of Figure 3-5). The mean open time constant from this analysis was 0.18 ms. Even though the mini-conductance events tended to be close to the lower limit of detection, the possibility of them all being truncated sub-conductance events was ruled out due to the occurrence of longer openings with an observable dwell time at this current level. These longer openings were not observed in every patch examined and yet in a cumulative plot such as the top panel of Figure 3-5 they appear as an extended foot to the main population of currents. When the open durations of mini-conductance events evoked by 1 μM GABA were plotted on a linear time scale, the graph could be fitted better with two exponentials (r^2=0.998) rather than one (r^2= 0.973) (see Figure 3-6), with time constants of 0.10 ms and 2.83 ms. While the shorter time constant was estimated from a line extrapolated to below our limit of detection, the apparent presence of a longer duration population raises the possibility of this being a true amplitude state. The sub- and full-conductance current populations can both be defined by the sum of two exponentials by defining the probability density function of Sigworth-Sine plots and fitting exponentials to the linear graphed version of the data (middle and bottom panels of Figure 3-5 and 3-6). Therefore, there was a population of both short and long sub- and full-conductance openings. The open duration and the proportion of sub- and full-conductance events that open either to the short or long population of currents as determined by the probability density function are summarized in Table 3-1. The time constants measured by exponential decay of the linearized open duration sub-

conductance currents at 1μM GABA were 0.39 and 5.97 ms, and 0.43 and 5.55 ms for the full-conductance currents. These curves were fitted best with two exponentials rather than one or three exponentials.

The sub-conductance open duration events were investigated at six concentrations between 1 nM and 30 μM GABA. The short time constant is on average around 0.36 ms, and the long time constant is around 2.28 ms. The proportions of the short and long sub-conductance events do not change with GABA concentration over this range (top panel of Figure 3-7).

The full-conductance open duration events were investigated at 1 μM, 10 μM and 30 μM GABA. The short full-conductance events have a time constant of about 0.31 ms, and the long full-conductance events have a time constant of about 4.45 ms. This agrees with the open duration time constants determined by Mortensen *et al.* (2004) for the full-conductance current openings. The proportion of the short full-conductance events decreased to the proportion of long full-conductance events with increasing GABA concentration (bottom panel of Figure 3-7). At 1 μM GABA, the predominant full-conductance population exhibited the short time constant, while at 30 μM the predominant population demonstrated the long time constant.

Discussion

The detection of transient events such as single channel currents is fraught with technical limitations associated with the detection equipment itself. The necessity of reducing noise in the system requires the use of a filter, among other precautions, and to maintain a reassuring signal to noise ratio, a -3dB frequency of 3 kHz was chosen. A

high order Bessel filter has a $t_{10\text{-}90}$ of 100 μs, and so the attenuation of a step signal is complete after 150 μs. Choosing this value as the lower limit of acceptance for the duration of signals ensures that amplitude is accurately recorded at all times. It is more than likely that this arbitrary cutoff duration fails to capture numbers of shorter currents such as those seen in nAChR by Hallermann *et al.* (2005), and this loss will bias the estimates of channel open time upwards and might affect current duration population fits but will not affect the estimates of current amplitude.

We have identified three different amplitude states, which we have called the mini-, sub-, and full-conductance states. Based on the open duration analysis, we have identified a single population of very short mini-conductance openings as well as a possible small population of longer mini-conductance openings. Due to the small size of the population of longer duration mini-conductance events and the ambiguity in establishing its separate existence, even at 1 μM GABA when these events have reached their maximum frequency, it is difficult to comment definitively on the relationship of the two. This must remain an open question to be answered only by more rigorous attention to the reduction of baseline noise such as was used by Parzefall *et al.* (1998).

Two populations each of sub-, and full-conductance openings were identified. This amounts in total to at least five activated states. While it has long been recognized that the open duration of the full-conductance state is fitted best by two exponentials (Jackson *et al.*, 1982), this is the first time that the open duration has been considered for the lesser conductance states. Such kinetic modeling as has been attempted to date has focused exclusively on the full-conductance state (Lema & Auerbach, 2006). The number of conductance states that could be elucidated was determined by compiling

amplitude histograms of recordings analyzed using the Strathcylde electrophysiology software WinEDR 2.4.9. We have considered the frequency of each conductance state as a pharmacological response that can be quantified and compared over a range of concentrations. The frequency of the lesser conductance states was also measured in an effort to understand their behaviour as well as to prove their authenticity.

Although a recombinant expression system using HEK 293 cells is extensively used for expressing receptor proteins (Thomas & Smart, 2005), there is evidence to suggest that it does not necessarily always generate a homogenous population of $GABA_A$Rs (Ebert *et al.*, 1996). Of most consequence to this work, there are reports that α and β subunits can assemble into functional receptors in the absence of the γ subunit (Verdoorn *et al.*, 1990b; Ebert *et al.*, 1996; Tretter *et al.*, 1997). These receptors display smaller conductances than receptors composed of all three subunits (Verdoorn *et al.*, 1990a), and Angelotti & Macdonald (1993) reported the conductance currents of the sub-conductance and full-conductance states of an α1β1 receptor to be 10 pS and 15 pS, respectively, while the corresponding values of an α1β1γ2s receptor were 21 pS and 29 pS, respectively. The realization that expression systems do not always produce a pentamer constructed from three subunits has led to the investigation of this expression problem. Angelotti *et al.* (1993) demonstrated that in a different cell type (L929 cells) in the presence of the γ2s subunit, α1β1γ2s receptors were preferentially expressed over α1β1 receptors. Much work has been done recently with HEK293 expression systems in forcing subunit assembly by creating chimeras of the subunits to ensure that the αβγ subunits are expressed in the desired stoichiometry (Boileau & Czajkowski, 1999; Baumann *et al.*, 2001; Boileau *et al.*, 2005). We have used the γ2L variant without

linkage to the other subunits and have apparently achieved homogeneous populations of receptors in our cells since our single channel conductance values agree consistently with those of proven $\alpha 1\beta 2\gamma 2$ receptors.

From our observations of the multiple conductance states in single channel recordings of $GABA_AR$ and using the criteria for substates of a channel, recommended by Fox (1987), it appears that the sub-conductance currents reflect substates of the $GABA_AR$. First, the bursting behaviour shows transitions between each of the states with the three conductance states converting between each other. Second, these three states are always seen in the presence of each other, and none of these was seen in a patch independently of the other two. Finally, the sum of a mini-conductance current and a sub-conductance current or the sum of two sub-conductance currents does not add up to the value of the full-conductance current. Thus, taken together, these findings strongly suggest that these states are indeed substates of a single channel and not separate channels. Therefore, we have no evidence that the mini- or sub-conductance states are a consequence of an additional $GABA_AR$ in the patch based on Fox's criteria.

Since the contribution of the sub-conductance currents to total current passed through the receptor has never been established nor a physiological role ever ascribed to the sub-conductance currents, we believed it was important to determine some information about the behaviour of these currents as well as determine their relationship to the full-conductance currents. Channel activation with GABA has shown that the frequency of occurrence of the various conductance states is influenced by the concentration of GABA. At low GABA concentrations, there are predominantly openings to the mini- and sub-conductance states. With increasing GABA

concentrations, we witnessed an increase in the incidence of long full-conductance events. Conventional pharmacological theory maintains that, on average, at low concentrations of agonist, high affinity binding sites will bind ligand preferentially over low affinity sites. As the concentration of agonist is increased there is a higher incidence of low affinity binding. It follows that the binding event that produces the mini-conductance currents has a higher affinity for GABA compared to the binding event that produces the full-conductance currents. The sub-conductance currents are produced by a binding event involving high to moderate affinity for GABA. It follows that the binding event that produces the mini-conductance currents has a very high affinity for GABA compared to the binding event that produces the full-conductance currents. The sub-conductance currents are produced by a binding event with high to moderate affinity for GABA.

In Figure 3-4, the frequency of events for each conductance current rises over different GABA concentration ranges and the mean frequency curves for each of the conductance states have different estimated EC_{50} values. This is consistent with each of the conductance currents being a product of a binding event independent from the events that produce the other conductance currents, but not necessarily in a linear scheme. The frequency curve generated for the mini-conductance currents illustrates a very steep rise in frequency and a very low estimated EC_{50} value for this curve. Again, this points to the mini-conductance currents being generated by a binding site with very high affinity for agonist. Due to the biphasic nature of both the sub- and full-conductance mean frequency curves, two EC_{50} values were estimated for each curve. This behaviour is indicative of agonist binding to two binding sites that have different affinities for agonist.

Since the incidence of each of these activation states depicts multiple different estimated EC_{50} values for GABA, it is suggested that individual conductance states reflect the occupation of a series of binding sites by agonist.

On the basis of controlled iontophoresis studies at the frog neuromuscular junction, Dionne *et al.* (1978) predicted that the data were consistent with the presence of at least two binding sites, although they suggested that additional sites may also be present. This has led to extensive kinetic modelling of activation at the nicotinic acetylcholine receptor based on a monoliganded and diliganded paradigm (Edmonds *et al.*, 1995). Unlike the nicotinic receptor, the $GABA_A$ receptor is recognized to be well endowed with both high affinity and lower affinity binding sites, which originally could have been explained by multiple receptor types in the preparation. However, apparently homogenous preparations also exhibit multiple agonist binding sites (Newell *et al.*, 2000).

In our work we can distiguish five different activated states of the receptor, although association of these states with known binding loci remains to be attempted. Further evidence is required before a model of activation can be constructed. Maconochie *et al.* (1994) noted that the rate at which receptors responded to GABA was dependent on agonist concentration and concluded that more than one molecule of GABA binds to the $GABA_AR$, and that the final binding step has low affinity. In considering the mean frequency curves generated for each of the conductance states, the full-conductance states appear to have a lower affinity for GABA than the mini- and initial sub-conductance states. As well, the full-conductance currents occur most often at high concentrations of GABA. The stochastic nature of ligand binding would not

preclude the occupancy and activation of a low affinity site at low agonist concentrations, and this is substantiated by our raw recordings, where full conductance events do occur, albeit rarely, among the relatively more plentiful sub- and mini-conductance events at low GABA concentrations.

The proportion of the short and long sub-conductance currents is not influenced by GABA concentration and we interpret this to mean that these states are generated by two independent binding events. However, the short and long full-conductance states do appear to have reciprocal dependence on each other that can be seen as GABA concentration is increased (bottom panel of Figure 3-7). The virtually complete disappearance of the short full-conductance currents at 30 μM GABA is consistent with a degree of cooperativity between the events producing these two currents. If both are the product of binding events to different binding sites, if both sites were occupied simultaneously this might result in a more stable conformational change and a longer lasting current or currents would result. As was pointed out above, sufficient binding sites apparently occur on the $GABA_AR$ pentamer to accommodate such a suggestion.

It is true that the majority of current that passes through the $GABA_AR$ at concentrations of GABA higher than 10 μM is through the full-conductance state (Newland *et al.*, 1991). The mini- and sub-conductance states seem to play a more evident role at very low concentrations of GABA and this correlates well with whole cell data that shows small amounts of current passing at low concentrations of GABA. The rise in the whole cell concentration-response curve beginning at 1 μM corresponds to the increase in the incidence of full-conductance currents and their tendency to being longer in duration.

Once ligand binding has occurred in a LGIC, a conformational change is thought to occur in the receptor, which allows the ion pore to open, possibly repetitively (Grosman *et al.*, 2000). If there are a number of independent binding sites on the $GABA_AR$ the conformation of the receptor need not change to the same extent as each of these binding sites interact with an agonist molecule, leading to the different activated states of the receptor.

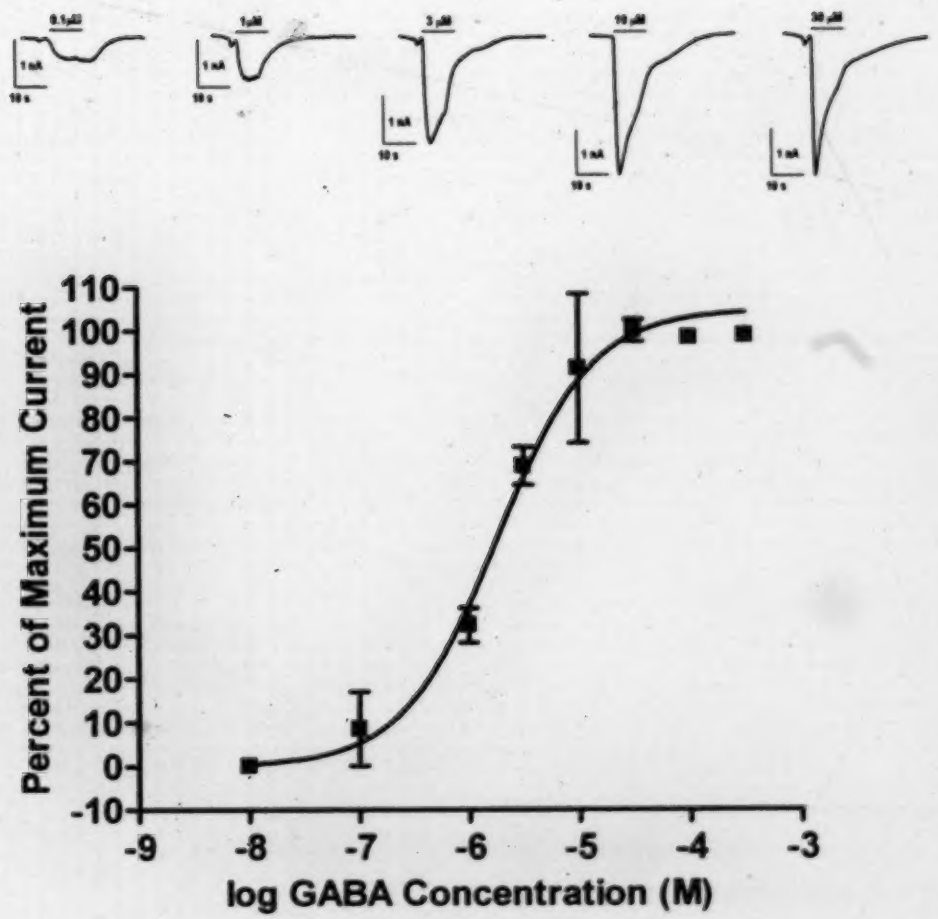

Figure 3-1: Whole cell $GABA_AR$ currents. Top panel shows examples of whole cell currents elicited by 0.1, 1, 3, 10 and 30 μM GABA at a holding potential of -50 mV. Bottom panel shows the concentration-effect curve of GABA to HEK 293 cells transiently expressing α1β2γ2L $GABA_AR$. Current is reported as the average percent of maximal current ± S.E.M. from three individual dose-response curves derived from three separate transfections. EC_{50} = 1.94 ± 0.16 μM, Hill slope =1.59 ± 0.31.

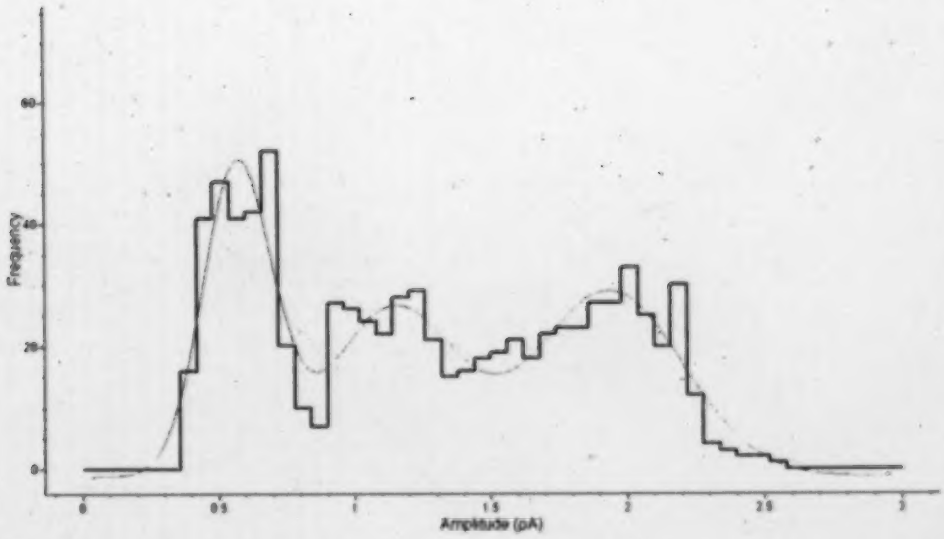

Figure 3-2: Amplitude histogram from $GABA_AR$ activation with GABA. Amplitude analysis produced amplitude histograms that were fitted best with three Gaussian populations of current. The above illustrates these three populations in the cumulative amplitude analysis from 3 patches at 10 μM GABA (r^2=0.86).

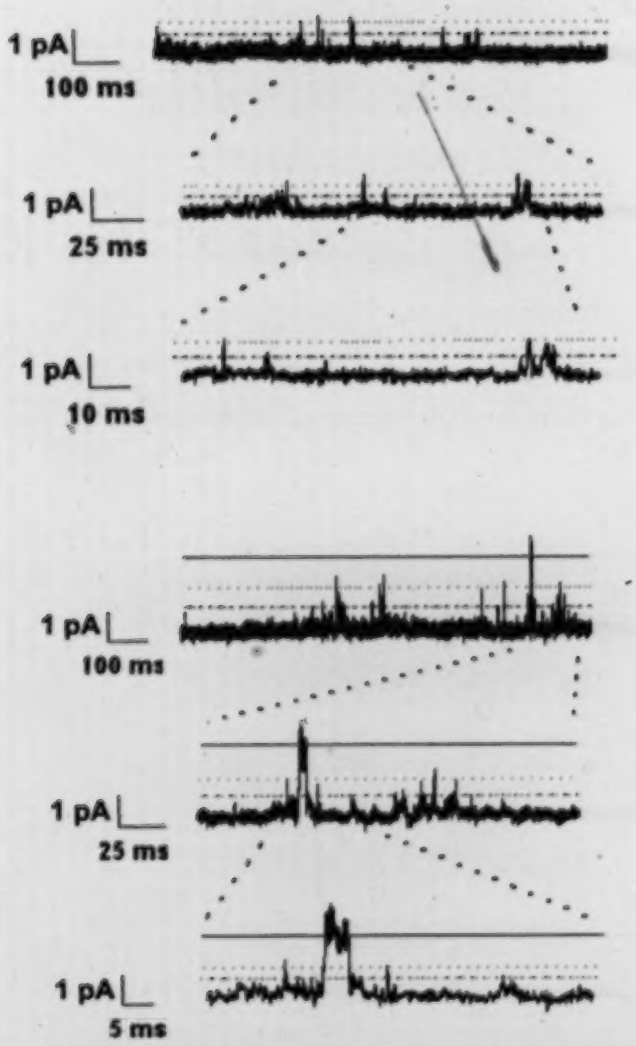

Figure 3-3a: Single channel current conductances of $GABA_AR$ activated by GABA. Examples of single channel currents activated by GABA in excised inside-out patches of HEK 293 cells expressing $\alpha1\beta2\gamma2L$ $GABA_AR$ at an electrode holding potential of +70 mV. Channel openings are a deflection upward from baseline. The full-conductance state is shown with a solid line (-) at 2.1 pA (29 pS), the sub-conductance state is illustrated with a dotted line (··) at 1.2 pA (16 pS), and the mini-conductance state is shown with a dashed line (--) at 0.6 pA (7 pS). Top panel: 100 pM GABA, bottom panel: 10 nM GABA. At these concentrations, the incidence of mini- and sub-conductance events is greater than that of full-conductance events.

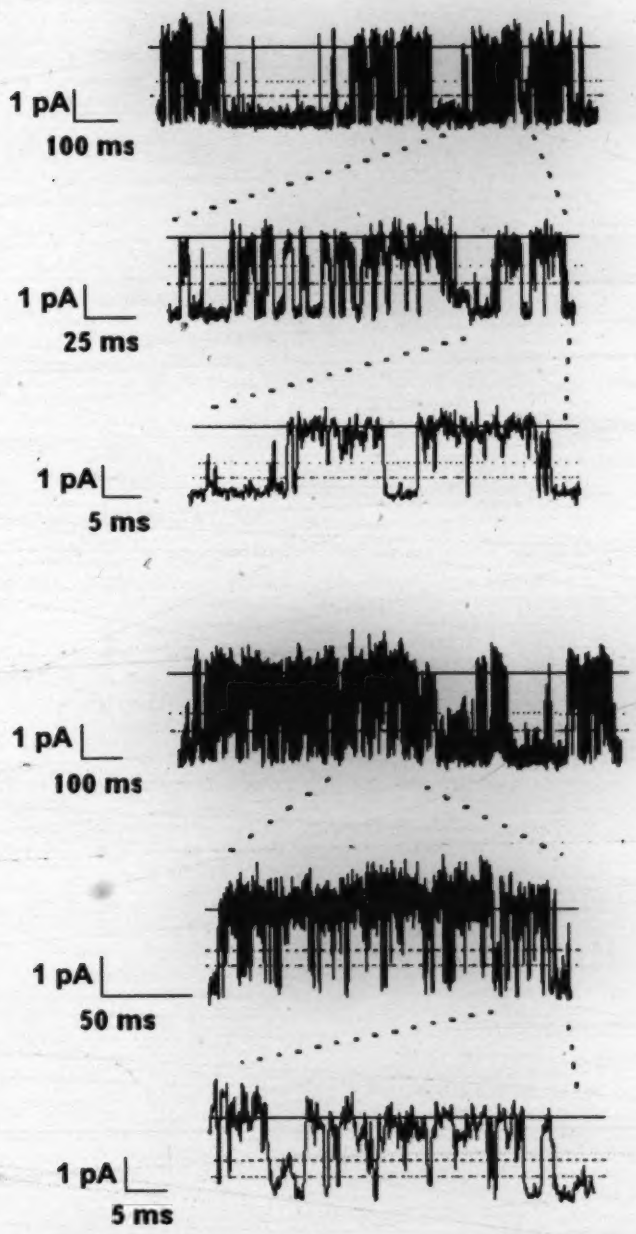

Figure 3-3b: Single channel current conductances of $GABA_AR$ activated by GABA: Examples of single channel currents activated by GABA. Legend as stated in Figure 3-3a. Top panel: 1 μM GABA, bottom panel: 100 μM GABA. At these concentrations full-conductance events are very frequent, although openings and closings to the lesser conductance states are still evident.

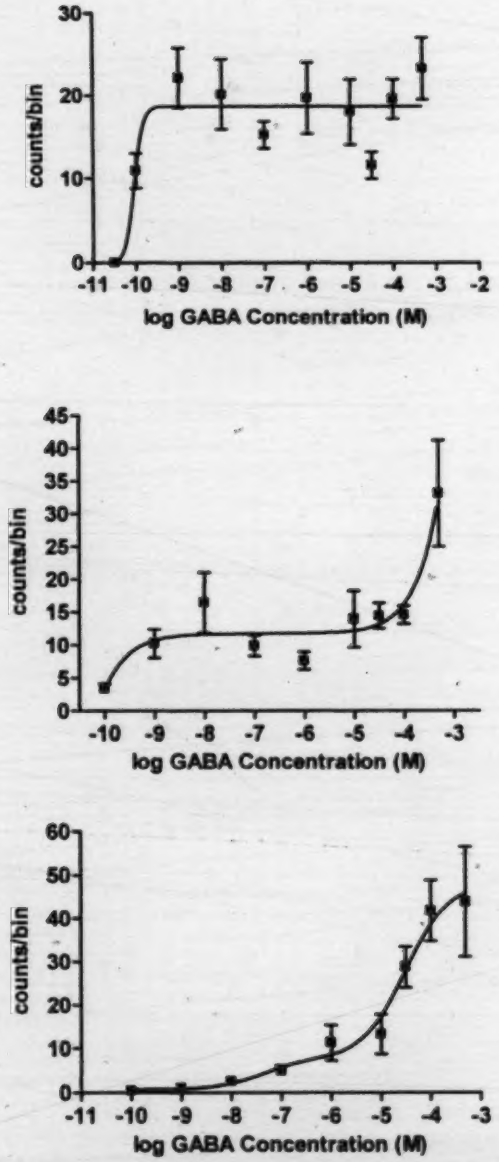

Figure 3-4: Number of events per 500 ms bins. Graphs show the average number of events per 500 ms bin from at least 25 bins accumulated from three to four different patches ± S.E.M. at each GABA concentration, except for 100 μM GABA (1 patch), for: mini-conductance events (top panel), sub-conductance events (middle panel) and full-conductance events (bottom panel). The mini-conductance events were fitted with a sigmoidal dose-response curve, while the sub- and full-conductance events were fitted with a two-site competition curve.

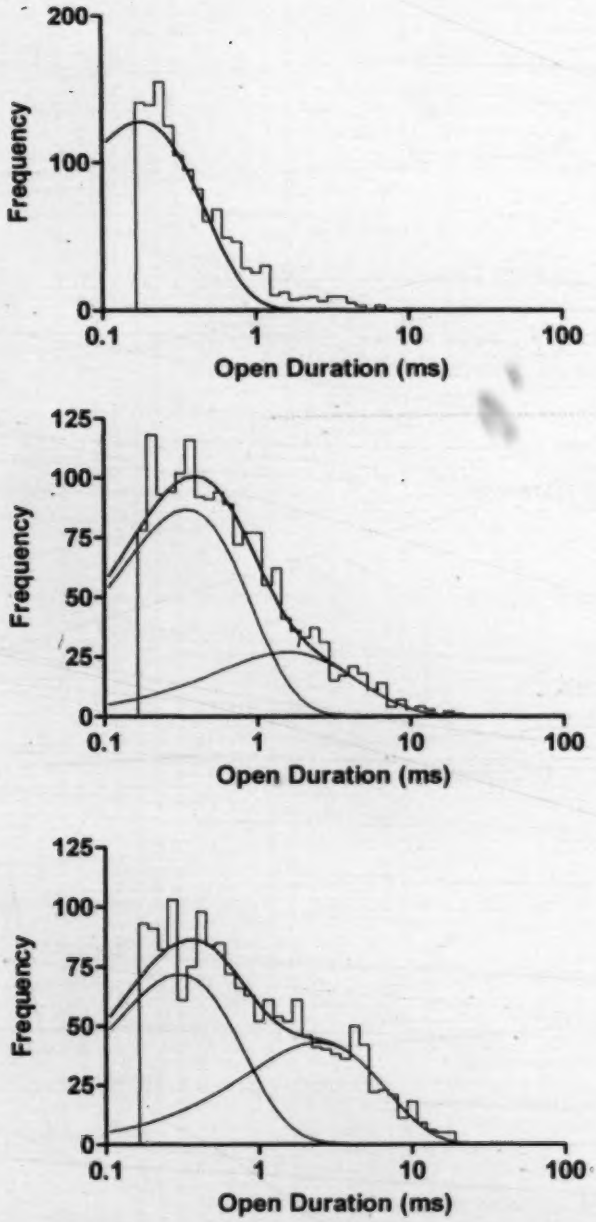

Figure 3-5: Open duration of $GABA_A$Rs activated by GABA: mini-, sub, and full-conductance current durations at 1 μM GABA. The open duration of the mini-conductance state (top panel) is fitted with a single exponential, while the sub-conductance (middle panel) and full-conductance (bottom panel) open durations are both fitted by two exponentials in Sigworth-Sine plots.

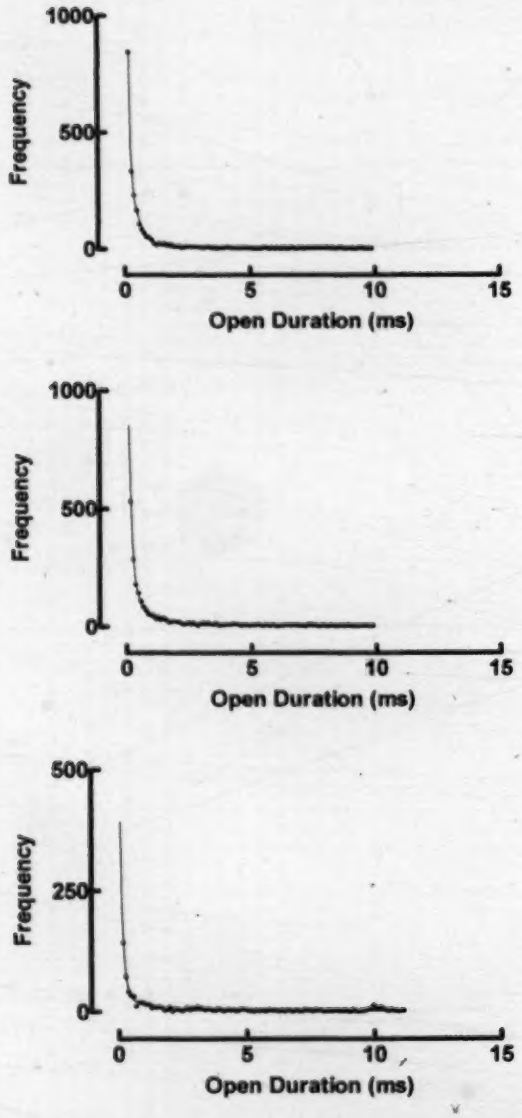

Figure 3-6: Open duration analysis of $GABA_A$Rs activated by 1 μM GABA. When plotted on a linear time scale, the open duration of the mini-conductance currents (top panel) could be fitted best with two exponentials with tau values of 0.10 and 2.83 ms. The open duration of the sub- (middle panel) and full- (bottom panel) conductance currents were both fitted best with two exponentials. For the sub-conductance currents, the tau values are 0.39 and 5.97 ms, while for full-conductance currents these values are 0.43 and 5.55 ms.

	Mini-conductance		Sub-conductance				Full-conductance			
	τ	Area	τ1	Area 1	τ2	Area 2	τ1	Area 1	τ2	Area 2
GABA										
1 nM			0.40 ± 0.07	91.01 ± 5.70	2.44 ± 0.82	19.95 ± 11.14				
10 nM			0.34 ± 0.05	94.03 ± 3.97	2.31 ± 1.93	9.56 ± 3.16				
100 nM	0.21 ± 0.03	100 ± 3.52	0.42 ± 0.05	94.14 ± 20	2.29 ± 0.92	16.71 ± 26.76				
1 μM	0.19 ± 0.01	100 ± 3.55	0.41 ± 0.09	72.69 ± 9.31	3.25 ± 0.46	37.51 ± 6.29	0.35 ±0.14	83.49 ± 15.19	5.77 ± 0.57	27.49 ± 20.68
10 μM	0.18 ± 0.01	100 ± 2.57	0.35 ± 0.03	80.93 ±9.60	1.98 ± 0.47	26.54 ±11.40	0.26 ± 0.06	59.48 ±11.67	2.92 ± 0.23	47.77 ±15.14
30 μM	0.17 ± 0.01	100 ± 2.33	0.29 ± 0.06	92.99 ±19.19	1.41 ± 0.32	17.20 ± 15.53	0.30 ± 0.02	6.37 ±5.46	4.67 ± 0.36	93.07 ±7.11

Table 3-1: Open duration analysis summary. The open duration and proportion of current that activates to the long and short sub- and full-conductance openings are summarized above. These values were calculated using the probability density function from the Sigworth-Sine plots. Tau values are in milliseconds while area is reported as a percent. Results are expressed as means ± S.E.M.

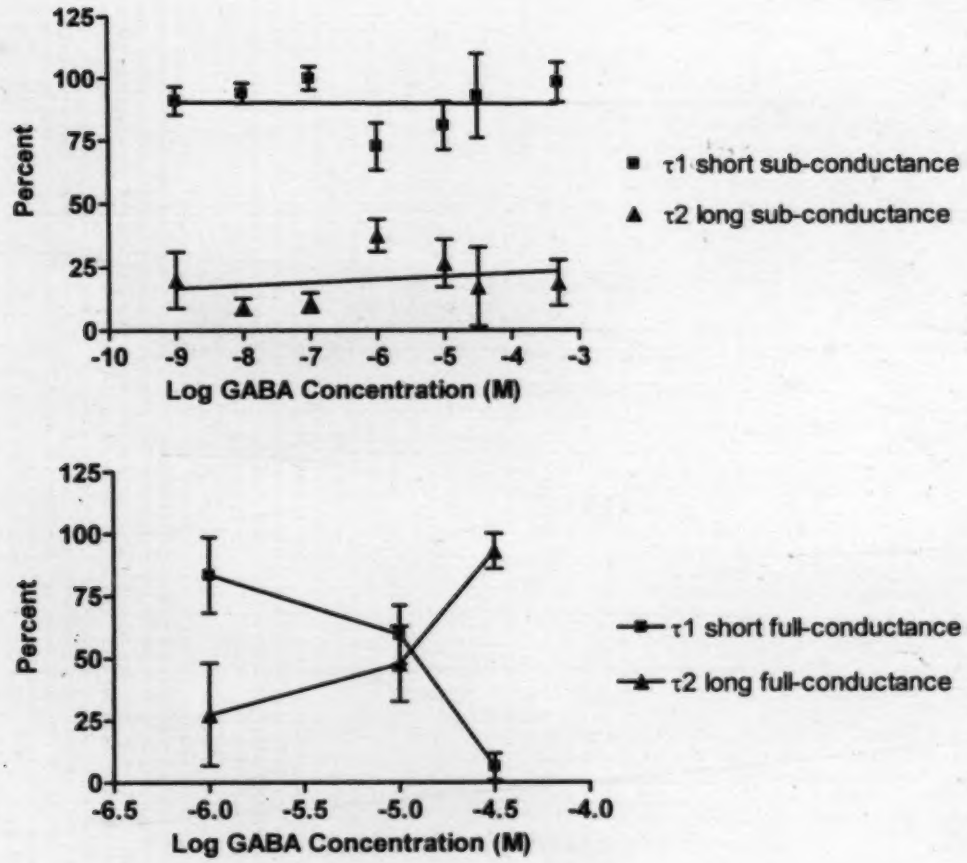

Figure 3-7: Proportion of the long and short events with concentration of GABA. Top panel: Long and short duration currents as a proportion of sub-conductance. Bottom panel: Proportion of long and short full-conductance events to total full-conductance events. Results are expressed as means ± S.E.M.

Bibliography

Angelotti TP & Macdonald RL. (1993). Assembly of GABAA receptor subunits: alpha 1 beta 1 and alpha 1 beta 1 gamma 2S subunits produce unique ion channels with dissimilar single-channel properties. *J Neurosci* **13,** 1429-1440.

Angelotti TP, Uhler MD & Macdonald RL. (1993). Assembly of GABAA receptor subunits: analysis of transient single-cell expression utilizing a fluorescent substrate/marker gene technique. *J Neurosci* **13,** 1418-1428.

Baumann SW, Baur R & Sigel E. (2001). Subunit arrangement of gamma-aminobutyric acid type A receptors. *J Biol Chem* **276,** 36275-36280.

Boileau AJ & Czajkowski C. (1999). Identification of transduction elements for benzodiazepine modulation of the GABA(A) receptor: three residues are required for allosteric coupling. *J Neurosci* **19,** 10213-10220.

Boileau AJ, Pearce RA & Czajkowski C. (2005). Tandem subunits effectively constrain GABAA receptor stoichiometry and recapitulate receptor kinetics but are insensitive to GABAA receptor-associated protein. *J Neurosci* **25,** 11219-11230.

Colmenares PJ. (1993). Role of a stochastic friction coefficient in open channel noise. *J Theor Biol* **161,** 175-198.

Dionne VE, Steinbach JH & Stevens CF. (1978). An analysis of the dose-response relationship at voltage-clamped frog neuromuscular junctions. *J Physiol* **281,** 421-444.

Ebert V, Scholze P & Sieghart W. (1996). Extensive heterogeneity of recombinant gamma-aminobutyric acidA receptors expressed in alpha 4 beta 3 gamma 2-transfected human embryonic kidney 293 cells. *Neuropharmacology* **35,** 1323-1330.

Edmonds B, Gibb AJ & Colquhoun D. (1995). Mechanisms of activation of muscle nicotinic acetylcholine receptors and the time course of endplate currents. *Annu Rev Physiol* **57,** 469-493.

Fox JA. (1987). Ion channel subconductance states. *J Membr Biol* **97,** 1-8.

Gage PW. (1998). Signal transmission in ligand-gated receptors. *Immunol Cell Biol* **76,** 436-440.

Grosman C, Zhou M & Auerbach A. (2000). Mapping the conformational wave of acetylcholine receptor channel gating. *Nature* **403,** 773-776.

Guyon A, Laurent S, Paupardin-Tritsch D, Rossier J & Eugene D. (1999). Incremental conductance levels of GABAA receptors in dopaminergic neurones of the rat substantia nigra pars compacta. *J Physiol* **516,** 719-737.

Hales TG, Tang H, Bollan KA, Johnson SJ, King DP, McDonald NA, Cheng A & Connolly CN. (2005). The epilepsy mutation, gamma2(R43Q) disrupts a highly conserved inter-subunit contact site, perturbing the biogenesis of GABAA receptors. *Mol Cell Neurosci* **29,** 120-127.

Hallermann S, Heckmann S, Dudel J & Heckmann M. (2005). Short openings in high resolution single channel recordings of mouse nicotinic receptors. *J Physiol* **563,** 645-662.

Hamill OP, Bormann J & Sakmann B. (1983). Activation of multiple-conductance state chloride channels in spinal neurones by glycine and GABA. *Nature* **305,** 805-808.

Jackson MB, Lecar H, Mathers DA & Barker JL. (1982). Single channel currents activated by gamma-aminobutyric acid, muscimol, and (-)-pentobarbital in cultured mouse spinal neurons. *J Neurosci* **2,** 889-894.

Kaneda M, Farrant M & Cull-Candy SG. (1995). Whole-cell and single-channel currents activated by GABA and glycine in granule cells of the rat cerebellum. *J Physiol* **485,** 419-435.

Kash TL, Jenkins A, Kelley JC, Trudell JR & Harrison NL. (2003). Coupling of agonist binding to channel gating in the GABA(A) receptor. *Nature* **421,** 272-275.

Lema GM & Auerbach A. (2006). Modes and models of GABAA receptor gating. *J Physiol.*

Maconochie DJ, Zempel JM & Steinbach JH. (1994). How quickly can GABAA receptors open? *Neuron* **12,** 61-71.

Miledi R, Parker I & Sumikawa K. (1983). Recording of single gamma-aminobutyrate- and acetylcholine-activated receptor channels translated by exogenous mRNA in Xenopus oocytes. *Proc R Soc Lond B Biol Sci* **218,** 481-484.

Mortensen M, Kristiansen U, Ebert B, Frolund B, Krogsgaard-Larsen P & Smart TG. (2004). Activation of single heteromeric GABA(A) receptor ion channels by full and partial agonists. *J Physiol* **557,** 389-413. Epub 2004 Feb 2027.

Newell JG, Davies M, Bateson AN & Dunn SM. (2000). Tyrosine 62 of the gamma-aminobutyric acid type A receptor beta 2 subunit is an important determinant of high affinity agonist binding. *J Biol Chem* **275,** 14198-14204.

Newland CF, Colquhoun D & Cull-Candy SG. (1991). Single channels activated by high concentrations of GABA in superior cervical ganglion neurones of the rat. *J Physiol* **432,** 203-233.

Parzefall F, Wilhelm R, Heckmann M & Dudel J. (1998). Single channel currents at six microsecond resolution elicited by acetylcholine in mouse myoballs. *J Physiol* **512**, 181-188.

Sigworth FJ. (1985). Open channel noise. I. Noise in acetylcholine receptor currents suggests conformational fluctuations. *Biophys J* **47,** 709-720.

Thomas P & Smart TG. (2005). HEK293 cell line: a vehicle for the expression of recombinant proteins. *J Pharmacol Toxicol Methods* **51,** 187-200.

Tretter V, Ehya N, Fuchs K & Sieghart W. (1997). Stoichiometry and assembly of a recombinant GABAA receptor subtype. *J Neurosci* **17,** 2728-2737.

Twyman RE & Macdonald RL. (1992). Neurosteroid regulation of GABAA receptor single-channel kinetic properties of mouse spinal cord neurons in culture. *J Physiol* **456,** 215-245.

Verdoorn TA, Draguhn A, Ymer S, Seeburg PH & Sakmann B. (1990a). Functional properties of recombinant rat GABAA receptors depend upon subunit composition. *Neuron* **4,** 919-928.

Verdoorn TA, Draguhn A, Ymer S, Seeburg PH & Sakmann B. (1990b). Functional properties of recombinant rat GABAA receptors depend upon subunit composition. *Neuron* **4,** 919-928.

CHAPTER 4

THE SINGLE CHANNEL BASIS FOR PARTIAL AGONISM AT THE $\alpha1\beta2\gamma2L$ $GABA_A$ RECEPTOR

A version of this chapter has been submitted for publication.

Introduction

Earlier investigations of the sub-conductance states of the $\alpha1\beta2\gamma2L$ $GABA_AR$ identified three separate conductance currents, the mini-, sub- and full-conductance currents (Chapter 3). In other receptor systems, a link has been observed between the incidence of sub-conductance events and partial agonism. With the nAChR, ion flux studies showed that arecolone methiodide was more potent than ACh but never achieved the same maximum flux rate as ACh (Kawai *et al.*, 2000). The single channel nAChR currents evoked by carbamylcholine (a nAChR full agonist) and arecolone methiodide illustrate two amplitudes of current. The sub-conductance currents appear to be favoured over the full-conductance currents when the receptor in activated by arecolone methiodide, which led Kawai *et al.* (2000) to hypothesize that partial agonists preferentially activate the sub-conductance state of the receptor over the full-conductance state. This may explain why the total current evoked with partial agonists is less than with full agonists. Study of the single channel activity of AMPA-type glutamate receptors activated by a series of partial agonists led Jin *et al.* (2003) to propose that the receptor can achieve a number of conformational states which are dependent on the ligand that activates the channel. These studies point towards ligand specific activation of ligand-gated receptors, which can be observed at the single channel level as differences in the proportion of sub- to full-conductance currents.

Having previously characterized the activated states of the $GABA_AR$ when activated by GABA, the question arose as to how the behaviour of the channel might be different when the receptor is activated with partial agonists and whether the same trends in sub-conductance currents as described above also occur with $GABA_ARs$. 4,5,6,7-

Tetrahydroisoxazolo-[5,4-c]pyridin-3-ol (THIP) and piperidine-4-sulphonic acid (P4S) were chosen as compounds of interest since both of these agonists show less intrinsic activity than GABA at this particular $GABA_AR$. Also, the structure of these two compounds tends to be more rigid than that of GABA (see Figure 4-1), which has been suggested to increase the occurrence of sub-conductance currents (Kawai *et al.*, 2000).

The present study focuses on comparing the frequency of all the conductance states induced by THIP or P4S to receptor activation by GABA at the $\alpha1\beta2\gamma2L$ $GABA_AR$ construct. The same three conductance currents were observed, and while the same trends in frequency were observed, the concentration ranges that elicited the same responses were different. With both THIP and P4S, the receptor did not reach the same maximum frequency of full-conductance currents that was seen with GABA, which suggests one explanation for why these compounds are partial agonists at this particular $GABA_AR$.

Methods

Human $\alpha1\beta2\gamma2L$ $GABA_ARs$ were transiently expressed in HEK293 cultures. Single channel or whole cell electrophysiology was performed on HEK293 cells expressing these receptors as described previously (Chapter 2). In this chapter, whole cell experiments were performed using a perfusion rate of 500 µl/min in a 2ml bath volume. The frequency of channel opening to each current amplitude was determined by counting the number of openings within 500 ms time blocks. Frequency is expressed as the average number of times the channel opened to each current amplitude within 500 ms ± S.E.M.

Results

Concentration-effect Relationship of THIP and P4S Compared to that of GABA

The whole cell currents of HEK293 cells expressing $\alpha1\beta2\gamma2L$ $GABA_A$Rs were recorded after application of a range of concentrations of THIP and P4S. Examples of these currents are illustrated in the top panel of Figure 4-2. The resulting concentration-response curves are shown in the middle panel of Figure 4-2. The response of these receptors to THIP is shifted to the right of the GABA concentration-response curve, with an EC_{50} of around 1 mM and reached at least 81% of the maximum GABA response. P4S has an EC_{50} around 5 μM and reached around 58% of the maximum GABA response. The Hill slope of the GABA concentration-response curve is 1.59 ± 0.3, while this value is 0.90 ± 0.03 for the THIP curve and 1.03 ± 0.35 for the P4S curve. As illustrated, even at 100 nM P4S, whole cell current was still evoked and recordable. At this time, an explanation is not available for this observation. The whole cell responses were used as a parameter for deciding the concentration ranges that would be investigated at the single channel level.

Single Channel Currents

Single channel recordings were made from excised inside-out patches. The membrane holding potential was set at 70 mV with the cytoplasmic face negative to the extracellular face. Three amplitudes of current were seen when the receptor was activated by THIP or P4S, and these amplitudes of current were the same as were seen previously with GABA (Chapter 3). These were defined as the mini-conductance state at 7 pS, the sub-conductance state at 16 pS and the full-conductance state at 29 pS. Sample

single channel currents are shown in Figures 4-3 and 4-4. Amplitude analysis confirmed these current amplitudes as conforming best to three Gaussian populations (Figure 4-5). The mean conductance was determined from the peak of each Gaussian curve, and these values were the same at electrode holding potentials of either +70 mV or -70 mV. GFP did not influence these states (results not shown). Channels closed not only to baseline, but also from full-conductance openings to the sub-, or mini-conductance state, or from sub-conductance openings to the mini-conductance state. These types of closures were regarded as channel closure from the initial current level.

Frequency of Channel Openings to the Various Current Amplitudes

The channel activity at each concentration of THIP and P4S was compared by considering the changes in frequency of openings to each of the three amplitude states. This also gave a means by which to compare the results we found previously with channel activation by GABA. The number of openings to each conductance state was counted in 500 ms time segments from several patches and averaged to determine the mean frequency of openings to any given conductance state at the various concentrations of THIP and P4S investigated.

The frequency of the mini-conductance events rose over the concentration range of 1 μM to 100 μM THIP to around 20 events/bin at 100 μM through to 3 mM THIP (top panel of Figure 4-6). The concentration-effect curves for both the sub- (middle panel of Figure 4-6), and full- (bottom panel of Figure 4-6) conductance currents both increased in a biphasic manner with THIP and P4S. With THIP, the first rise in frequency occurred over the concentration range of 1 μM to 100 μM. The second rise in frequency occurred

over the concentration range of 1 mM and 3 mM THIP to about 40 events/bin. Full-conductance currents increased in frequency initially over the concentration range of 1 μM to 100 μM, and a second time over the concentration range of 1 mM to 3 mM to a maximum of around 25 events/bin.

The frequency of mini-conductance events was greater at lower concentrations of P4S than THIP with the frequency rising over the concentration of 1 nM to 10 nM P4S to around 12 events/bin (top panel of Figure 4-7). This remained constant for the higher concentration of P4S investigated. While the frequency of mini-conductance events increased at lower concentrations of P4S than THIP, the maximum frequency reached with P4S was slightly lower than that of THIP. With P4S, the initial rise in sub-conductance frequency occurred over the concentration range of 1 nM and 10 nM, with the second rise occurring at 100 μM P4S to around 40 events/bin (middle panel of Figure 4-7). The frequency of the full-conductance currents rose initially over the concentration range of 1 nM to 10 nM and the second increase occurred between 1 μM and 100 μM P4S to around 15 events/bin (bottom panel of Figure 4-7).

The frequency of each conductance state elicited by the various concentrations of THIP or P4S are compared with the corresponding GABA induced currents in Figure 4-8. The concentration-effect curves of current frequencies evoked by THIP are consistently shifted to the right of the frequency curves generated from GABA evoked currents. The maximum frequency of mini- and sub-conductance currents was similar for THIP and GABA, but the maximum frequency of full-conductance currents evoked by THIP did not reach the same maximum as with GABA at the respective highest agonist concentrations investigated. The concentration-effect curves evoked by P4S rose along

the same concentration ranges as with GABA, but in the case of the mini- and full-conductance currents, did not rise to the same maximum frequency that GABA evoked currents did at the relative maximal concentrations of these agonists.

Open Duration of the Multiple Amplitude Currents

The open duration of each of the current amplitudes was plotted on Sigworth-Sine plots (Sigworth & Sine, 1987). The average open dwell time was taken from multiple patches. The open durations of the mini-conductance currents evoked by either THIP or P4S were fitted by a single exponential with an average open time of approximately 0.18 ms (see top panels of Figures 4-9 and 4-10). When plotted on a linear time scale, the mini-conductance currents were fitted best by a single exponential (see top panel of Figure 4-11), with a time constant of 0.16 ms for THIP evoked currents and 0.23 ms for P4S evoked currents. As with GABA evoked mini-conductance currents, the duration of the mini-conductance currents are very close to our limit of detection. However, the observation of longer duration openings to this current amplitude suggests that it is a true amplitude state. The sub- and full-conductance currents were both fitted best with two exponentials. Using the probability density function, the mean open durations of THIP evoked sub-conductance currents were determined to be 0.23 ms and 1.23 ms (see middle panel of Figure 4-9), while with P4S the mean durations were 0.30 ms and 2.52 ms (see middle panel of Figure 4-10). The mean open durations of the full-conductance currents were 0.32 ms and 2.07 ms with THIP (see bottom panel of Figure 4-9) and 0.27 ms and 1.51 ms with P4S (see bottom panel of Figure 4-10). This is summarized in Table 4-1. The open durations of sub- and full-conductance currents were also plotted on a linear

time scale and the time constants were measured by exponential decay. Both the sub- and full-conductance currents were fitted best with two exponentials. The time constants of THIP induced sub-conductance currents are 0.32 and 2.15 ms (middle panel of Figure 4-11), and 0.40 and 1.81 ms (bottom panel of Figure 4-11) for full-conductance currents at 100 μM THIP. For currents evoked by 10 μM P4S, the time constants of the sub-conductance currents are 0.50 and 1.37 ms (middle panel Figure 4-12) and for the full-conductance currents the time constants are 0.28 and 1.17 ms (bottom panel Figure 4-12).

Using the probability density function, the proportion of long to short sub- and full-conductance events were compared. The proportion of long and short duration sub-conductance events to total sub-conductance events did not change significantly with concentration of THIP with there being a larger population of short sub-conductance currents to long sub-conductance currents at the concentrations considered (top panel of Figure 4-13). With P4S, there was a predominance of short sub-conductance currents at 1 μM to slightly more long sub-conductance currents at 10 μM and 100 μM P4S. The proportion of short and long full-conductance currents did not change significantly with concentration of THIP or P4S (bottom panel of Figure 4-13) and at all the concentrations considered there was a greater proportion of short full-conductance currents to long full-conductance currents.

Discussion

Using Fox's criteria for substates (1987), initial studies by our laboratory provided evidence for the sub-conductance currents of the $\alpha1\beta2\gamma2L$ $GABA_AR$ being true substates of the channel (Chapter 3). These criteria include transitions observed between conductance states, the observation that all of the conductance currents occurred in the

same patches without any occurring in the absence of the others and the lack of summation of these currents. The frequency of openings to each current amplitude state and the open duration of each current state were originally determined at various concentrations of GABA to typify the behaviour of the sub-conductance currents. In an attempt to characterize the sub-conductance currents of the $GABA_AR$ further, these same parameters of channel activation were investigated using the partial agonists THIP or P4S to activate the receptor. The three amplitudes of current that were elicited with GABA were also elicited by either THIP or P4S. These agonists do not change the conductance of the channel and this indicates that three different agonists of various efficacies can activate the same three amplitude states of the receptor. This is further supported by the open duration analysis of the amplitude states. More certainly than with GABA, there is apparently only one discernable population of mini-conductance currents, and two populations each of sub- and full-conductance currents. It follows that GABA, THIP and P4S generate the same activated states of the $GABA_AR$.

Classical whole cell recording techniques illustrated the differences in the intrinsic activity of THIP or P4S compared to GABA. These results compare well with the findings of other laboratories (Ebert *et al.*, 1994; Mortensen *et al.*, 2004). The intrinsic activity of these compounds compared to GABA is: GABA > THIP > P4S. However, the potency of these compounds is GABA >P4S > THIP.

The frequency of the channel opening to each conductance state was chosen as a means to compare the activity of each conductance state at various concentrations of agonist. The frequency of openings of the three conductance states followed the same trends in increasing frequency with increasing concentration of agonist. These agonists

differed in the concentrations that were required to achieve the same frequency of response from any particular conductance state. This was hypothesized from the whole cell concentration-effect curves since these compounds do differ in potency.

Mini-conductance events evoked by THIP increased in frequency over a concentration range significantly higher than the range of GABA concentrations required for the same effect. The THIP concentration-effect curve was also shifted to the right of the GABA curve. With P4S, the curve was shifted to the right of GABA concentration-effect curve, and never achieved the same maximum number of events as with GABA or THIP. The sub-conductance events evoked by THIP and P4S both increased in frequency in a biphasic manner, just as with GABA. Again, the THIP concentration-effect curve was shifted to the right of the GABA concentration-effect curve while P4S rose over the same concentration ranges as GABA. The frequency of full-conductance events showed the same trend again, with THIP increasing over a higher concentration range than GABA or P4S. As was observed with GABA, the frequency of each of the different current amplitude events increased over different concentrations of agonist. This further supports each of these currents being the product of different binding events with each ligand having different affinity for each binding site.

Neither THIP nor P4S achieved the same maximum frequency of full-conductance events as was seen with GABA (around 40/ 500 ms), but THIP was closer at around 30 events/ 500 ms than P4S which was significantly lower at around 15 events/ 500 ms. This may partly explain why P4S has lower intrinsic activity than GABA. The greatest amount of current will flow through the full-conductance state, and since this state is not achieved as frequently with P4S as with GABA, total current passed in a set

frame of time will be less as well. THIP, on the other hand, reached around 80% of the maximum GABA whole cell response and achieved slightly lower full-conductance opening frequency at the maximum concentrations investigated. This suggests that P4S, and to a lesser extent THIP, do not allow the receptor to achieve the full-conductance state as readily as GABA. This may represent an inability of the receptor construct to achieve a specific conformation that allows current to flow as readily through the full-conductance state. The second observation noted from the concentration-frequency curves was that none of the conductance states appear to be dependent upon the others. An increase in the frequency of the sub-conductance events does not do so at the expense of the mini-conductance events, and an increase in the frequency of the full-conductance events does not do so at the expense of the sub- or mini-conductance events. These states, therefore, do not appear to show any cooperativity or dependence to each other. This is further supported by the examination of the proportion of short and long full-conductance events across a range of agonist concentration. With increasing GABA concentrations we noted an increase in the proportion of long full-conductance to short full-conductance events (Chapter 3). This same trend did not hold true with THIP or P4S. It appears as though neither THIP nor P4S are capable of achieving a dominance of long full-conductance currents. This may offer an additional reason for why these two compounds have a lower intrinsic activity than GABA.

The data presented here support the hypothesis that separate binding sites lead to different activated states of the receptor, based on the different estimated EC_{50} values obtained for the frequency plots of each conductance state. It appears that individual agonists cause different proportions of openings to the different conductance states and

that the EC_{50} values for each frequency plot are dependent upon the agonist used to elicit the response. It would follow that the generation of fewer full-conductance events, and additionally fewer long full-conductance events, as was seen with channel activation with P4S and to a lesser extend THIP when compared with GABA, provides a functional reason for P4S and THIP being partial agonists at this particular $GABA_AR$ construct.

Guyon *et al.* (1999) argued that there are not enough binding sites to accommodate a theory that involves each conductance state representing an activated state of a single receptor. However, it was proposed by Newell *et al.* (2000) that while the conventional agonist binding sites are at the β-α subunit interfaces (see Smith & Olsen, 1995), an addition binding site may be located at the α-β subunit interface (Newell *et al.*, 2000). This site was proposed to play a role in stabilizing the desensitized state of the receptor but its ability to bind agonist would suggest that binding might be manifest as a distinct active state. While this binding site is not accepted by all (Baur & Sigel, 2003), binding studies of the nAChR have yielded results that point to the possibility of subsites for binding at the conventional ACh binding site (Dunn & Raftery, 1997b, 1997a). Therefore, additional binding sites for GABA on the $GABA_AR$ complex that influence channel behaviour besides the two binding sites on the β-α interfaces cannot be dismissed.

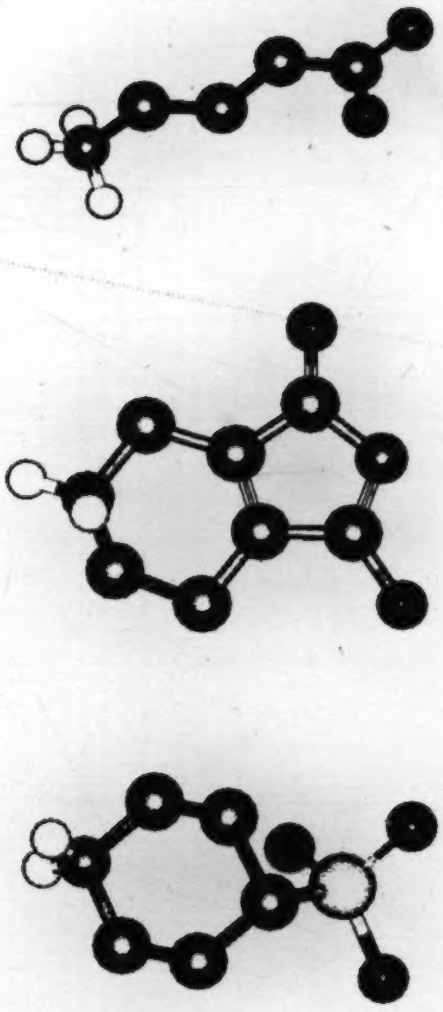

Figure 4-1: Three $GABA_AR$ agonists. From top to bottom, the structures of GABA (γ-aminobutyric acid), THIP (4,5,6,7-tetrahydroisoxazolo-[5,4-c]pyridin-3-ol) and P4S (piperidine-4-sulphonic acid).

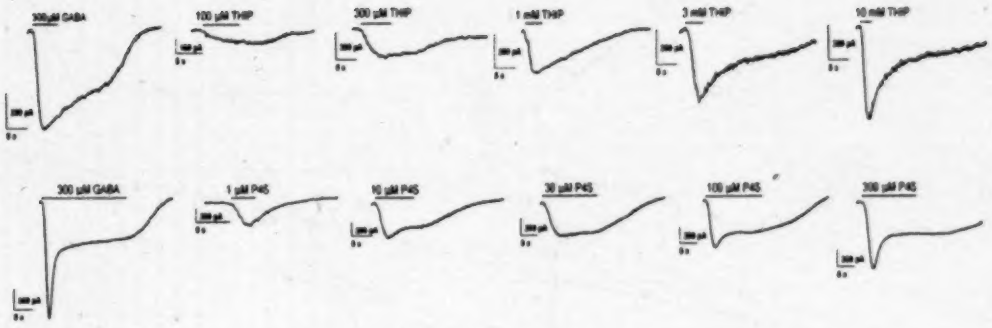

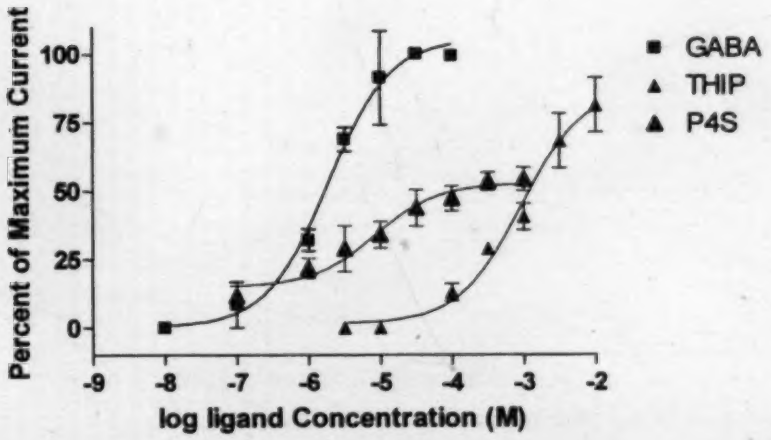

Ligand	log EC_{50} (M)	% Max I	Hill slope
GABA	-5.72 ± 0.04	100	1.59 ± 0.3
THIP	-3.14 ± 0.06	81.4 ± 5.7	0.90 ± 0.03
P4S	-5.45 ± 0.41	57.7 ± 1.1	1.03 ± 0.35

Figure 4-2: Whole cell responses to GABA, THIP or P4S. Top panel shows sample whole cell currents from HEK293 cells expressing α1β2γ2L $GABA_AR$. The top line compares THIP induced currents to the cells maximal response to GABA. The second line compares P4S currents to maximal GABA induced current. Below are the corresponding whole cell concentration-effect curves for GABA, THIP and P4S. The table illustrates the potency and intrinsic activity of each of these compounds. Results represent means ± S.E.M from three different cells.

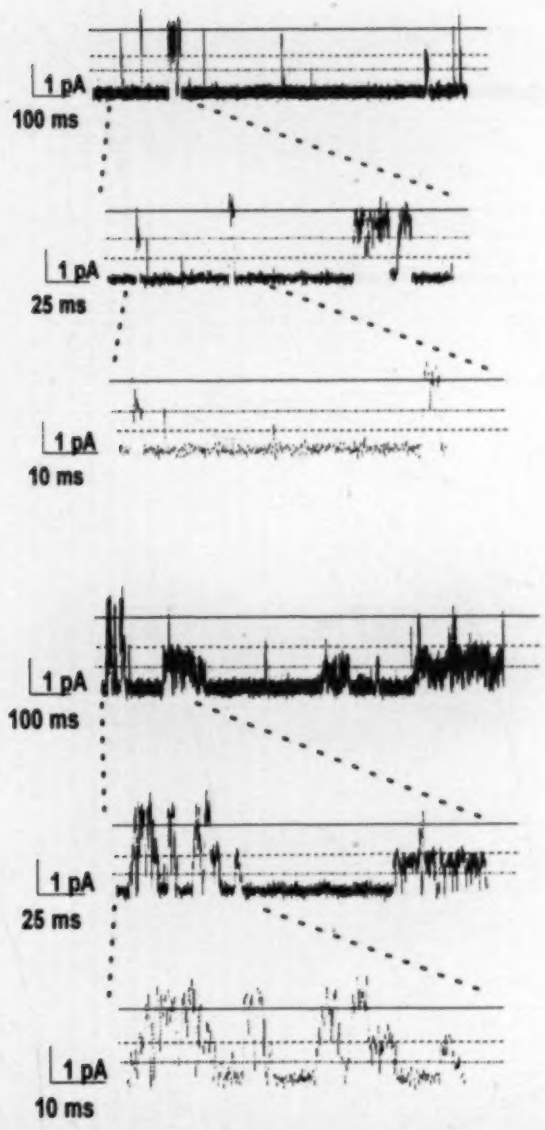

Figure 4-3: Sample single channel recordings evoked by THIP. HEK293 cells expressing $\alpha 1\beta 2\gamma 2L$ $GABA_AR$ were exposed to THIP. Top 3: currents evoked by exposure to 10 μM THIP. Channel opening to mini-, sub-, and full-conductance levels are evident. Bottom 3: currents induced by 1mM THIP. The incidence of sub- and full-conductance events appears to increase with concentration, and mini-conductance openings are still evident. Solid lines indicate full-conductance currents, dashed lines illustrate sub-conductance currents and dotted lines depict mini-conductance currents.

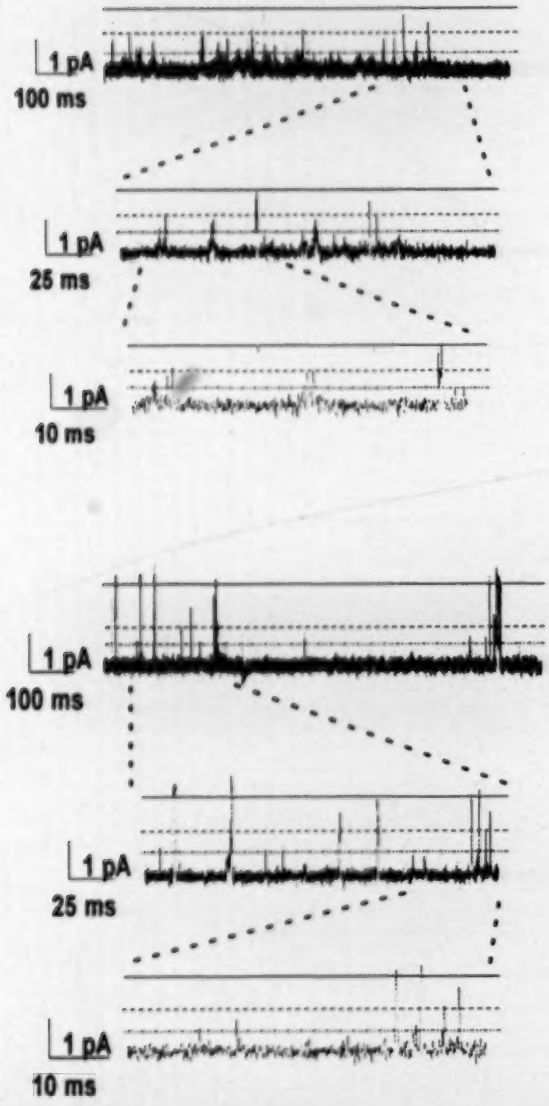

Figure 4-4: Sample single channel recordings evoked by P4S. HEK293 cells expressing $\alpha 1\beta 2\gamma 2L$ $GABA_AR$ were exposed to P4S. Top 3: currents induced by exposure to 10 nM P4S. While full-conductance currents are evident, mini- and sub-conductance currents appear to occur more frequently. Bottom 3: currents induced by 10 μM P4S. The incidence of full-conductance events increases with concentration, however, the appearance of mini- and sub-conductance currents are still very apparent. Solid lines indicate full-conductance currents, dashed lines illustrate sub-conductance currents and dotted lines depict mini-conductance currents.

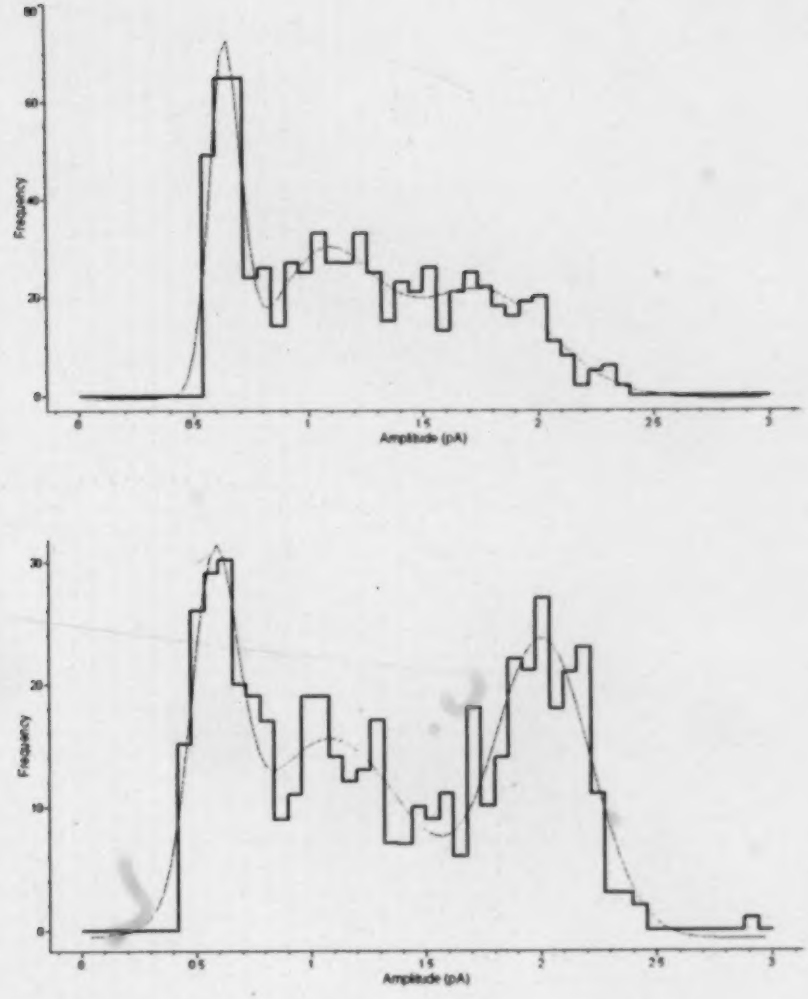

Figure 4-5: Amplitude histograms from channel activation with THIP or P4S. Amplitude analysis of the single channel currents from α1β2γ2L $GABA_A$Rs activated by THIP (top panel) or P4S (bottom panel) are fitted best with three Gaussian populations with r^2 values of 0.82 and 0.79 respectively. These results correspond very closely to the results we obtained for receptors activated by GABA (see Figure 3-3). Top: 100 μM THIP. Bottom: 10 μM P4S.

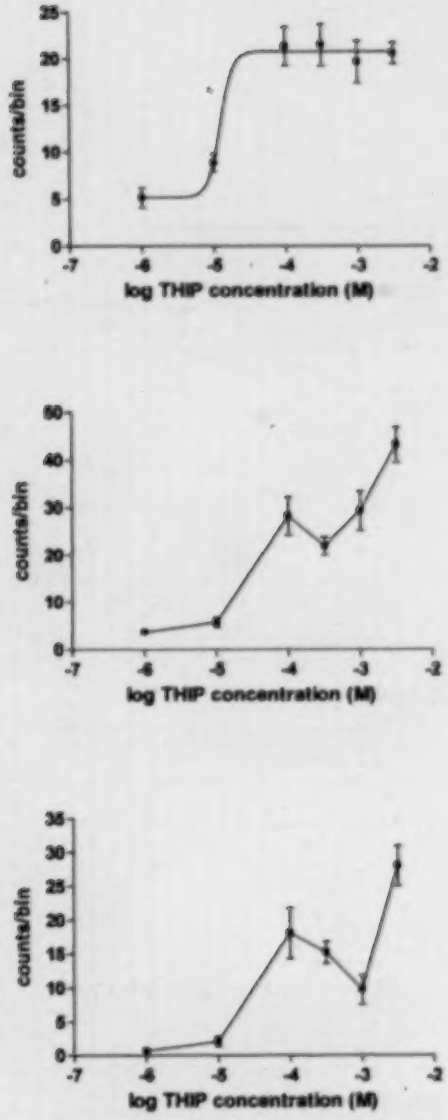

Figure 4-6: Frequency of conductance events at various concentrations of THIP. Graphs show the average number of events ± S.E.M. per 500 ms bin from at least 25 bins accumulated from 3 to 4 different patches at each THIP concentration for: mini-conductance events (top panel), sub-conductance events (middle panel) and full-conductance events (bottom panel). The mini-conductance events were fitted with a sigmoidal concentration-effect curve while the points were joined for the sub- and full-conductance events.

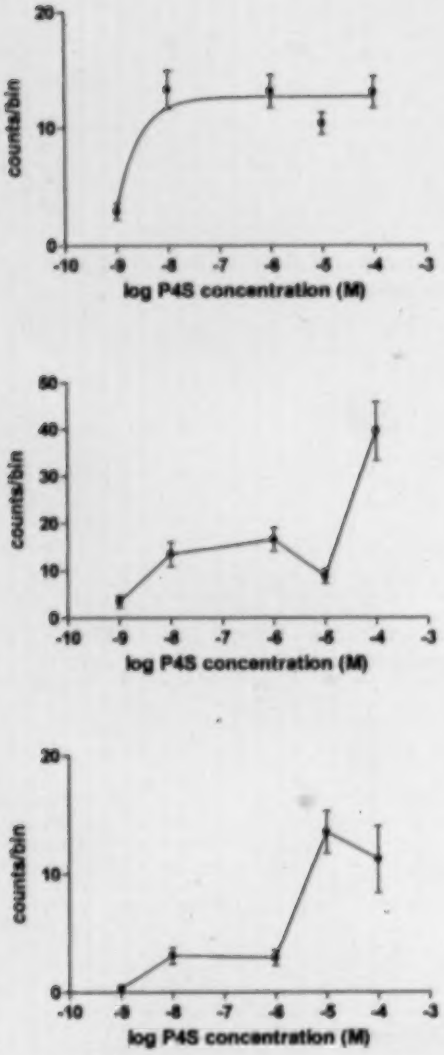

Figure 4-7: Frequency of conductance events at various concentrations of P4S. Graphs show the average number of events ± S.E.M. per 500 ms bin from at least 25 bins accumulated from 3 to 4 different patches at each P4S concentration for: mini-conductance events (top panel), sub-conductance events (middle panel) and full-conductance events (bottom panel). The mini-conductance events were fitted with a sigmoidal concentration-effect curve while the points were joined for the sub- and full-conductance events.

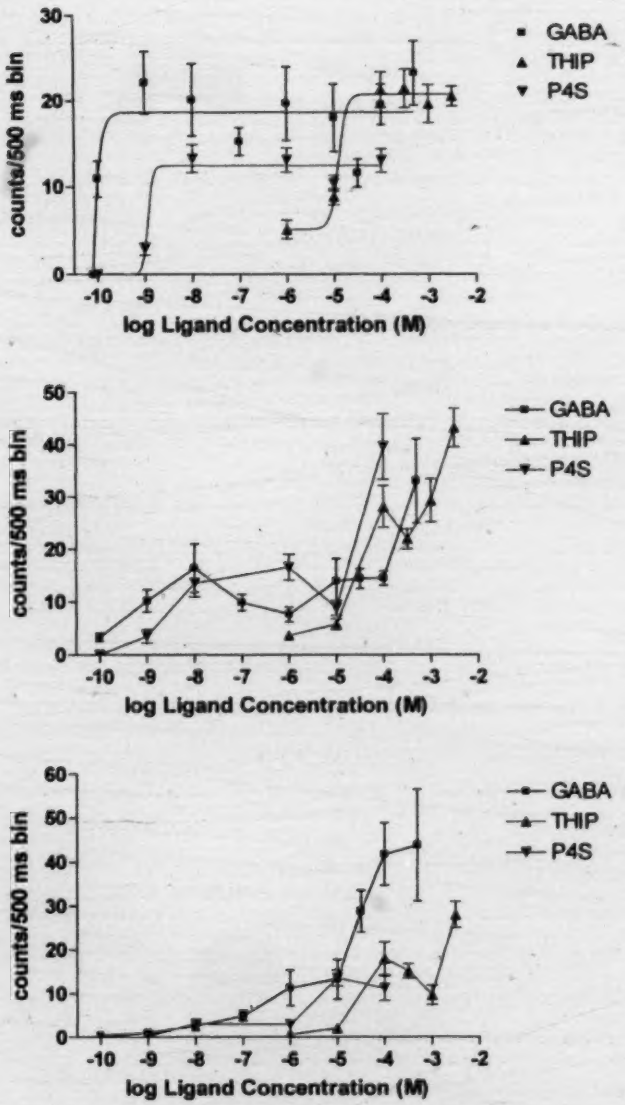

Figure 4-8: Comparison of the frequency of conductance events at various concentrations of agonists. Each of these concentration-effect plots has been shown individually previously (GABA Figure 3-4, THIP Figure 4-6 and P4S Figure 4-7). From top to bottom: mini-conductance events, sub-conductance events and full-conductance events. Results are expressed as means ± S.E.M.

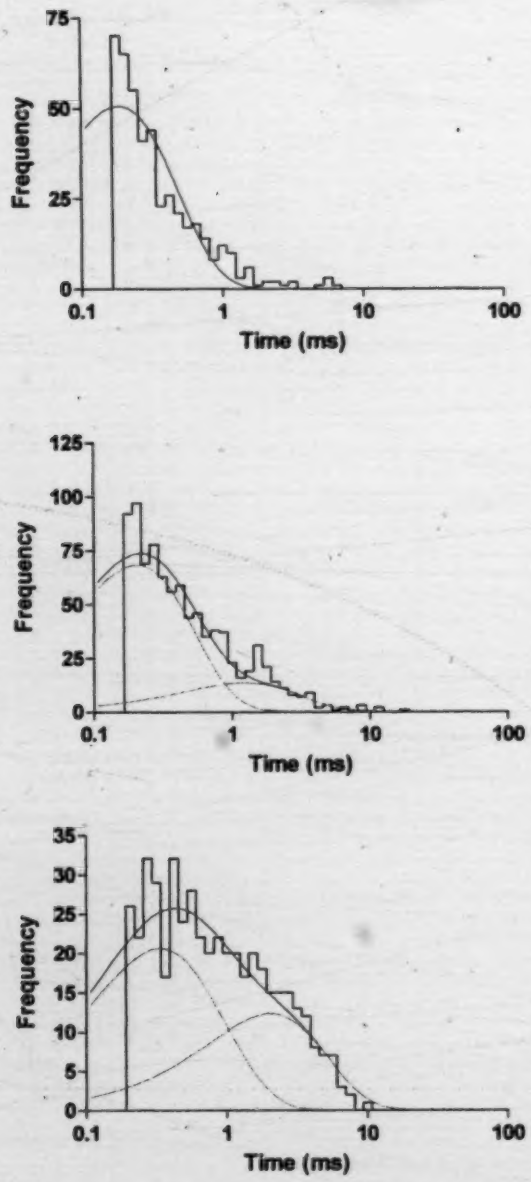

Figure 4-9: Open duration of $GABA_A$Rs activated by THIP: mini-, sub, and full-conductance current durations at 100 μM THIP. The open duration of the mini-conductance state (top panel) is fitted with a single exponential, while the sub-conductance (middle panel) and full-conductance (bottom panel) open durations are both fitted by two exponentials in the above Sigworth-Sine plots.

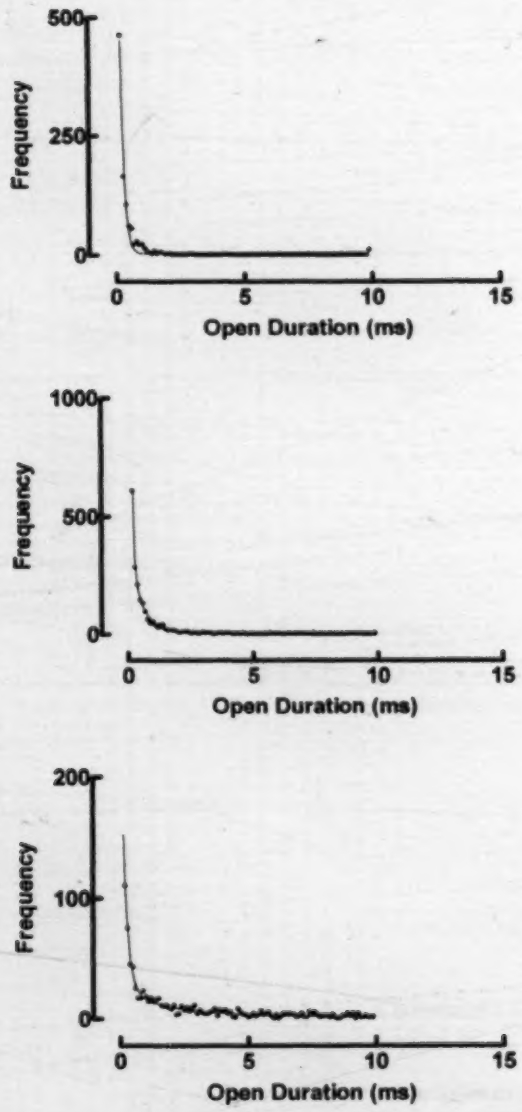

Figure 4-10: Open duration analysis of $GABA_A$Rs activated by 100 μM THIP. When plotted on a linear time scale, the open duration of the mini-conductance currents (top panel) were fitted best with a single exponential with a tau value of 0.16 ms. The open duration of both the sub- (middle panel) and full- (bottom panel) conductance currents were both fitted best with two exponentials. For the sub-conductance currents, the tau values are 0.32 and 2.15 ms, and for the full-conductance currents these values are 0.40 and 1.81 ms.

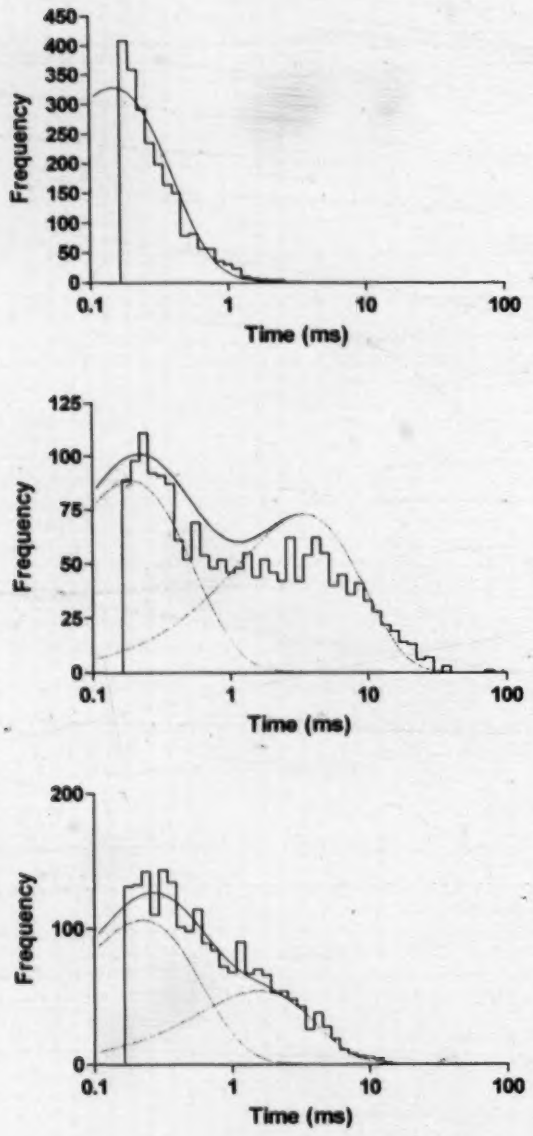

Figure 4-11: Open duration of $GABA_AR$ activated by P4S: mini-, sub, and full-conductance current durations at 10 μM P4S. The open duration of the mini-conductance state (top panel) is fitted with a single exponential, while the sub-conductance (middle panel) and full-conductance (bottom panel) open durations are both fitted with two exponentials.

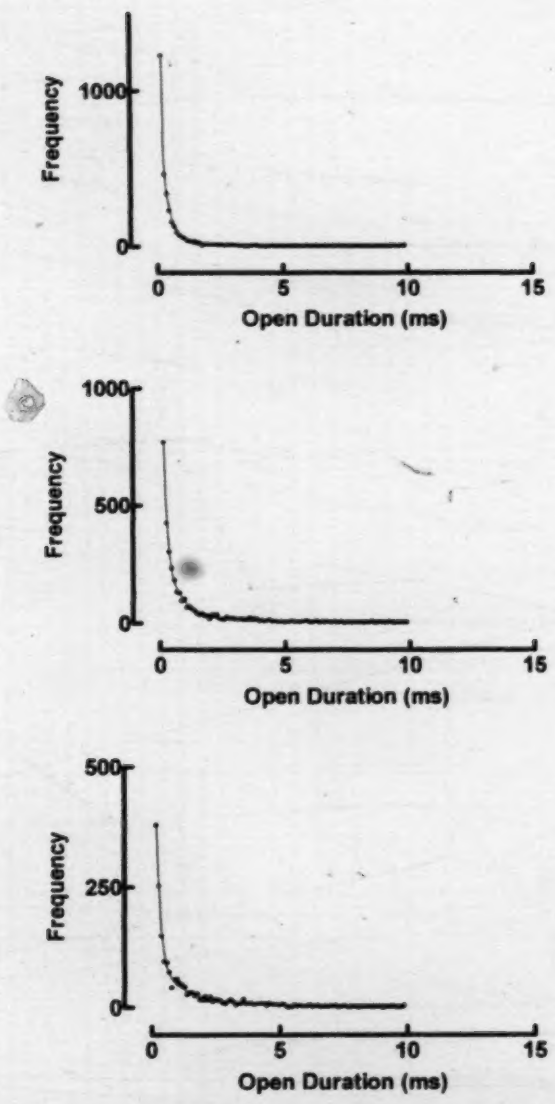

Figure 4-12: Open duration analysis of $GABA_AR$ activated by 10 μM P4S. When plotted on a linear time scale, the open duration of the mini-conductance currents (top panel) were fitted best with a single exponential with a tau value of 0.23 ms. The open duration of both the sub- (middle panel) and full- (bottom panel) conductance currents were both fitted best with two exponentials. For the sub-conductance currents, the tau values are 0.50 and 1.37 ms, and for the full-conductance currents these values are 0.28 and 1.17 ms.

	Mini-conductance		Sub-conductance				Full-conductance			
	τ	Area	τ1	Area 1	τ2	Area 2	τ1	Area 1	τ2	Area 2
THIP										
10 μM	0.19 ± 0.01	100 ± 1.52	0.24 ± 0.02	90.68 ± 2.19	1.22 ± 0.24	18.6 ± 18.68	0.27 ± 0.03	66.05 ± 6.59	2.01 ± 0.52	41.31 ± 6.71
100 μM	0.19 ± 0.02	100 ± 8.83	0.22 ± 0.02	93.06 ± 10.37	1.23 ± 0.12	18.23 ± 6.06	0.30 ± 0.09	69.23 ± 10.09	2.21 ± 0.19	39.37 ± 21.90
300 μM	0.15 ± 0.01	100 ± 4.06	0.24 ± 0.01	93.11 ± 4.05	1.24 ± 0.21	18.21 ± 2.29	0.38 ± 0.04	85.04 ± 8.72	2.00 ± 1.38	23.07 ± 9.02
P4S										
1 μM	0.23 ± 0.03	100 ± 1.22	0.51 ± 0.05	82.71 ± 5.17	2.25 ± 0.38	28.55 ± 4.12	0.30 ± 0.04	66.2 ± 17.82	1.22 ± 0.59	40.54 ± 17.75
10 μM	0.16 ± 0.01	100 ± 1.70	0.16 ± 0.03	41.39 ± 14.37	3.83 ± 0.35	61.21 ± 13.19	0.27 ± 0.04	73.06 ± 9.80	1.64 ± 0.16	36.63 ± 8.00
100 μM	0.17 ± 0.02	100 ± 3.01	0.23 ± 0.04	42.48 ± 12.3	1.47 ± 0.61	61.53 ± 13.9	0.25 ± 0.09	90.22 ± 7.32	1.66 ± 0.88	21.96 ± 4.36

Table 4-1: Summary of open duration analysis. The open time duration (τ) and the proportion of current at each amplitude of current that activates to either short (τ) or long (τ) sub- or full-conductance openings are summarized. Tau values are reported in milliseconds while area is a percentage. All values are reported as means ± S.E.M.

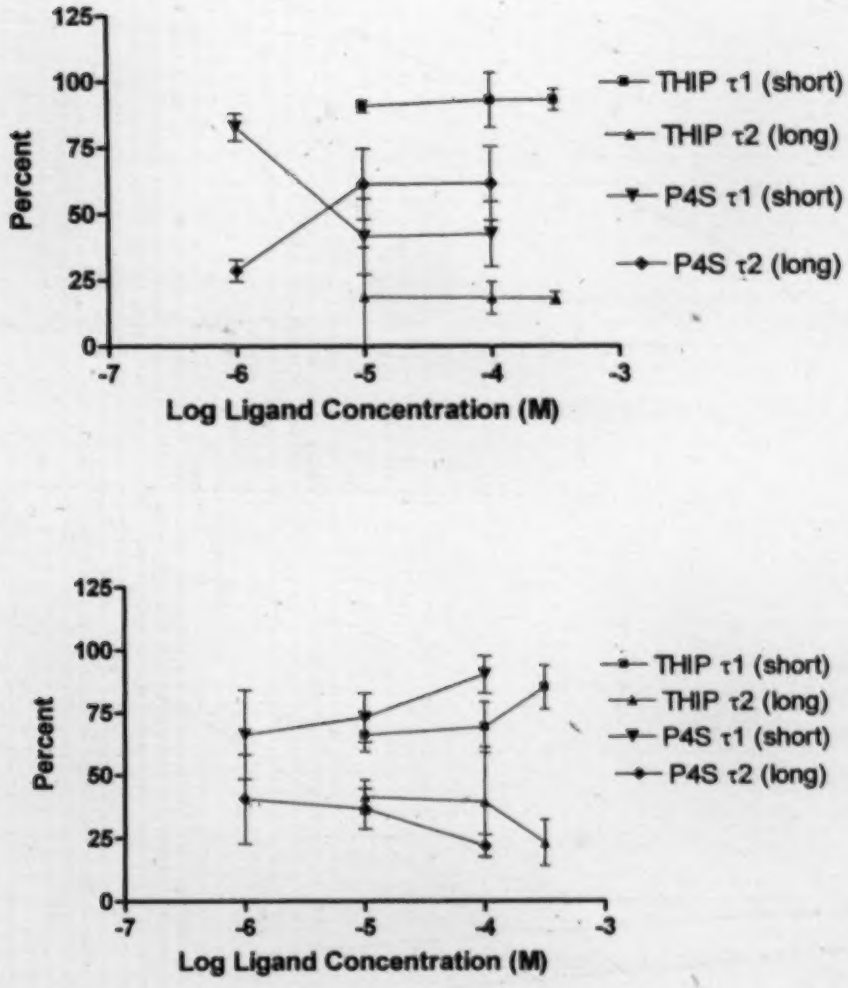

Figure 4-11: Proportion of long to short sub- or full-conductance openings. Top panel shows the proportion of short to long sub-conductance events at various concentrations of THIP or P4S. This proportion did not change significantly with the concentrations of THIP investigated. This proportion did change over the concentration range of 1 μM to 10 μM P4S, and then remained constant at 100 μM. Bottom panel shows the proportion of short to long full-conductance events to total full-conductance events. This proportion did not change significantly with the various concentrations of agonists investigated. Results are expressed as means ± S.E.M.

Bibliography

Baur R & Sigel E. (2003). On high- and low-affinity agonist sites in GABAA receptors. *J Neurochem* **87,** 325-332.

Dunn SM & Raftery MA. (1997a). Agonist binding to the Torpedo acetylcholine receptor. 1. Complexities revealed by dissociation kinetics. *Biochemistry* **36,** 3846-3853.

Dunn SM & Raftery MA. (1997b). Agonist binding to the Torpedo acetylcholine receptor. 2. Complexities revealed by association kinetics. *Biochemistry* **36,** 3854-3863.

Ebert B, Wafford KA, Whiting PJ, Krogsgaard-Larsen P & Kemp JA. (1994). Molecular pharmacology of gamma-aminobutyric acid type A receptor agonists and partial agonists in oocytes injected with different alpha, beta, and gamma receptor subunit combinations. *Mol Pharmacol* **46,** 957-963.

Guyon A, Laurent S, Paupardin-Tritsch D, Rossier J & Eugene D. (1999). Incremental conductance levels of GABAA receptors in dopaminergic neurones of the rat substantia nigra pars compacta. *J Physiol* **516 (Pt 3),** 719-737.

Jin R, Banke TG, Mayer ML, Traynelis SF & Gouaux E. (2003). Structural basis for partial agonist action at ionotropic glutamate receptors. *Nat Neurosci* **6,** 803-810.

Kawai H, Cao L, Dunn SM, Dryden WF & Raftery MA. (2000). Interaction of a semirigid agonist with Torpedo acetylcholine receptor. *Biochemistry* **39,** 3867-3876.

Mortensen M, Kristiansen U, Ebert B, Frolund B, Krogsgaard-Larsen P & Smart TG. (2004). Activation of single heteromeric GABA(A) receptor ion channels by full and partial agonists. *J Physiol* **557,** 389-413.

Newell JG, Davies M, Bateson AN & Dunn SM. (2000). Tyrosine 62 of the gamma-aminobutyric acid type A receptor beta 2 subunit is an important determinant of high affinity agonist binding. *J Biol Chem* **275,** 14198-14204.

Sigworth FJ & Sine SM. (1987). Data transformations for improved display and fitting of single-channel dwell time histograms. *Biophys J* **52,** 1047-1054.

Smith GB & Olsen RW. (1995). Functional domains of GABAA receptors. *Trends Pharmacol Sci* **16,** 162-168.

CHAPTER 5

PROBING $GABA_AR$ FUNCTION WITH NOVEL BISFUNCTIONAL LIGANDS: THE POLYMETHYLENE DIGABAMIDES

A version of this chapter will be submitted for publication
The concentration-dependence desensitization experiments were
performed with the assistance of Isabelle Paulsen

Introduction

Polymethylene digabamides were synthesized as novel $GABA_A$ receptor agonists (Carlier *et al.*, 2002). These compounds are composed of two GABA residues separated by a polymethylene chain (see Figure 5-1). Analogous bischoline compounds have been investigated with the nAChR and led to the hypothesis that there are multiple binding sites on the nAChR (Dunn and Raftery, 1997a&b; Carter *et al.*, 2006). On the premise that there are likely at least two binding sites for GABA on the $GABA_AR$ (Newell *et al.*, 2000), the polymethylene digabamides offer a unique tool for investigating the function of these binding sites. These compounds are termed bisfunctional ligands since they are capable of binding to two GABA binding sites simultaneously if the GABA residues and binding site separation are congruent. Using chloride flux methods in mouse synaptoneurosomes, one compound (butylene digabamide) was labelled a 'superagonist' (Carlier *et al.*, 2002). The present work was undertaken to investigate the 'superagonism' of butylene digabamide using conventional whole cell electrophysiology and to establish the effect of altering the distance between GABA moieties on receptor response. From information linking GABA moiety separation and response, the relationship of binding sites additional to the accepted high affinity binding pocket might be revealed. We have compared the potency, intrinsic activity and desensitization kinetics of a series of polymethylene digabamides in HEK293 cells and *Xenopus* oocytes expressing human $\alpha1\beta2\gamma2L$ $GABA_A$ receptors. The results observed with the polymethylene digabamides were compared with those of GABA as well as with the potent $GABA_AR$ agonist Z-3-[(aminoiminomethyl)thio] prop-2-enoic acid (ZAPA).

Methods

Human α1β2γ2L $GABA_A$Rs were expressed in HEK293 cells and *Xenopus laevis* oocytes as described in Chapter 2. Conventional whole cell and two-electrode voltage clamp techniques were used to measure current. Expression in HEK293 cells was used to generate whole cell concentration-response curves. In this chapter, whole cell experiments were performed as described previously but using a perfusion rate of 1 ml/min into a 2 ml recording dish. *Xenopus* oocytes were used in the desensitization experiments.

Results

The Polymethylene Digabamides

A series of polymethylene digabamides with between two methyl groups (n=2) and six methyl groups (n=6) separating the GABA moieties were investigated for their intrinsic activity and potency at the α1β2γ2L $GABA_A$R. The generic structure of these compounds is shown in Figure 5-1. When these compounds are fully extended, the maximum length separating the nitrogen groups of the GABA residues (max N-N distance) ranges between 16.4 and 21.2 Å within this series of compounds (see Table 5-1).

Whole Cell Currents of α1β2γ2 $GABA_A$R Activated by the Polymethlyene Digabamides

The whole cell concentration-effect curves were determined from transiently transfected HEK293 cells expressing the α1β2γ2L $GABA_A$R. Sample currents elicited

by the various polymethylene digabamides are shown in Figure 5-2a. The resulting concentration-effect curves are shown in Figure 5-2b. Due to the rate of the perfusion system, the exchange times are not particularly fast, but the concentration-response curves none the less provide a means of comparing the intrinsic activities and potencies of the various compounds. Compared to the perfusion system used in Chapters 3 and 4, this system flowed twice as fast and this difference could be observed in the resulting GABA concentration-effect curves. In this chapter, the GABA concentration-effect curve is further to the right than in the previous chapters, suggested that desensitization may have truncated the maximal current responses in Chapters 3 and 4.

The shortest polymethylene digabamide compound investigated, ethylene digabamide, showed very little intrinsic activity. However, the next compound in the series, propylene digabamide, showed significantly greater intrinsic activity. However, this compound was still a partial agonist compared with GABA with an intrinsic activity of approximately 60%.

Butylene digabamide was shown in ion flux experiments in mouse synaptosomes to evoke more Cl^- flux through the $GABA_A$Rs than GABA, and was thus referred to as a 'superagonist' (Carlier *et al.*, 2002). In whole cell experiments, butylene digabamide did not evoke a greater current than GABA, and therefore does not appear to behave as a 'superagonist' under the conditions of our experiments. Butlyene, pentylene or hexylene digabamides are all partial agonists at this receptor, and an increase in chain length from four methyl groups to six methyl groups reduced the potency of these compounds as seen by the rightward shift in the concentration-effect curves. ZAPA appears as a full agonist at this $GABA_A$R, and is more potent than GABA. The maximum current elicited by each

compound compared to GABA and their corresponding EC_{50} values are summarized in Table 2. Butylene digabamide was also tested in *Xenopus* oocytes expressing the same receptors as the HEK293 cells to verify that it could not elicit more current than GABA. The results seen in oocytes were comparable to the HEK293 data, however a difference in the current decay, or the rate of desensitization with butlyene digabamide compared to GABA was noted and further investigated.

Desensitization of $GABA_AR$ with Polymethlyene Digabamides

The desensitization of $GABA_AR$ in the presence of the polymethylene digabamides was compared to that seen with GABA and ZAPA. Samples of these currents can be seen in Figure 5-4. Both GABA and ZAPA currents decayed exponentially with two phases, a fast component and a slow component. The decay of current was fitted with exponentials by best fit analysis using Clampfit 9. Since ethylene digabamide has such low intrinsic activity, the rate of desensitization with this compound could not be determined. Propylene digabamide evoked the same fast and slow components of desensitization that GABA and ZAPA evoked, while with the butylene, pentylene or hexylene digabamides only the slow rate of desensitization could be seen. These results are summarized in Table 5-3. Jones and Westbrook (1995) described a two binding site model for $GABA_AR$ activation and desensitization. This model described mono-liganded receptors activating to a brief open state then desensitizing to a long desensitized state while bi-liganded receptors enter a longer open state that leads to a rapid desensitized state. With low concentrations of ligand, this model would predict receptors predominantly entering the long desensitized state over the short desensitized

state. A shift of more receptors entering the short desensitized state would be predicted with increasing ligand concentration. While this model may be useful in describing the results observed with the polymethylene digabamides, the validity of this model was further tested by considering the desensitization rate of this $GABA_AR$ at sub-maximal concentrations of GABA.

Concentration Dependence of $GABA_AR$ Desensitization with GABA or ZAPA

The rate of $GABA_AR$ desensitization was measured at concentrations of GABA ranging from 30 μM to 10 mM and concentrations of ZAPA from 10 μM to 1 mM. The activation and desensitization of these currents at various concentrations of agonist can be seen in Figure 5-4. At concentrations of agonist less than approximately the EC_{70} value, the desensitization of these currents resulted in only a single exponential of decay that corresponds to the slow desensitization component. Graphing the proportion of current that desensitizes in the fast and slow components of desensitization (see Figure 5-5) illustrates that at concentrations greater than the EC_{75} of the agonist, both a fast and slow component of desensitization were measurable, while at concentrations less than this value only the slow component of desensitization was measurable. The proportion of the fast component rose dramatically from 0% to between 20-25%, which remained constant at the higher concentrations of agonist, while the corresponding proportion of the slow component decreased from 100% to around 75-80%.

Discussion

The polymethylene digabamide compounds offer a unique opportunity to study the activation of the $GABA_AR$ due to the two GABA residues that make up each compound. The initial goal of this investigation was to determine if there is an optimal distance of separation between the two GABA moieties as this may reflect the relative distance separating two binding sites on the receptor construct. Secondly, due to the observation that one of these compounds, butylene digabamide, appeared as a 'superagonist' in ion flux experiments (Carlier *et al.*, 2001), this compound was examined for any indication of behaviour that would point to this compound having greater intrinsic activity than GABA.

Whole cell currents

By measuring whole cell currents evoked by each polymethylene digabamide compound, it was determined that the entire series of polymethylene digabamide compounds investigated are partial agonists at the $\alpha1\beta2\gamma2L$ $GABA_A$ receptor. While the shortest polymethylene digabamide compound, ethylene digabamide, showed little intrinsic activity, there was a dramatic increase in intrinsic activity between ethylene digabamide and propylene digabamide. This suggests that ethylene digabamide lacks the ability either to bind to the receptor or to initiate channel activation. It may be possible, due to its shorter structure than the other polymethylene digabamides, that there is a higher degree of steric hindrance which reduces its ability to bind to the receptor binding pocket. Clearly there is a functional significance of adding one additional methyl group to ethylene digabamide. The result is a dramatic difference in the intrinsic activity of a

digabamide compound with a maximal separation of 17.4 Å between amino groups in the GABA moieties with that of a digabamide compound with the same separation distance being 16.4 Å. Since these measurements are the maximal length that the compound can achieve, it is also possible that the difference in the compounds seen at the receptor is greater than a single Angstrom if these two compounds fold slightly differently from each other in solution.

Butylene digabamide

The highlighted compound butylene digabamide does not behave as a 'superagonist' at the $\alpha1\beta2\gamma2L$ $GABA_AR$ according to the whole cell currents that it can evoke. Also, the compounds with 4, 5 and 6 methyl groups between GABA moieties showed a trend towards a decrease in affinity with increasing length. A separation of GABA moieties greater than 18.7 Å, therefore, reduces the potency of these bisfunctional ligands. Another trend noted with these particular compounds was that the desensitization observed showed only a single exponential of decay, corresponding to the slow component of desensitization observed with 1 mM GABA. Both a fast and a slow component were seen when receptors were desensitized by GABA, ZAPA or propylene digabamide at concentrations that evoke maximal response. Together with the high intrinsic activity of butylene digabamide, the lack of the fast desensitization rate may explain why this compound appeared as a 'superagonist' in ion flux experiments in mouse synaptosomes as reported by Carlier *et al.* (2002). This reduction in desensitization equates to greater charge transfer with activation by butylene digabamide compared to GABA over the duration of ion flux measurements. Charge is the integral of

current with respect to time which, in the case of the $GABA_AR$, is carried by chloride ions. Thus, the 'superagonism' observed by Carlier *et al.* (2002) can be explained in terms of slower overall desensitization of the receptor. Of course, the presence of a heterogeneous population of $GABA_A$ receptors in the mouse synaptosomes used by Carlier *et al.* (2002) may offer an alternative explanation, since these compounds may exhibit different affinities and potencies at different $GABA_AR$ constructs.

Desensitization

Since desensitization is a behaviour of bound receptors, the lack of a fast desensitization component may indicate differences in binding between the butylene, pentylene or hexylene digabamides and GABA, ZAPA or the shorter polymethylene digabamides. The observation of multiple rate constants of this current decay has classically been interpreted to be the product of different receptor desensitized states. Several authors have suggested that the multiple rates of desensitization of cys-loop LGIC are products of agonist binding to separate binding sites with different affinities (Jones & Westbrook, 1995; Haas & Macdonald, 1999 and see Giniatullin *et al.*, 2005). It is likely that these multiple components of desensitization could correspond to different conformations of the ligand bound receptor. The compounds that showed only a single exponential of current decay had GABA residues separated by at least 18 Å. This distance corresponds with the internal diameter of the AChBP crystal structure (Brejc *et al.*, 2001).

Despite the two functional groups of the butylene, pentylene and hexylene digabamides, the desensitization kinetics of these polymethylene digabamides resembles

the desensitization kinetics observed with low concentrations of GABA. In agreement with Frosch *et al.* (1992), low concentrations of GABA exposure resulted in a single slow rate of desensitization. This was also observed with ZAPA. At higher concentrations, desensitization became a bi-exponential event with either GABA or ZAPA (see Figure 5-5). Due to the limitations of both this system and the analysis used, it is likely that due to the smaller population of receptors activated at lower agonist concentrations, we can not statistically distinguish the fast desensitization phase from the slow phase until the agonist evoked response reaches approximately 75% of maximum evoked current.

Modeling

Jones and Westbrook (1995) suggested that slow desensitization is caused by a mono-liganded state of the receptor and fast desensitization is an effect of the di-liganded state. In this context, with the longer polymethylene digabamide compounds, two GABA binding sites may be bound at the same time and prevent entry into the fast desensitized state. An alternative explanation is these compounds may be long enough to inhibit binding by steric hindrance at an adjacent binding site, thereby preventing the binding that leads to the fast desensitized state. This model would also explain the existence of only a single exponential of current decay with low concentrations of GABA. Bai *et al.* (2001) also proposed a model involving both mono- and di-liganded states of the receptor when investigating tonic current. In their model, the mono-liganded state opens to a low conductance state while the di-liganded state could desensitize with either fast or slow entry into the desensitized states or this agonist bound state could lead to an open state

(Bai *et al.*, 2001). These two models differed primarily in the origin of the state leading to desensitization.

Considering that the distance separating the GABA moieties of the compounds that desensitize with a single exponential corresponds to the diameter of the AChBP cavity, it may be plausible that these compounds can stretch the distance of the two low affinity GABA binding sites on the β-α interfaces. However, this would require the assumption that ligand can access the binding pocket from inside the external vestibule (Miyazawa *et al.*, 1999) as opposed to the external perimeter of the vestibule (Brejc *et al.*, 2001). Both the N-terminal domain and the TM1 domain of the receptor have been implicated as structures involved in desensitization (Bianchi *et al.*, 2001; Bianchi and Macdonald, 2002). Therefore, the interaction of these compounds with the N-terminal ligand binding domain may account for the differences in desensitization that were observed with the polymethylene digabamides. Modeling of these compounds bound to the receptor may provide more evidence for where the two GABA moieties could be interacting on the receptor.

Binding sites

With the nAChR, additional binding sites for ligand on the same subunit interfaces as the characterized binding sites has been suggested from the association and dissociation kinetics of suberyldicholine (Dunn & Raftery, 1997a&b). Trp 86 of the *Torpedo* nAChR was postulated to be a residue that interacts with suberyldicholine (Kapur *et al.*, 2006). This residue was previously labeled with a nAChR competitive agonist (Galzi *et al.*, 1990) and, based on the AChBP structure, is approximately 18 Å

away from the characterized binding site. Using bisquaternary ligands, comparing the dimensions of these compounds to the AChBP structure suggests the interaction of one end of the compound in the characterized binding pocket, and the other end interacting with Trp 82, the equivalent position to Trp 86 on the *Torpedo* nAChR (Carter *et al.*, 2007). Previous single channel investigations of the $GABA_AR$ from our laboratory suggests that there are multiple binding sites for GABA on the receptor complex and it may be possible that these binding sites are located in similar positions to that of ACh on the nAChR.

Other kinetic models

Haas & Macdonald (1999) introduced a third component of desensitization to a linear kinetic model of $\alpha1\beta3\gamma2L$ $GABA_AR$ activation and desensitization and is shown below. This was necessary to account for their observation of triphasic desensitization. In this model, fast desensitization develops from the third closed state while intermediate desensitization develops from the fourth closed state. The slow desensitization state develops from and recovers to the intermediate desensitization state.

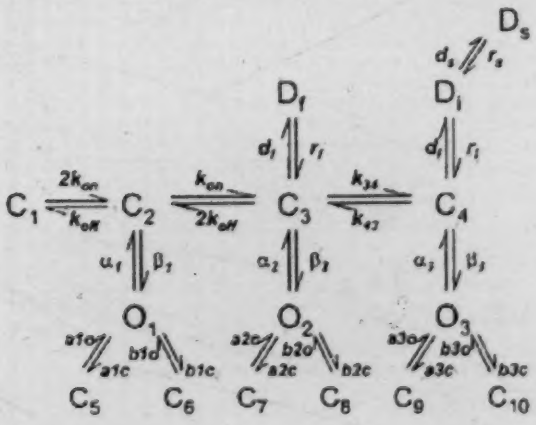

In this model, states of the receptor are denoted by O for open states, C for closed states and D for desensitized states. The three desensitized states are referred to in the text as fast, intermediate and slow which are illustrated above as D subscript f, i and s respectively. Since these authors did not see any change in the rate of desensitization with increasing concentrations of GABA, they proposed that the desensitization states are achieved only from di-liganded states of the receptor, in contrast to that proposed by Jones & Westbrook (1995) or Bai *et al.* (2001). A fourth desensitization state was later reported for $\alpha 1\beta 3\gamma 2L$ $GABA_AR$ using excised patches and an ultra fast perfusion system (Bianchi & Macdonald, 2002). This state has yet to be included into a kinetic model.

Conclusion

The *Xenopus* oocyte platform is not ideal for the study of fast desensitization due to the large size of the cell (stage V and VI oocytes have diameters between 1 and 1.3 mm (Goldin, 1992)). This means that there is large membrane capacitance and therefore slow response time of the clamp. A bath perfusion system was also used which delivers drugs more slowly than a delivery pipette positioned close to the clamped cell. However, this system is useful for measuring slower rates of desensitization. Using excised patches and an extremely fast perfusion system, Bianchi & Macdonald (2002) were able to resolve four components of fast desensitization. This suggests that the two state model of Jones & Westbrook (1995) is a simplified model of receptor activation and desensitization.

While it is likely that there are faster phases of $GABA_AR$ desensitization that could not be measured by using *Xenopus* oocytes, the influence of the long

polymethylene digabamide compounds on desensitization is dramatic. This could be a reflection of ligand interaction at an additional GABA binding site on the receptor construct which can be bound in addition to the characterized binding site when the bisfunctional ligand is of sufficient length and/or an inability of the receptor to change conformation in the presence of these ligands to achieve the fast desensitized state.

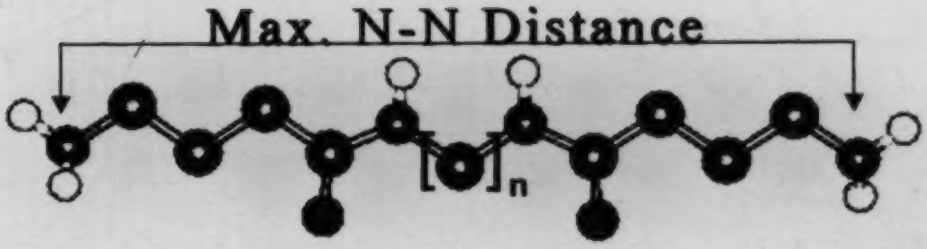

Figure 5-1: Generic structure of polymethylene digabamides. The polymethylene digabamide compounds are composed of two GABA moieties separated by a polymethylene chain of variable length. Shown here, these compounds are in their fully extended conformation.

n=	Maximum length (Å)
2	16.4
3	17.4
4	18.7
5	19.9
6	21.2

Table 5-1: Maximum distance separating GABA moieties in each of the series of polymethylene digabamides. In their fully extended form, the maximum distance between the amine groups in the GABA residue of each polymethylene digabamide is listed above.

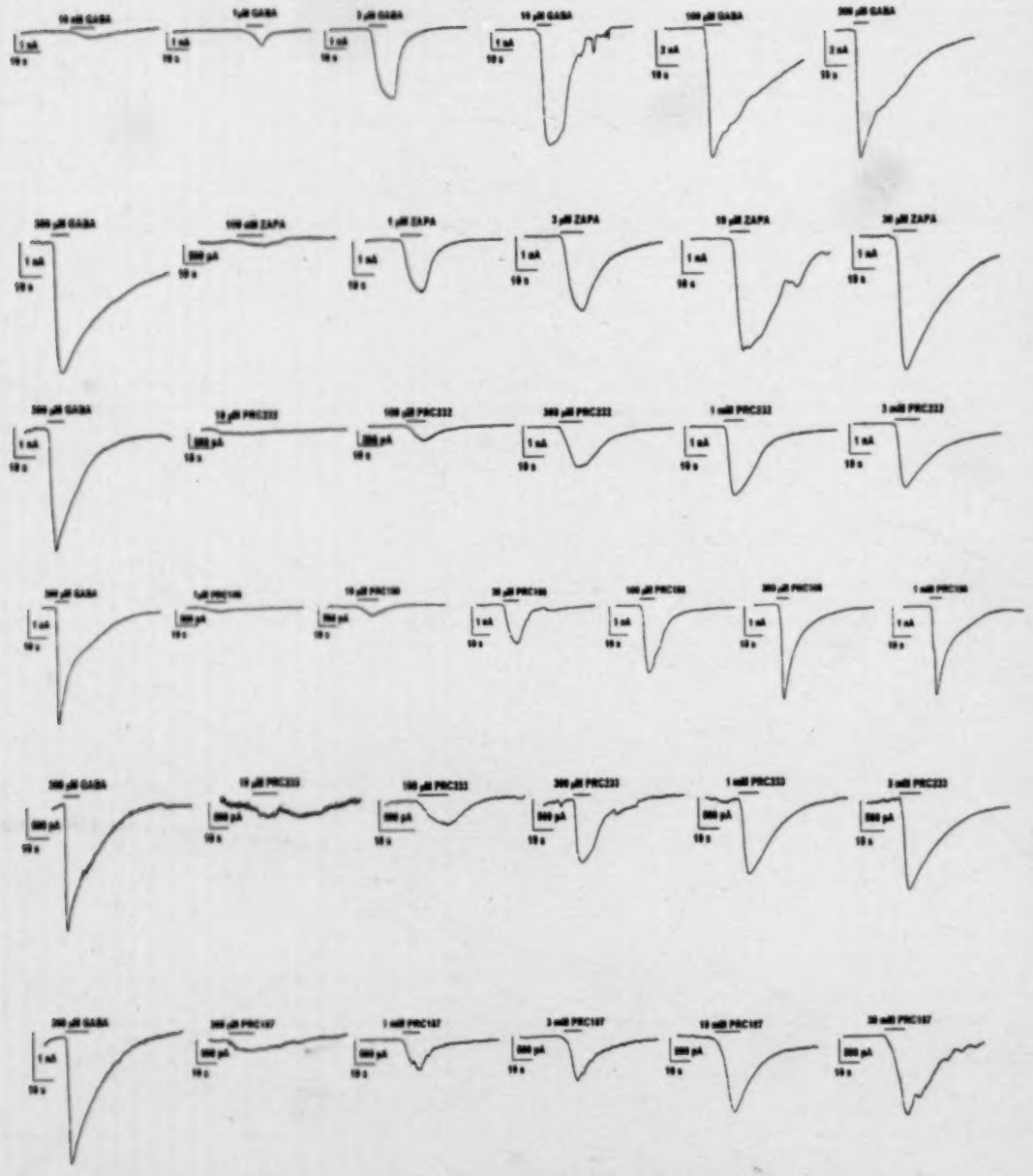

Figure 5-2: Sample whole cell currents elicited by GABA, ZAPA, PRC232, PRC186, PRC233 and PRC187. Currents were measured from HEK293 cells expressing $\alpha1\beta2\gamma2L$ $GABA_AR$ at a holding potential of -50 mV. From top to bottom: GABA, ZAPA, PRC232 (n=3), PRC186 (n=4), PRC233 (n=5) and PRC187 (n=6). The response to each compound is compared to the response to 300 μM GABA.

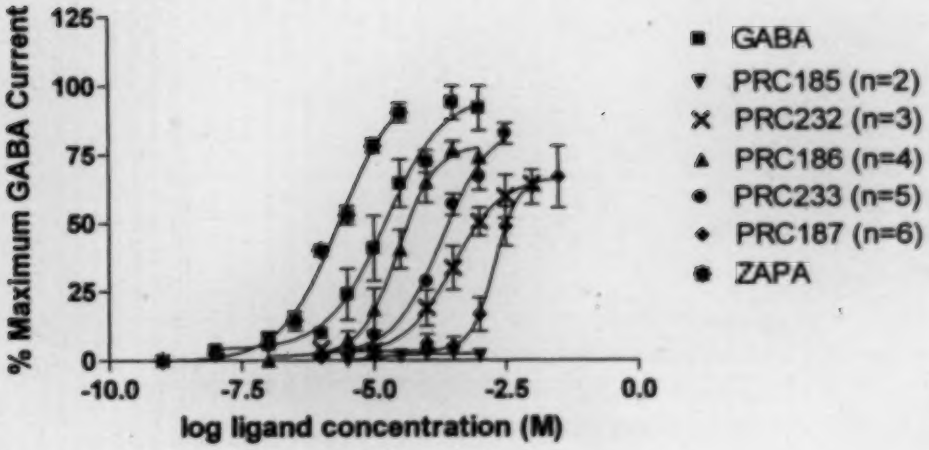

Figure 5-3: Concentration-response curves of polymethylene digabamide compounds compared to GABA and ZAPA. The resulting concentration-response curves of the polymethylene digabamide compounds to HEK 293 cells transiently expressing $\alpha 1\beta 2\gamma 2L$ $GABA_AR$ are shown above. Current is reported as an average percent of maximal current ± S.E.M. from at least three individual dose-response curves derived from at least two separate transfections for each drug.

Ligand	Log EC_{50} (M)	Intrinsic Activity (%)
GABA	-4.82 ± 0.19	
ZAPA	-5.70 ± 0.10	
PRC185 (n=2)	-5.07 ± 0.35	2.9 ± 0.9
PRC232 (n=3)	-3.35 ± 0.11	61.4 ± 6.5
PRC186 (n=4)	-4.69 ± 0.20	76.1 ± 4.7
PRC233 (n=5)	-3.74 ± 0.10	82.3 ± 2.7
PRC187 (n=6)	-2.82 ± 0.09	75.7 ± 6.5

Table 5-2: Potency and intrinsic activity of the series of polymethylene digabamide compounds compared to GABA and ZAPA. Values are reported as an average percent of maximal current or the average EC_{50} ± S.E.M. from at least three individual dose-response curves derived from at least two separate transfections for each drug.

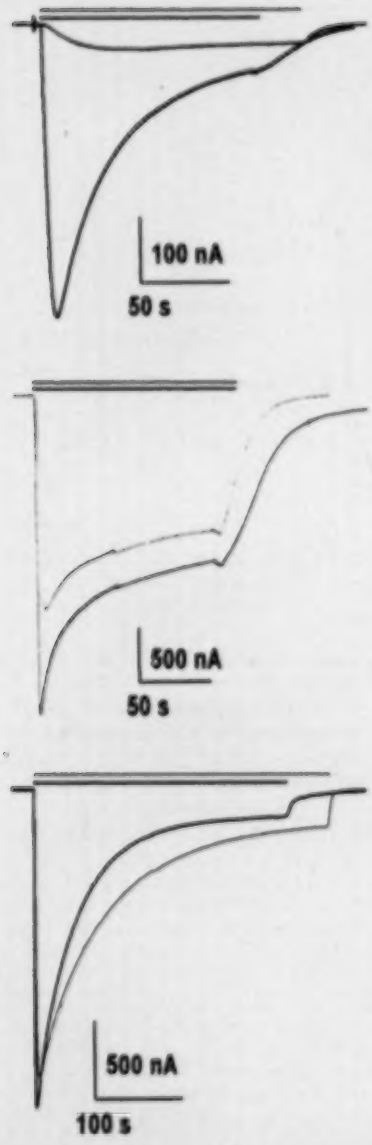

Figure 5-4: Two-electrode voltage clamp currents from *Xenopus* oocytes. Currents evoked by GABA are in black and currents evoked by the polymethylene digabamide compounds are in red. The lines above the current traces denote the duration of drug application to the oocyte. Top panel: currents evoked by 1 mM PRC185 do not show any desensitization over the duration we investigated. Middle panel: currents evoked by 3 mM PRC232 decay in a biexponential manner, while currents evoked by 0.5 mM PRC186 (bottom panel) decay with only a single exponential.

		Desensitization (s)		Amplitude (%)		Time to Peak (s)
Ligand	Conc (mM)	Tau 1	Tau 2	A1	A2	
GABA	1	16.7 ± 2.4	57.9 ± 7.3	24.8 ± 4.3	75.2 ± 4.3	6.8 ± 0.6
ZAPA	1	13.3 ± 3.1	52.4 ± 7.8	23.3 ± 5.1	76.7 ± 5.1	5.2 ± 0.8
PRC185 (n=2)	1	Desensitization Not Measurable		-	-	35.3 ± 3.3
PRC232 (n=3)	3	13.8 ± 3.6	83.3 ± 10.4	14.4 ± 5.9	85.6 ± 5.9	12.1 ± 1.9
PRC186 (n=4)	0.5	-	67.2 ± 7.1	-	-	9.3 ± 0.9
PRC233 (n=5)	3	-	80.8 ± 2.3	-	-	17.2 ± 4.3
PRC187 (n=6)	10	-	64.4 ± 16.9	-	-	6.5 ± 1.1

Table 5-3: Desensitization rates of GABA, ZAPA and the polymethylene digabamides. GABA, ZAPA and PRC232 currents displayed biexponential decay with two time constants. The proportion of amplitude that contributes to each is displayed above. PRC186, 233 and 187 currents showed only a single exponential of decay. Also listed are the average times required for the current to reach its peak response with each compound. Values are reported as mean ± S.E.M. and are obtained from a minimum analysis of four currents for each drug.

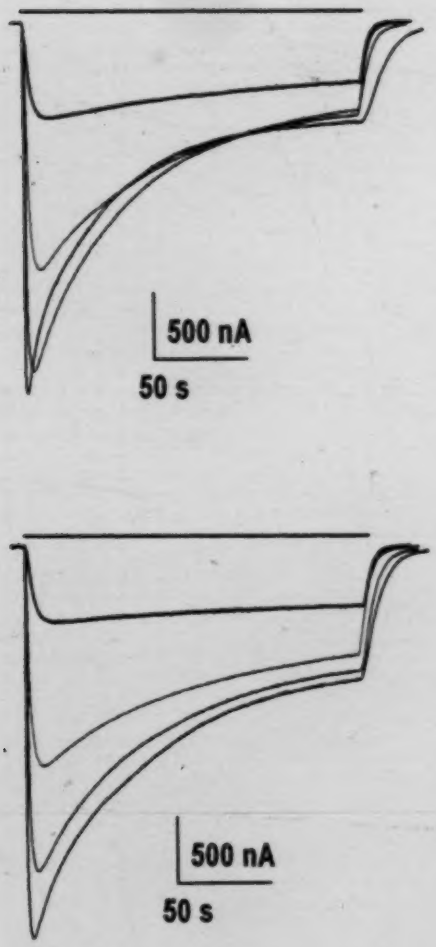

Figure 5-5: Concentration-dependence of desensitization. The concentration of agonist applied to oocytes increases from black, red, green to blue. Top panel: GABA 10 μM, 30 μM, 100 μM, and 1 mM. Currents evoked with 10 and 30 μM GABA are fitted best by a single exponential of decay while currents evoked by 100 μM and 1 mM GABA decay biexponentially. Bottom panel: ZAPA 3 μM, 10 μM, 30 μM and 100 μM. As with GABA, the two lowest concentrations of ZAPA decay with a single exponential while the two higher concentrations show two exponentials of decay.

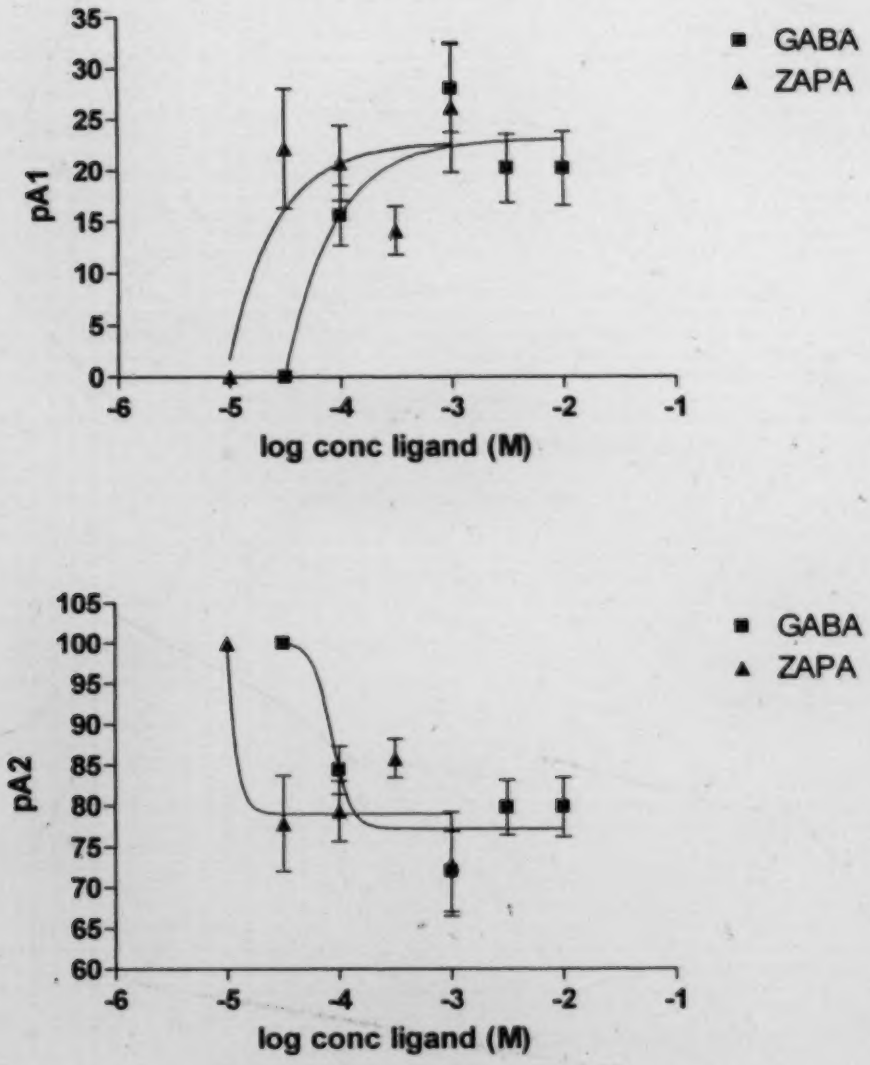

Figure 5-6: Proportion of the maximum current entering slow or fast desensitization when exposed to GABA (green squares) or ZAPA (blue triangles). Top panel: the proportion of the fast component (pA1) of desensitization is zero at concentrations under 100 μM GABA and 30 μM ZAPA. These concentrations appear to be the threshold concentration at which the fast component can be measured. Bottom panel: the respective proportion of the slow component (pA2) of desensitization decreases as the proportion of the fast component increases.

Bibliography

Bai D, Zhu G, Pennefather P, Jackson MF, MacDonald JF & Orser BA. (2001). Distinct functional and pharmacological properties of tonic and quantal inhibitory postsynaptic currents mediated by gamma-aminobutyric acid(A) receptors in hippocampal neurons. *Mol Pharmacol* **59,** 814-824.

Bianchi MT & Macdonald RL. (2002). Slow phases of GABA(A) receptor desensitization: structural determinants and possible relevance for synaptic function. *J Physiol* **544,** 3-18.

Brejc K, van Dijk WJ, Klaassen RV, Schuurmans M, van Der Oost J, Smit AB & Sixma TK. (2001). Crystal structure of an ACh-binding protein reveals the ligand-binding domain of nicotinic receptors. *Nature* **411,** 269-276.

Carlier PR, Chow ES, Barlow RL & Bloomquist JR. (2002). Discovery of non-zwitterionic GABA(A) receptor full agonists and a superagonist. *Bioorg Med Chem Lett* **12,** 1985-1988.

Carter CR, Cao L, Kawai H, Smith PA, Dryden WF, Raftery MA & Dunn SM. (2007). Chain length dependence of the interactions of bisquaternary ligands with the Torpedo nicotinic acetylcholine receptor. *Biochem Pharmacol* **73**, 417-426.

Dunn SM & Raftery MA. (1997a). Agonist binding to the Torpedo acetylcholine receptor. 1. Complexities revealed by dissociation kinetics. *Biochemistry* **36,** 3846-3853.

Dunn SM & Raftery MA. (1997b). Agonist binding to the Torpedo acetylcholine receptor. 2. Complexities revealed by association kinetics. *Biochemistry* **36,** 3854-3863.

Frosch MP, Lipton SA & Dichter MA. (1992). Desensitization of GABA-activated currents and channels in cultured cortical neurons. *J Neurosci* **12,** 3042-3053.

Galzi JL, Revah F, Black D, Goeldner M, Hirth C & Changeux JP. (1990). Identification of a novel amino acid alpha-tyrosine 93 within the cholinergic ligands-binding sites of the acetylcholine receptor by photoaffinity labeling. Additional evidence for a three-loop model of the cholinergic ligands-binding sites. *J Biol Chem* **265,** 10430-10437.

Giniatullin R, Nistri A & Yakel JL. (2005). Desensitization of nicotinic ACh receptors: shaping cholinergic signaling. *Trends Neurosci* **28,** 371-378.

Goldin AL. (1992). Maintenance of Xenopus laevis and oocyte injection. *Methods Enzymol* **207,** 266-279.

Haas KF & Macdonald RL. (1999). GABAA receptor subunit gamma2 and delta subtypes confer unique kinetic properties on recombinant GABAA receptor currents in mouse fibroblasts. *J Physiol* **514 (Pt 1),** 27-45.

Jones MV & Westbrook GL. (1995). Desensitized states prolong GABAA channel responses to brief agonist pulses. *Neuron* **15,** 181-191.

Kapur A, Davies M, Dryden WF & Dunn SM. (2006). Tryptophan 86 of the alpha subunit in the Torpedo nicotinic acetylcholine receptor is important for channel activation by the bisquaternary ligand suberyldicholine. *Biochemistry* **45,** 10337-10343.

Miyazawa A, Fujiyoshi Y, Stowell M & Unwin N. (1999). Nicotinic acetylcholine receptor at 4.6 A resolution: transverse tunnels in the channel wall. *J Mol Biol* **288,** 765-786.

Newell JG, Davies M, Bateson AN & Dunn SM. (2000). Tyrosine 62 of the gamma-aminobutyric acid type A receptor beta 2 subunit is an important determinant of high affinity agonist binding. *J Biol Chem* **275,** 14198-14204.

Olsen RW, Bergman MO, Van Ness PC, Lummis SC, Watkins AE, Napias C & Greenlee DV. (1981). gamma-Aminobutyric acid receptor binding in mammalian brain. Heterogeneity of binding sites. *Mol Pharmacol* **19,** 217-227.

CHAPTER 6

GENERAL DISCUSSION

General Discussion

Based on the results from Chapters 3 and 4 we have identified in total at least five activated states of the α1β2γ2L $GABA_AR$. These are manifested as different conductance amplitudes and different populations of open durations of these amplitude states. Current receptor theory views different activated states as derived from differential binding to the receptor complex, and is reflected in the concentration dependence observed for each conductance state. Our results are consistent with these states being derived from separate binding events. Each binding site is thought to have different affinities for a ligand, and in addition, have unique affinities for separate ligands. Only two of these states demonstrated co-operativity with each other, and even then, this was observed only when the receptor was activated with GABA and not with the partial agonists THIP or P4S.

It is widely accepted that there are two binding sites for GABA at each of the β-α subunit interfaces. These two sites have been postulated to have different affinities for GABA and, therefore, were not regarded as equivalent binding sites (Baumann *et al.*, 2003). This disparity was proposed to be attributable to the influence of the subunits adjacent to those forming the interface since these subunits are not identical (Baumann *et al.*, 2003). Dunn & Raftery (1997a&b) further proposed additional "sub-sites" within the binding pocket of the nAChR, a circumstance that is likely to extend to the $GABA_AR$ given the homology between members of the cys-loop LGIC family. A putative high affinity binding site at the α-β interface with a role in desensitization has also been suggested (Newell *et al.*, 2000).

Based on the total number of postulated binding sites for both the nAChR and the $GABA_AR$, there are theoretically enough binding sites on the receptor complex to accommodate a model that involves multiple binding events. From the single channel studies using GABA, THIP or P4S to activate the channel, we propose the following model as a summary of these results. Each of the small blue circles represents a ligand molecule binding to a distinct binding site on the receptor (illustrated as the larger blue circles). Each binding event leads to an activated state of the receptor which is more permissive to channel opening(s). The co-operativity observed between the short and long full-conductance states was not observed when the receptor was activated by either THIP or P4S. It may be that the rate of conversion from the short full-conductance state to the long full-conductance state is very long when the receptor is activated by THIP or P4S, or that the affinity for P4S and THIP at the site that produces the long full-conductance currents is very low.

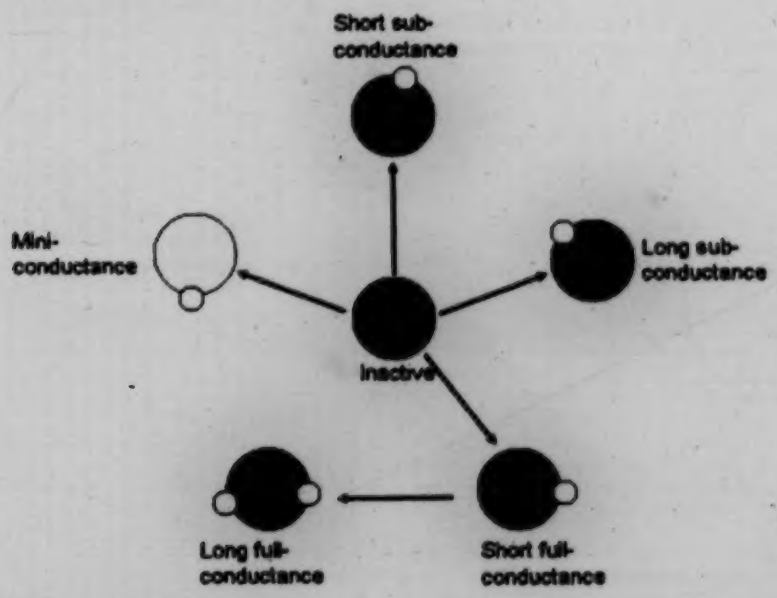

From the results obtained in Chapter 5 it is not possible to predict where the two desensitization states we observed would fit into the above model. It is possible, based on the desensitization studies performed by other investigators (Haas & Macdonald, 1999; Bianchi & Macdonald, 2002) that there are additional fast desensitized states of the receptor that we could not measure using the *Xenopus* oocyte system and best fit least squares analysis. Due to the millisecond time constants of these particular desensitization states, they are incompatible with our model since such time frames do not match the observed occurrence of the mini-, sub- or full-conductance currents.

The investigation of the desensitization rates of these $GABA_AR$s activated by the series of polymethylene digabamide compounds illustrated a difference in desensitization kinetics of compounds longer than 18.7 Å (butylene digabamide) compared to the shorter polymethylene digabamide compounds or GABA or ZAPA. As this difference in desensitization may reflect differences in binding, one possibility for this observation is that compounds longer than 18 Å might be capable of binding to two binding sites on the receptor. This would suggest that two of the binding sites might be found within approximately 18 Å of each other.

Single channel work with butylene digabamide was attempted but, unfortunately, the open channel noise was too great to analyze the recordings in the same manner as the GABA, THIP and P4S recordings. Even very low concentrations of butylene digabamide yielded very noisy results. However, the conductance amplitudes that were observed appeared to be close to those which were observed with GABA, THIP or P4S evoked channel activation. Certainly there was no 'super'-conductance state observed, which may have provided an explanation for the 'superagonism' that Carlier *et al.* (2002)

reported for this compound in ion flux experiments. The differences that were observed in channel desensitization kinetics seems the most likely explanation for this compound appearing as a 'super agonist' in ion flux experiments but appearing as a partial agonist in whole cell recordings.

While the mechanism involved in determining the conductance of the cys-loop LGICs has not been completely elucidated, it has been shown that the channel conductance is influenced by both the TM2 domain (Imoto *et al.*, 1988) as well as the TM3-TM4 intracellular loop (Kelley *et al.*, 2003). However, at this time it is not clear what structures of the receptor are involved in generating the sub-conductance currents that are so commonly observed in $GABA_AR$ single channel recordings. Whether agonist binding can lead to various conformations of the receptor pore and/or the intracellular vestibules is unknown.

These five activated states that we observed may reflect different conformations that the receptor undergoes during channel activation. Depending on the structure and size of the agonist, certain conformations may be energetically more favourable than others, explaining why certain conductance states are seen more often than others with different agonists. When each of these binding sites is bound with an agonist molecule, the conformation need not change to the same extent, leading to the different activated states of the receptor. The effect that such graded conformational changes have on gating are more difficult to conceive in detail. As ion permeation through the channel is single file, variations in conductance must derive from changes in the rate of ion transition through the channel. In turn, the rates of ion transition are determined by the positioning of energy barriers within the transition pathway such as described for the nAChR by

Cymes *et al.* (2005) and Hung *et al.* (2005). Thus variances in conduction values may reflect variable repositioning of these energy barriers to ion passage.

Future Directions

Progress has been made in identifying the structures within the $5HT_3R$ that control the conductance of this channel. Kelley *et al.* (2003) implicated three conserved arginines (432, 436 and 440) of the internal vestibule (the portals) in controlling the conductance of this channel. While these arginines are not conserved in the $GABA_AR$, so much homology is shared within the cy-loop LGIC superfamily, especially in terms of structure, that it is possible that there are regions within the internal vestibule of this receptor that determine the conductance of this channel as well. Furthermore, it may be possible that the conductance currents are controlled within this region, possibly at the interfaces of different subunits. It is not clear at this time how the channel gate would be able to control the portals, but it might not be a stretch of the imagination to consider how the rotation of the TM2 after agonist binding (Miyazawa *et al.*, 2003) might be translated along the entire length of this segment of the protein and cause movements in the internal vestibule. There remains much work to be done to elucidate how the different conductance currents are achieved, and considering the internal vestibules may be an appropriate place to begin. For simplicity's sake, this would probably best be achieved using an $\alpha\beta$ $GABA_AR$, since this receptor only demonstrates two conductance states (Angelotti & Macdonald, 1993a) and likewise will only have α-β and β-α interfaces. While some of this work has been started with the nAChR (Hales *et al.*, 2006; Peters *et*

al., 2006), it will be interesting to see how this translates to the glycine receptors and $GABA_ARs$.

There is also evidence that the conductance of a cys-loop LGIC might also be controlled at and around the TM2 domain (Imoto *et al.*, 1988). This region could serve to be further investigated. As ligand binds to each of the ligand binding sites, the energy barriers to ion passage in the pore region of the receptor may be removed at different extents as the TM2 domains rotate. This may lead to different activated states of the receptor, as mentioned above.

Mutagenic studies on both of these regions may provide more evidence for the structures that determine the multiple channel conductance currents. These types of studies introduce their own uncertainties, due to the possibility that the changes observed are caused by allosteric effects of the mutation as opposed to a direct action of the mutation. However, coupled with functional studies, mutational work could provide clues to the roles of specific amino acid residues in the pore region of the receptor.

Despite the poor results obtained from single channel work with butylene digabamide, it may be useful to try to obtain single channel recordings of channel activation by the other polymethylene digabamide compounds. While the same type of single channel analysis done for GABA, THIP and P4S activated channels may not be possible, nor even required, further single channel investigation may provide further insights into the channel behaviour. For example, if all of these compounds produce very noisy single channel recordings, this might point to less stable interactions of these compounds to the binding sites leading to less stable conformational states of the

receptor. If the other compounds generate analyzable results, it may be possible to investigate whether the behaviour of any of the conductance states changes.

Modeling of these polymethylene digabamide compounds to the binding pocket, such as was accomplished with the bisquaternary ligands at the nAChR (Carter *et al.*, 2006), would also be an interesting venture. This type of data could provide information into the distances that these compounds can reach from the binding pocket and determine if there are any other regions of the receptor within the vicinity of the second functional group where this group could bind once the first group is bound to the binding site. Modeling of this sort could determine if there are other binding sites that have not yet been characterized and novel interactions of these compounds with the receptor may be determined. While the interpretation of the results obtained from using these types of bisfunctional ligands can be difficult, these are still interesting tools to use in probing the function of the $GABA_AR$.

Despite the great strides that have been made in determining the structure, ligand binding domains and channel gating of members of the cys-loop LGIC superfamily, none of these processes has been completely explained. Considering the importance of these receptors in normal function, and specifically the role of $GABA_AR$ in fast inhibitory synaptic activity, understanding their activity could provide great insight into greater functionality of the central nervous system. Also, certain disease states such as Angelman's syndrome and some types of epilepsy are caused by or involve specific problems involving $GABA_AR$. Understanding the normal activity of these receptors may provide more basis for understanding abnormal activity in disease states and bring us closer to creating therapies that directly target the malfunction of the receptor.

Bibliography

Amin J & Weiss DS. (1993). GABAA receptor needs two homologous domains of the beta-subunit for activation by GABA but not by pentobarbital. *Nature* **366,** 565-569.

Angelotti TP & Macdonald RL. (1993a). Assembly of GABAA receptor subunits: alpha 1 beta 1 and alpha 1 beta 1 gamma 2S subunits produce unique ion channels with dissimilar single-channel properties. *J Neurosci* **13,** 1429-1440.

Angelotti TP & Macdonald RL. (1993b). Assembly of GABAA receptor subunits: alpha 1 beta 1 and alpha 1 beta 1 gamma 2S subunits produce unique ion channels with dissimilar single-channel properties. *J Neurosci* **13,** 1429-1440.

Angelotti TP, Uhler MD & Macdonald RL. (1993). Assembly of GABAA receptor subunits: analysis of transient single-cell expression utilizing a fluorescent substrate/marker gene technique. *J Neurosci* **13,** 1418-1428.

Baumann SW, Baur R & Sigel E. (2003). Individual properties of the two functional agonist sites in GABA(A) receptors. *J Neurosci* **23,** 11158-11166.

Baur R & Sigel E. (2003). On high- and low-affinity agonist sites in GABAA receptors. *J Neurochem* **87,** 325-332.

Bianchi MT & Macdonald RL. (2002). Slow phases of GABA(A) receptor desensitization: structural determinants and possible relevance for synaptic function. *J Physiol* **544,** 3-18.

Boileau AJ, Baur R, Sharkey LM, Sigel E & Czajkowski C. (2002). The relative amount of cRNA coding for gamma2 subunits affects stimulation by benzodiazepines in GABA(A) receptors expressed in Xenopus oocytes. *Neuropharmacology* **43,** 695-700.

Bormann J & Clapham DE. (1985). gamma-Aminobutyric acid receptor channels in adrenal chromaffin cells: a patch-clamp study. *Proc Natl Acad Sci U S A* **82,** 2168-2172.

Brejc K, van Dijk WJ, Klaassen RV, Schuurmans M, van Der Oost J, Smit AB & Sixma TK. (2001). Crystal structure of an ACh-binding protein reveals the ligand-binding domain of nicotinic receptors. *Nature* **411,** 269-276.

Carlier PR, Chow ES, Barlow RL & Bloomquist JR. (2002). Discovery of non-zwitterionic GABA(A) receptor full agonists and a superagonist. *Bioorg Med Chem Lett* **12,** 1985-1988.

Carter CR, Cao L, Kawai H, Smith PA, Dryden WF, Raftery MA & Dunn SM. (2006). Chain length dependence of the interactions of bisquaternary ligands with the Torpedo nicotinic acetylcholine receptor. *Biochem Pharmacol.*

Chen CA & Okayama H. (1988). Calcium phosphate-mediated gene transfer: a highly efficient transfection system for stably transforming cells with plasmid DNA. *Biotechniques* **6,** 632-638.

Cymes GD, Ni Y & Grosman C. (2005). Probing ion-channel pores one proton at a time. *Nature* **438,** 975-980.

Dunn SM & Raftery MA. (1997a). Agonist binding to the Torpedo acetylcholine receptor. 1. Complexities revealed by dissociation kinetics. *Biochemistry* **36,** 3846-3853.

Dunn SM & Raftery MA. (1997b). Agonist binding to the Torpedo acetylcholine receptor. 2. Complexities revealed by association kinetics. *Biochemistry* **36,** 3854-3863.

Fox JA. (1987). Ion channel subconductance states. *J Membr Biol* **97,** 1-8.

Gage PW. (1998). Signal transmission in ligand-gated receptors. *Immunol Cell Biol* **76,** 436-440.

Guyon A, Laurent S, Paupardin-Tritsch D, Rossier J & Eugene D. (1999). Incremental conductance levels of GABAA receptors in dopaminergic neurones of the rat substantia nigra pars compacta. *J Physiol* **516,** 719-737.

Hales TG, Dunlop JI, Deeb TZ, Carland JE, Kelley SP, Lambert JJ & Peters JA. (2006). Common determinants of single channel conductance within the large cytoplasmic loop of 5-hydroxytryptamine type 3 and alpha4beta2 nicotinic acetylcholine receptors. *J Biol Chem* **281,** 8062-8071.

Hamill OP, Bormann J & Sakmann B. (1983). Activation of multiple-conductance state chloride channels in spinal neurones by glycine and GABA. *Nature* **305,** 805-808.

Haas KF & Macdonald RL. (1999). GABAA receptor subunit gamma2 and delta subtypes confer unique kinetic properties on recombinant GABAA receptor currents in mouse fibroblasts. *J Physiol* **514 (Pt 1),** 27-45.

Hung A, Tai K & Sansom MS. (2005). Molecular dynamics simulation of the M2 helices within the nicotinic acetylcholine receptor transmembrane domain: structure and collective motions. *Biophys J* **88,** 3321-3333.

Imoto K, Busch C, Sakmann B, Mishina M, Konno T, Nakai J, Bujo H, Mori Y, Fukuda K & Numa S. (1988). Rings of negatively charged amino acids determine the acetylcholine receptor channel conductance. *Nature* **335,** 645-648.

Jackson MB. (1989). Perfection of a synaptic receptor: kinetics and energetics of the acetylcholine receptor. *Proc Natl Acad Sci U S A* **86,** 2199-2203.

Kaneda M, Farrant M & Cull-Candy SG. (1995). Whole-cell and single-channel currents activated by GABA and glycine in granule cells of the rat cerebellum. *J Physiol* **485,** 419-435.

Kelley SP, Dunlop JI, Kirkness EF, Lambert JJ & Peters JA. (2003). A cytoplasmic region determines single-channel conductance in 5-HT3 receptors. *Nature* **424,** 321-324.

Miledi R, Parker I & Sumikawa K. (1983). Recording of single gamma-aminobutyrate- and acetylcholine-activated receptor channels translated by exogenous mRNA in Xenopus oocytes. *Proc R Soc Lond B Biol Sci* **218,** 481-484.

Miyazawa A, Fujiyoshi Y, Stowell M & Unwin N. (1999). Nicotinic acetylcholine receptor at 4.6 A resolution: transverse tunnels in the channel wall. *J Mol Biol* **288,** 765-786.

Miyazawa A, Fujiyoshi Y & Unwin N. (2003). Structure and gating mechanism of the acetylcholine receptor pore. *Nature* **423,** 949-955.

Mortensen M, Kristiansen U, Ebert B, Frolund B, Krogsgaard-Larsen P & Smart TG. (2004). Activation of single heteromeric GABA(A) receptor ion channels by full and partial agonists. *J Physiol* **557,** 389-413.

Newell JG & Czajkowski C. (2003). The GABAA receptor alpha 1 subunit Pro174-Asp191 segment is involved in GABA binding and channel gating. *J Biol Chem* **278,** 13166-13172.

Newell JG, Davies M, Bateson AN & Dunn SM. (2000). Tyrosine 62 of the gamma-aminobutyric acid type A receptor beta 2 subunit is an important determinant of high affinity agonist binding. *J Biol Chem* **275,** 14198-14204.

Newland CF, Colquhoun D & Cull-Candy SG. (1991a). Single channels activated by high concentrations of GABA in superior cervical ganglion neurones of the rat. *J Physiol* **432,** 203-233.

Newland CF, Colquhoun D & Cull-Candy SG. (1991b). Single channels activated by high concentrations of GABA in superior cervical ganglion neurones of the rat. *J Physiol* **432,** 203-233.

Peters JA, Carland JE, Cooper MA, Livesey MR, Deeb TZ, Hales TG & Lambert JJ. (2006). Novel structural determinants of single-channel conductance in nicotinic acetylcholine and 5-hydroxytryptamine type-3 receptors. *Biochem Soc Trans* **34,** 882-886.

Sigel E, Baur R, Kellenberger S & Malherbe P. (1992). Point mutations affecting antagonist affinity and agonist dependent gating of GABAA receptor channels. *Embo J* **11,** 2017-2023.

Smith GB & Olsen RW. (1994). Identification of a [^{3}H]muscimol photoaffinity substrate in the bovine gamma-aminobutyric acidA receptor alpha subunit. *J Biol Chem* **269,** 20380-20387.

Smith GB & Olsen RW. (1995). Functional domains of GABAA receptors. *Trends Pharmacol Sci* **16,** 162-168.

Twyman RE & Macdonald RL. (1992). Neurosteroid regulation of GABAA receptor single-channel kinetic properties of mouse spinal cord neurons in culture. *J Physiol* **456,** 215-245.

Unwin N. (1995). Acetylcholine receptor channel imaged in the open state. *Nature* **373,** 37-43.

Wagner DA & Czajkowski C. (2001). Structure and dynamics of the GABA binding pocket: A narrowing cleft that constricts during activation. *J Neurosci* **21,** 67-74.

Westh-Hansen SE, Witt MR, Dekermendjian K, Liljefors T, Rasmussen PB & Nielsen M. (1999). Arginine residue 120 of the human GABAA receptor alpha 1, subunit is essential for GABA binding and chloride ion current gating. *Neuroreport* **10,** 2417-2421.